ERDC/CHL TR-12-14

Coastal and Hydraulics Laboratory

US Army Corps
of Engineers®
Engineer Research and
Development Center

Coastal Inlets Research Program

St. Augustine Inlet, Florida: Application of the Coastal Modeling System

Report 2

Tanya M. Beck and Kelly Legault

August 2012

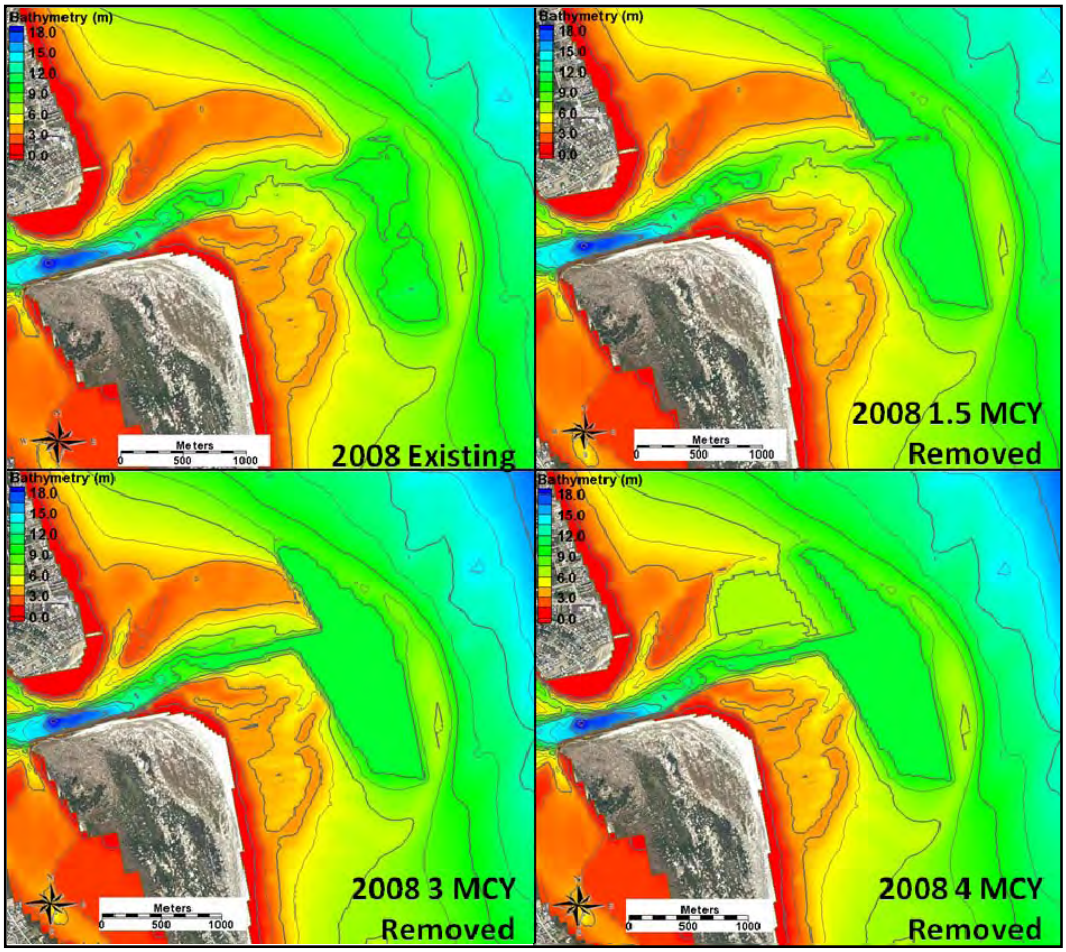

ERDC/CHL TR-12-14
August 2012

St. Augustine Inlet, Florida: Applying the Coastal Modeling System

Report 2

Tanya M. Beck and Kelly Legault

Coastal and Hydraulics Laboratory
U.S. Army Engineer Research and Development Center
3909 Halls Ferry Road
Vicksburg, MS 39180-6199

Report 2 of a series

Prepared for U.S. Army Engineer District, Jacksonville
701 San Marco Blvd.,
Jacksonville, FL 32207

Under Coastal Inlets Research Program

Monitored by Coastal and Hydraulics Laboratory
U.S. Army Engineer Research and Development Center
3909 Halls Ferry Road,
Vicksburg, MS 39180-6199

Abstract

This report, the second in a series, documents a numerical modeling study performed with the Coastal Modeling System (CMS), supported by field data collection, to quantify the impact of historical and future planned mining of the ebb-tidal delta at St. Augustine Inlet, FL. Recently, in the years 2001-2003 and 2005, two nourishment intervals utilized beach-quality sediment from the ebb-tidal delta at St. Augustine Inlet, resulting in 4.7 and 2.5 million cubic yards of sediment removed from the inlet system, respectively, for the two time periods. The CMS was used to determine the impact of these historical mining operations, as well as potential future minings on the natural littoral system in the vicinity of the inlet as well as the morphodynamics of the inlet. Quantitative comparisons of planform evolution, volumetric change, and transport pathway spatial distribution and magnitude were made for the historical and future scenarios. Results showed little to no changes in the ebb-tidal delta trajectory in these three quantitative comparisons. The footprint of the ebb-tidal delta mining did not change the bypassing patterns in a way such as to cause significant morphologic change to the inlet system. Modeling of planned alternatives including the removal of an additional 1.5, 3, and 4 million cubic yards (mcy) of sediment also illustrated a tipping point in morphodynamic response in varying volume removed and mining design.

Contents

Figures and Tables

Figures

Tables

Preface

This report documents a quantitative analysis of sediment transport and morphologic processes at St. Augustine Inlet, FL, performed during fiscal year 2010 at the request of the U.S. Army Engineer District, Jacksonville District (hereafter, the Jacksonville District). This study follows Report 1, Technical Report (Legault et al. 2012), which developed a sediment budget based on long-term profile evolution and attempts to answer questions posed by local authorities that address the impact of operations on the federal navigation channel at St. Augustine Inlet. The objective of this report is to determine the near field and far field effects to sediment transport processes under past and future dredging operations at the inlet ebb-tidal delta.

To address questions about the past and future behavior of the inlet ebb-tidal delta, the Coastal Modeling System (CMS) was applied to gain quantitative understanding of the hydrodynamics and sediment transport processes at the inlet and to evaluate alternatives dredging scenarios. The CMS, driven by tide and hindcast waves, was capable of reproducing observed trends in ebb-tidal delta morphodynamics and changes in volume of notable morphologic features. The modeling system was calibrated by reproducing observed water levels in the Tolomato-Matanzas estuary, current velocities in the inlet, and morphology change at the ebb-tidal delta. The CMS was then applied to evaluate alternatives trajectories of past ebb-tidal delta configurations and to future alternatives to determine the capacity of the inlet to function under different dredging scenarios.

This study was performed by Tanya M. Beck, Coastal Engineering Branch (CEB), Navigation Division (ND), Coastal and Hydraulics Laboratory (CHL), and Dr. Kelly Legault, Coastal Engineering, U.S. Army Engineer District, Jacksonville. Dr. Julie Dean Rosati, Flood and Coastal Division, Coastal Processes Branch (CPB), CHL, and Coastal Inlets Research Program (CIRP) Program Manager, reviewed a preliminary draft of this document. Information and coordination in support of this study, as well as study review, were provided by Jacksonville District personnel Jason Engle and Lori Hadley. Peer reviews of this study were provided by Dr. Christopher Reed, Reed & Reed Assoc., and Alison Sleath Grzegorzewski, CPB, CHL. This study was supported by the CIRP and the Regional

Sediment Management (RSM) Program, funded by the U.S. Army Corps of Engineers, Headquarters (HQUSACE). Linda Lillycrop (CEB), CHL, is Program Manager of the RSM Program. The CIRP and RSM Programs are administered for Headquarters at the U.S. Army Engineer Research and Development Center (ERDC), Coastal and Hydraulics Laboratory (CHL) under the Navigation Systems Program of the U.S. Army Corps of Engineers. James E. Walker is HQUSACE Navigation Business Line Manager overseeing CIRP and RSM. W. Jeff Lillycrop, CHL, is the Navigation Technical Director. This work was conducted under the general administrative supervision Dr. Jeffrey P. Waters, Chief, CEB, and Dr. Rose M. Kress, Chief, ND.

At the time of publication of this report, COL Kevin Wilson, EN, was Commander and Executive Director. Dr. Jeffery P. Holland was ERDC Director.

Unit Conversion Factors

Multiply	By	To Obtain
cubic feet	0.02831685	cubic meters
cubic yards	0.7645549	cubic meters

1 Introduction

St. Augustine Inlet is a federally maintained deep-draft navigation channel of the U.S. Army Engineer District, Jacksonville (hereafter, the Jacksonville District), located along the northeastern Florida Atlantic coast. The navigation channel is primarily maintained through maintenance dredging occurring on four to seven year intervals, consisting of a shore perpendicular channel dredged to a depth of 9 m below mean lower-low water (mllw). Inland water maintenance channel dredging is conducted by the Jacksonville District through the Atlantic Intracoastal Waterway (AIWW) in addition to the inlet navigation channel. The sediments removed in these projects have been used historically in a local Shore Protection Project along the St. Augustine Beach on Anastasia Island. Recently, in the years 2001-2003 and 2005, two nourishment intervals utilized beach-quality sediment from the ebb-tidal delta at St. Augustine Inlet resulting in 4.7 and 2.5 million cubic yards of sediment removed from the inlet system, respectively, for the two time periods. In 2009, the Jacksonville District initiated a study on the past impact of the mining of the ebb-tidal delta and the feasibility of utilizing this sediment source in the future.

This study on past and future impact from ebb-tidal delta mining at St. Augustine Inlet, FL, was performed at the request of the Jacksonville District. The objective was to evaluate whether past or future excavations of the ebb-tidal delta significantly altered or will alter the ebb-tidal delta morphology or local/regional sediment transport patterns in such a way that there have been or would be adverse effects on adjacent beaches and the functional nature of the inlet system. The Coastal Modeling System (CMS), a two-dimensional (2-D) hydrodynamic, sediment transport, and morphology change model, was used to address the following scientific questions:

1. How many cubic yards of sediment can be mined from the ebb-tidal delta in its present condition to minimize large-scale volumetric change to the ebb-tidal delta/inlet complex?
2. What is the volumetric limit for the removal of sediments which does not cause a significant change to the elevation and planform extent of the ebb-tidal delta either from the engineering activity itself at the borrow site, or due to ebb-tidal delta deflation or collapse after the engineering activity?

3. How would a significant change to the elevation and planform extent of the ebb-tidal delta affect shoreline position?

These questions were addressed through operation of the CMS, driven by tide and hindcast waves, which reproduced observed trends in hydrodynamics and ebb-tidal delta morphologic change. The modeling system was calibrated to observed water levels and currents in the Tolomato-Matanzas Bay and current velocity in the inlet. The CMS was then applied to evaluate features relative to the above questions for past and future conditions. The alternatives were developed in collaboration with the Jacksonville District to answer their questions.

1.1 Study area

The study area for this report covers St. Johns County, Florida, which stretches from Ponte Vedra Beach in the north to Matanzas Inlet to the south. Figure 1 illustrates the reach of the study area including the Matanzas-Tolomato Bay. St. Augustine Inlet is centrally located within the county area. The inlet serves the Matanzas River, which is located along the south reach of the bay, and the Tolomato River located along the north reach of the bay. These “rivers” were historically termed by locals, but are scientifically referred to as a coast parallel, lagoonal estuary that feeds a small tidal salt marsh. There is little riverine flow into the estuary, and much of the estuary is brackish to fully marine.

St. Augustine Inlet is located along the mesotidal, open Atlantic coast. Tides are semi-diurnal with a spring high tidal range of 1.8 m and a mean tidal range of 1.5 m (NOAA 2010a). Table 1 describes the general tide and wave characteristics of the area. The wave climate is seasonal with moderate wave exposure as defined by Walton and Adams (1976). Wave energy is typically greatest during the winter season from November to April, with subtropical frontal passages occurring every three to seven days (Taylor Engineering Inc. 1996). Wave heights during these storms are on average 1.2 to 1.8 m or greater, with longer mean wave periods of 9- 12 seconds (USACE 2010). Fair-weather conditions persist through the summer season from May to October, where wind swell waves are on average 0.3-1.0 m in height with shorter periods of 5-8 seconds (USACE 2010). This stretch of coast is also subject to the passages of tropical storms that can have larger wave heights of 1.8 to 3.7 m.

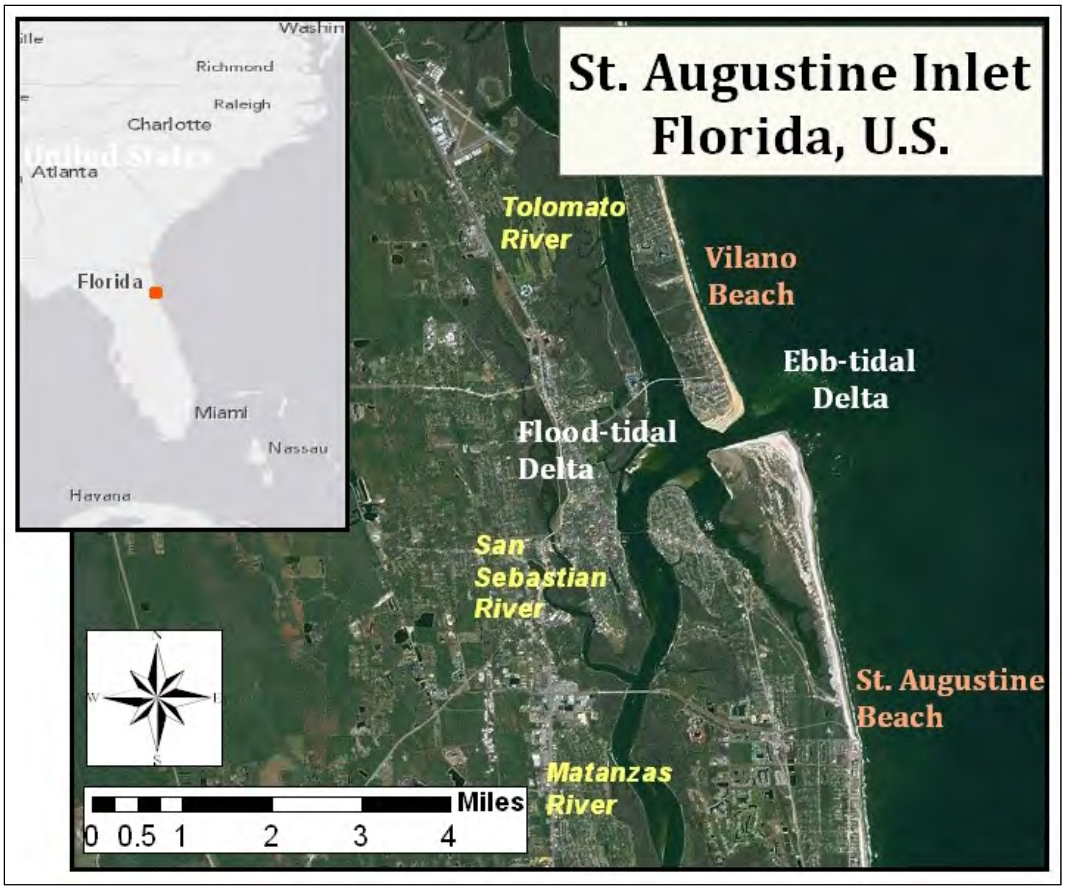

Figure 1. Study area location map for St. Johns County, Florida.

Table 1. General characteristics of the tide and waves in the vicinity of St. Augustine Inlet, Florida.

General Characteristic	Value	Description
Mean Tidal Range	1.4 m	Astronomical Tide (Taylor 1996)
Spring Mean Tidal Range	1.6 m	Astronomical Tide (Taylor 1996)
Mean Significant Wave Height	1.1 m	WIS Hindcast Database (USACE 2010)
Mean Peak Wave Period	7 s	WIS Hindcast Database (USACE 2010)
Range of Mean Significant Wave Height	0.6 – 1.8 m	WIS Hindcast Database (USACE 2010)
Range of Mean Peak Wave Period	4.8 - 10 s	WIS Hindcast Database (USACE 2010)

The classical interpretation of the inlet morphology based on the coastal classification of Hayes (1979) and Davis and Hayes (1984) is a mixed-energy straight morphology. This is indicative of relatively comparable forcing from both tides and waves where the inlet falls along a coastline that is nearly mesotidal and has a moderate wave exposure (Kana et al. 1999). This combination of energy results in spatial sediment transport patterns that

are not entirely tidal- or wave-driven, but rather are dominated by one forcing or the other spatially. Sediment bypassing at this inlet has been stable but partially influenced by significant episodic events such as the relocation of the inlet in 1940. Fitzgerald's (1988) classification of St. Augustine Inlet would fall under Stable Inlet Processes. More specific to the forcing, the updrift, northern portion of the inlet experiences greater wave forcing and operates as a wave-dominated shoal; whereas the northern flood marginal channel and southern shoal complex are greatly influenced by flood tidal currents.

Sediments alongshore and within much of the estuary primarily consist of sand-sized particles, and will be referred to as sand throughout this report. Some finer organic particles exist within the tidal creek estuary behind the barrier islands, but these sediments are not considered to be active in the sediment transport pathways of the nearshore and inlet system. The sand is a mixture of feldspar, carbonate shell hash, and primarily quartz. The carbonate shell hash and quartz make up the majority of sand concentration, and vary greatly in distribution alongshore. Carbonate shell hash along the study area is greatest in concentration along the northern Ponte Vedra and Vilano beaches, is small across the inlet ebb-tidal delta, and is lower in concentration but varies along the southern beaches of St. Augustine Beach and Crescent Beach. Figure 2 illustrates the mean grain size distribution across the beach and nearshore for 8 profiles along the South Ponte Vedra and Vilano beaches. Table 2 (from PBS&J 2009) describes the sediment characteristics and statistics of grain size distribution. Sand transport in the region is described extensively in Report 1 (Legault et al. 2012).

1.2 The coastal modeling system: description and justification

The CMS is a product of the Coastal Inlets Research Program (CIRP – http://cirp.usace.army.mil) conducted at the U.S. Army Engineer Research and Development Center and is composed of two coupled models, CMS-Flow (Buttolph et al. 2006; Wu et al. 2010) and CMS-Wave (Lin et al. 2008). Numerous other publications on the CMS are posted on the CIRP web site, which also maintains a Wiki for user interaction. CMS-Flow is a finite-volume, depth-averaged model that can calculate water surface elevation, flow velocity, sediment transport (Camenen and Larson 2007), and morphology change. In the Coastal Modeling System, CMS-Flow is coupled with CMS-Wave, which calculates spectral wave propagation including refraction, diffraction, reflection, shoaling, and breaking, and also provides wave information for the sediment transport formulas (Figure 3). CMS-Flow can

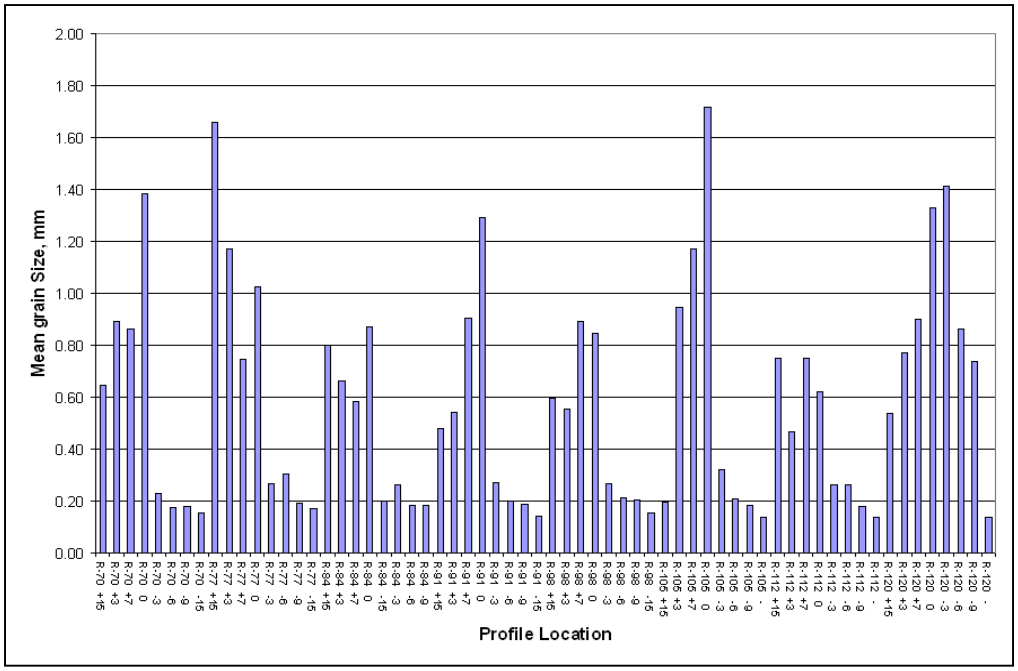

Figure 2. Mean grain size of eight cross-shore beach and nearshore locations from eight profiles along the South Ponte Vedra (north of Vilano) and Vilano beaches. Profiles are organized from north (left) to south (right) in the figure, where positive is landward and negative is oceanward.

Table 2. Maximum and minimum grain size statistics for South Ponte Vedre and Vilano Beaches (from PBS&J 2009).

Sample	USCS Class	Mean (mm)	Stand. Dev.	Skewness	Kurtosis	% Carbonate
Min	SP	0.14	0.78	-3.86	1.61	5
Max	SW	1.72	2.86	0.93	21.15	76
Average	SW-SP	0.55	1.22	-0.99	5.74	38

be driven by an ocean tide, as done here, by waves, and by wind forcing. This model was chosen for this study because of its capability to reproduce nearshore sediment dynamics at tidal inlets. A recent tidal inlet application of the CMS is found in Beck and Kraus (2010), also posted on the CIRP web site. The use of the CMS to accurately calculate sediment transport and morphologic evolution at inlets is advantageous over other morphological models because the CMS was specifically developed to represent inlet processes. A 2D model was used because vertical mixing and density stratification are not significant processes at St. Augustine Inlet. There is little freshwater input to the bay system of St. Augustine Inlet, and therefore, there are negligible salinity and density gradients. Wind shear is also neglected because the bay system is narrow, limiting the available fetch for wind forcing to play a major role.

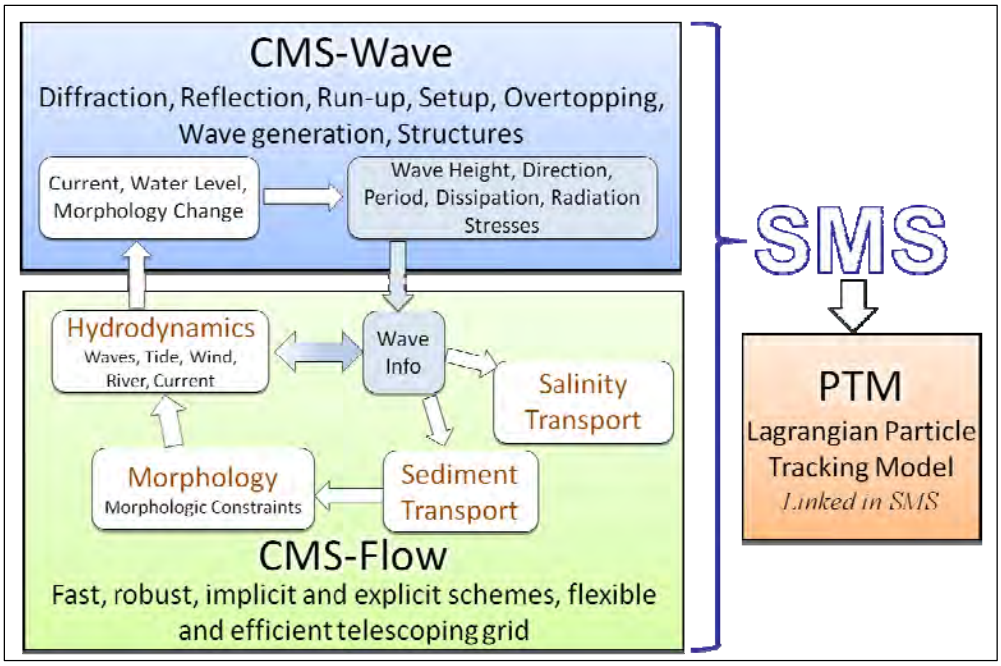

Figure 3. CMS framework and its components.

The CMS was selected because it is well suited to represent the physical processes controlling transport and morphology and can simulate some of the potentially large impacts. Significant changes in the depth and planform extent of the ebb-tidal delta could results in a realignment of the shoreline to such a degree that beach erosion would threaten upland infrastructure. Additionally, large-scale changes of the ebb-tidal delta bathymetry would interfere with gross transport to adjacent beaches or wave refraction patterns; therefore, the CMS was selected to examine changes in morphology of the ebb-tidal delta at St. Augustine Inlet.

Modeling outputs from CMS were applied to determine: 1) changes to the wave climate and response of inlet morphology as a function of mining of the ebb-tidal delta, 2) changes to the inlet planform morphology under long-term evolution of the mined ebb-tidal delta, 3) changes in sediment transport fluxes between control volumes and sediment reservoirs that connect the beach to the ebb-tidal delta through sediment transport pathways.

2 Model Setup

2.1 Hydrodynamic field data collection

Field measurements of water levels and currents were made at St. Augustine Inlet, St. Johns County, FL, in 2010 for validation of hydrodynamics calculated by the CMS. The field data collection plan was established to measure: a) the water level for confirming the ocean forcing boundary condition of the CMS; b) the current and water level in the two main channels in the Tolomato-Matanzas Bay system at Vilano Beach Pier and the St. Augustine Municipal Marina; and c) the vertical profile of the horizontal current across the ebb-tidal delta, across the inlet entrance, and along the Tolomato River and the Matanzas River.

The field campaign began 7 April 2010 and concluded 9 April 2010, took place over approximately 60 hours, and included instrument deployment, vertical profiling of the current, and instrument retrieval. On 7 April, three instruments were deployed beginning with the two horizontal current meters equipped with water level (pressure) gauges, followed by placement of the ocean-side water level gauge. Figure 4 shows the location of the three fixed instrument suites. Measured ocean water level is a main driver of the circulation during typical weather conditions, and CMS-computed water level and current can be compared with measurements within the modeling domain. The two fixed current meters, located within 1-2 km of the inlet entrance channel, each covered 50-70 m across the deepest part of the Tolomato River and Matanzas River. This horizontal current profiling provided time series measurements for comparison to the calculated current velocity in the CMS circulation model. A vessel mounted vertical current profiler was used to measure the structure of both the ebb and flood current field (item c) by sailing transects along reaches of the two rivers, through the inlet entrance channel, and over the ebb-tidal delta. These are used for further validation of the spatial distribution of current velocity.

The current meters deployed for the fixed horizontal profiles were RD Instrument (RDI) Acoustic Doppler Current Profiler (H-ADCP) Channel Masters with a 600 kHz frequency. This frequency gives a theoretical range of about 130 m from the sensor if there are sufficient depth and adequate particulate matter in the water to reflect the acoustic transmission back to the sensors. Current measurements were set to 1-min averages made every

Figure 4. Location map for fixed water level and velocity measurement gages.

15 min. The profile setup was established to collect data from a blanking distance of 1.7 m to 129 m in 128 1-m bins. These instruments were placed at mid-water depth at location and measured water levels, but were not tied to a vertical datum.

The first H-ADCP was deployed and became operational at 16:44 Coordinated Universal Time (UTC) on 7 April at the St. Augustine Municipal Marina, located directly south of the Bridge of Lions. The position of the gauge was at 29° 53.540' latitude and 81° 18.509' longitude (NAD83). The orientation of the horizontal beams had an azimuth of 94°. This gauge was retrieved at 12:44 UTC on 9 April for data collection of 44 hr. The second H-ADCP was deployed and operational at 20:41 UTC on 7 April at the Vilano Beach Pier, located directly south of the Vilano Beach Bridge. The position of the gauge was at 29° 55.000' latitude and 81° 18.005' longitude (NAD83). The orientation of the horizontal beams had an azimuth of 215°. This gauge was retrieved at 11:56 UTC on 9 April for data collection of 39 hr, 45 min.

The ocean side water level gauge collected 39.5 hr of data from 23:45 on 7 April 2010 to 15:15 on 9 April 2010. The pressure gauge, vented to the atmosphere, was installed at a NOAA station (St. Augustine Beach; 8720587) in the standardized housing available there for filtering short

period waves. Measurements were made every 15 min as an average over 1 min. The water level gauge was leveled to the local datum provided by benchmark D 322 1970 and set to mean sea level (MSL) for the local datum from the NOAA station (St. Augustine Beach; 8720587).

A 1,200 kHz acoustic Doppler current meter (D-ADCP) RDI Channel Master was used for the roaming, spatial coverage. Higher frequency allows smaller bins to be specified with greater reliability. Sampling through the vertical profile (vertical binning) was done every 0.25 m, and the frequency was adjusted in accordance with the range of depths to 18-m water depth. Vertical current profiling ran from 12:50 UTC (08:50 Local Standard Time - LST) to 21:00 UTC (17:00 LST) on 8 April 2010. Measurements began within the bay during the ebb-tidal cycle and consisted of transects across the ebb-tidal delta to cover the ebb jet and across the inlet throat. Slack tide occurred approximately between 14:30 and 16:30 UTC. The remainder of the measurements took place during the flood-tidal cycle from 16:30 to 21:00 UTC. Flood current was measured up both reaches of the bay (Tolomato River and Matanzas River), along four transects across the inlet throat, and in bay area adjacent to the inlet throat. The Vilano Beach Pier gage lost both water level and velocity measurement functions on the first day of deployment, and therefore was not usable for the calibration. Calibration to velocity does not rely on these horizontal measurements, and are not detailed in this report.

Measured water level is plotted in Figure 5 against the prediction for the St. Augustine Beach based on NOAA tidal constituents because NOAA no longer acquires water level data in the area. The comparison illustrates that there is little variation in minima and maxima and close correlation in phase. Measured and predicted values are plotted in Figure 6 and indicate close correlation in magnitude. The only notable departure is during the falling tide, where the measurements show a slightly greater decrease in level than the predicted tide. At every change in tide (six hours), the water level varies near zero because the measured level tends to rise and fall faster than the predicted level. Figure 7 gives the water levels for the study period for both H-ADCP locations, plotted about their record means.

Vertical current profile measurements were made over a flood and an ebb tidal cycle. The measurements were taken with consideration of boat location with respect to inlet morphologic features and the timing of the tidal cycle in an attempt to capture stronger current velocity near the inlet throat

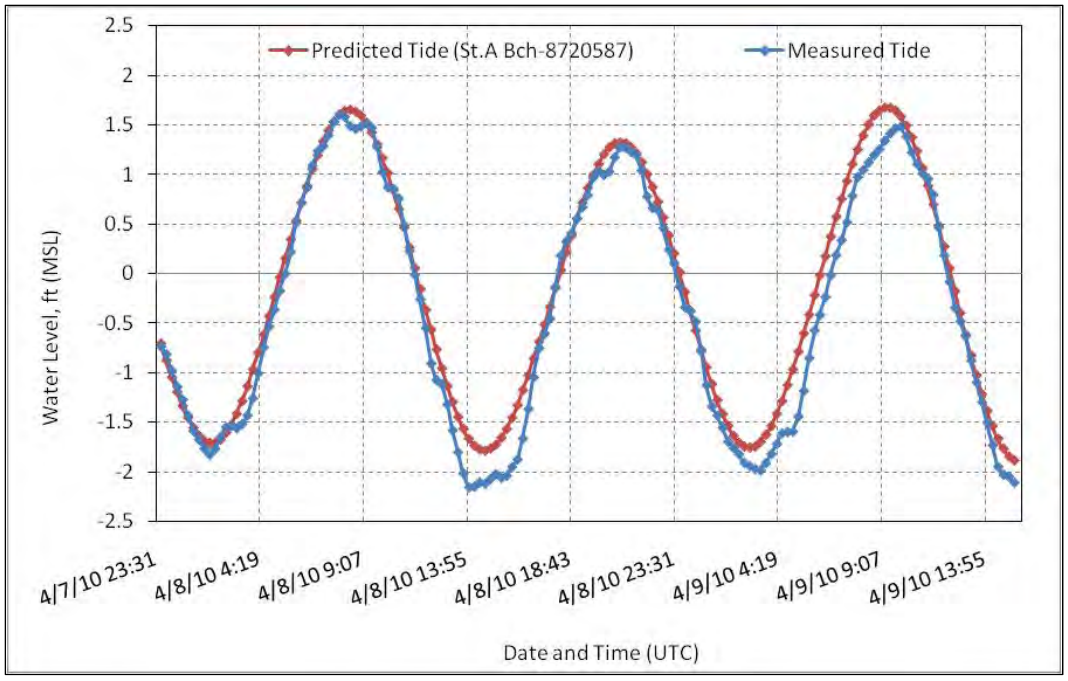

Figure 5. Measured and predicted water levels, St. Augustine Beach Pier, NOAA station 8720587.

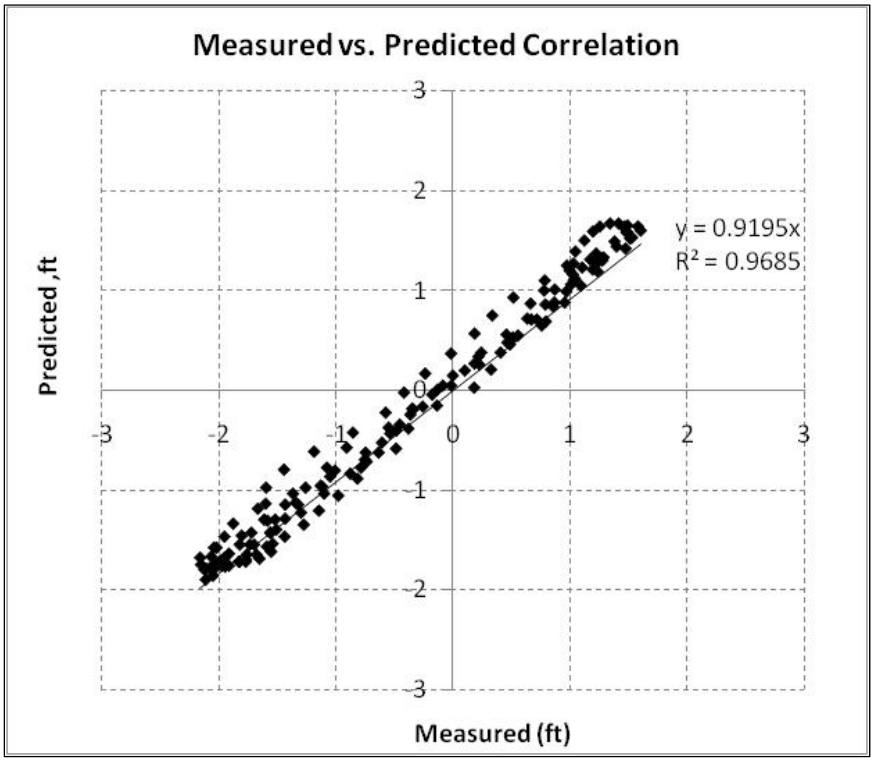

Figure 6. Correlation of measured vs. predicted water levels; Note $R^2 = 0.9685$.

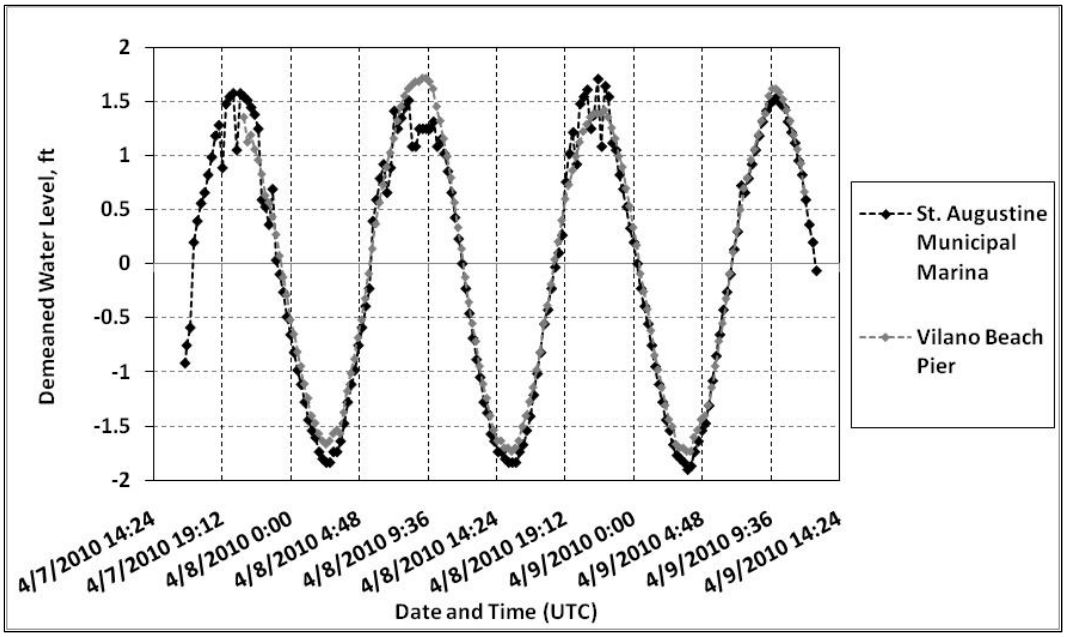

Figure 7. Measured water levels at both H-ADCP stations, St. Augustine Municipal Marina and the Vilano Beach Pier.

and general spatial characteristics of the bay system. Figures 8 through 12 illustrate snapshots of several transects that were grouped by a portion of the tidal cycle and depict velocity from a timeframe less than 1 hr. Figures 8 and 9 are of the ebb tide and illustrate the ebb jet exiting over the main navigation channel as well as peak ebb velocity through the inlet throat. Figure 10 shows the four transects across the inlet throat during flood tide. Two spatially extensive transects were collected during the flood tide (shown in Figures 11 and 12) to capture the maximum velocities in the Tolomato River and the Matanzas River.

2.2 Wave characteristics

Wave data from an extensive and detailed hindcast study, the Florida Coastal Forcing Project (FCFP), were supplied to CMS-Wave. Dally and Leadon (2003) and Leadon et al. (2009) developed a hindcast database of waves by modeling 30 years of wave transformation from a local offshore buoy data (NOAA), modeled hindcast winds, and a suite of wave gages offshore of St. Johns County. The spectral output of a centrally located observation point offshore of the inlet (Figure 13) was chosen as representative of the nearshore waves for the CMS grid and was used to force the CMS-Wave model boundary. The wave hindcast station lies along the wave grid boundary at 15-m water depth directly offshore of the inlet (offshore of R-monument 123), outside of the influence of nearshore perturbations such

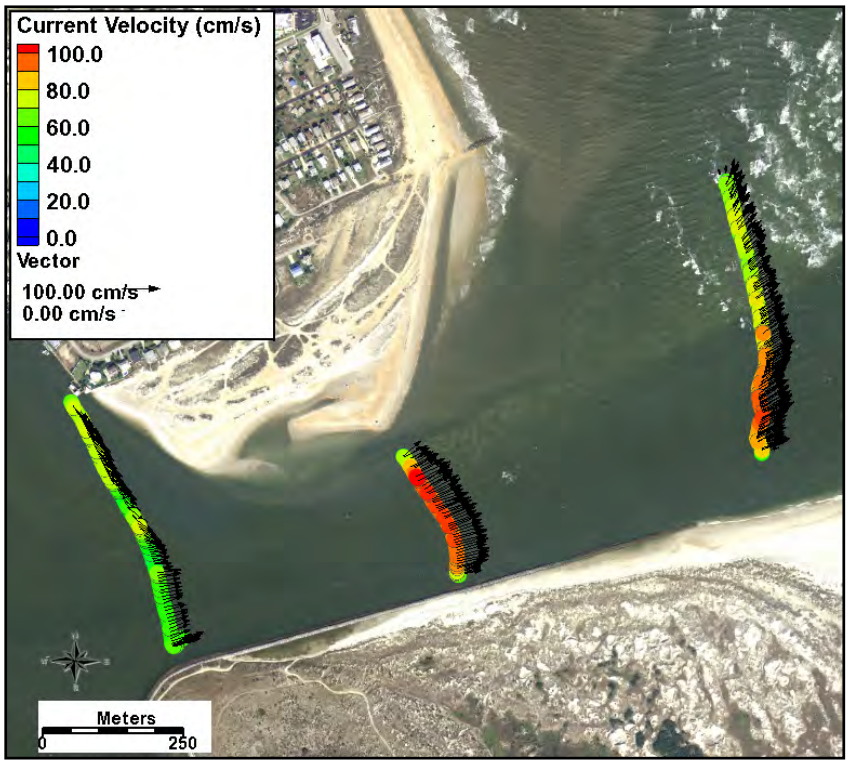

Figure 8. Depth-averaged ebb velocity across the inlet throat. These profiles were collected over the course of ~20 minutes.

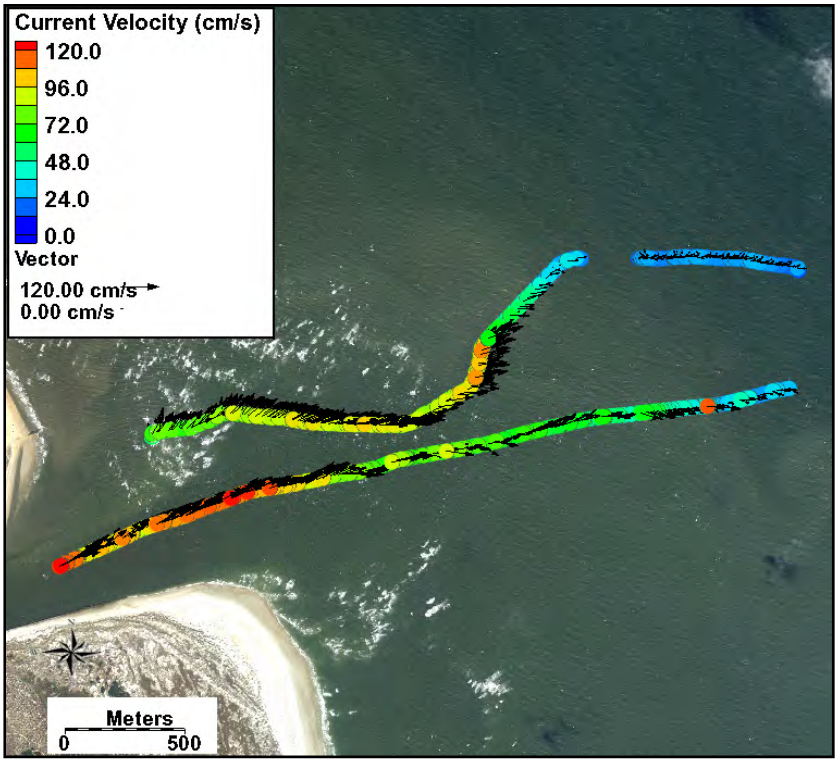

Figure 9. Depth-averaged velocity over the ebb-tidal delta toward the end of the ebb stage. These profiles were collected over the course of ~30 minutes.

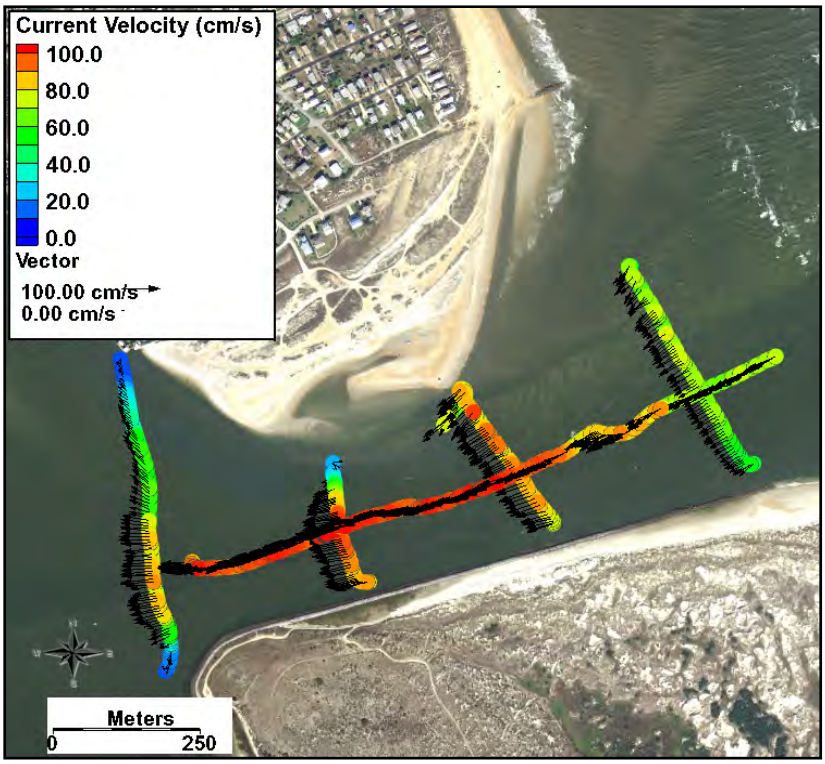

Figure 10. Depth-averaged flood velocity across the inlet throat. These profiles were collected over the course of ~40 minutes.

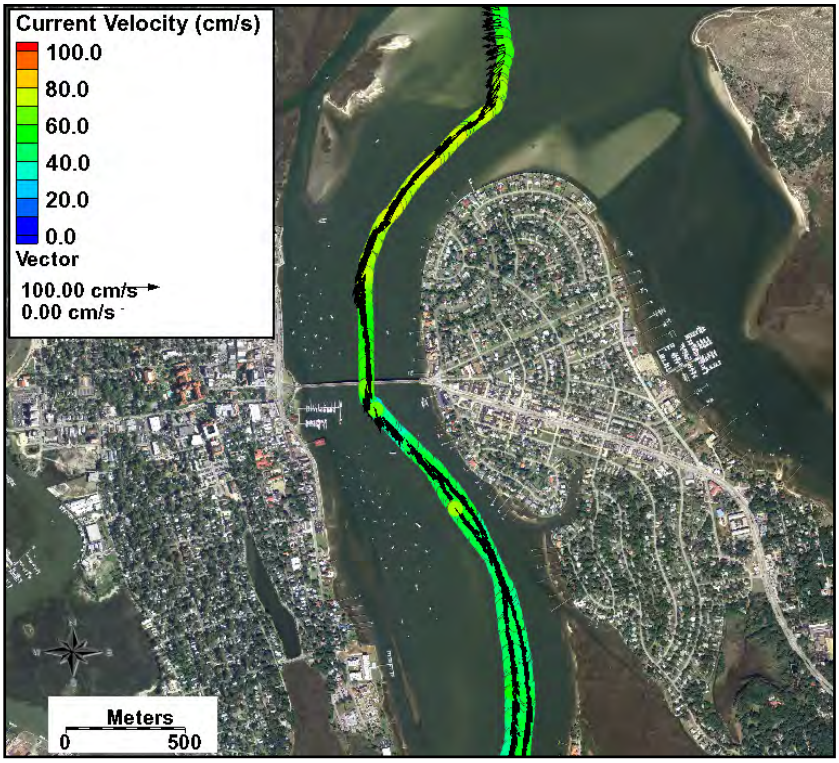

Figure 11. Depth-averaged flood velocity on a central transect along the Matanzas River. These profiles were collected over the course of ~45 minutes.

Figure 12. Depth-averaged flood velocity on a central transect along the Tolomato River. These profiles were collected over the course of ~30 minutes.

as the ebb-tidal delta. Due to numerous shore-oblique shoals existent along this stretch of coast, a centrally located wave station (82, 448) was preferable. The 2003-2005 calibration period used the spectral waves for the exact dates between June 2003 and November 2004 (1.4 years), and these spectral waves were applied to the alternatives modeled in this study.

A summary of the waves is given in rose plots for the significant wave height and peak period of the spectral waves. Figure 14 illustrates that the highest percent occurrence of waves are less than 1 m high and occur in the East-Southeast quadrant (110-135 degrees), and that less common larger waves approach the coast from the Northeast and East. Figure 15 illustrates a similar focus of energy in that there are calmer waves with short wave periods out of the Southeast, and longer swell-type waves approaching from the East (77. 5-107.5).

2.3 Bathymetry and shoreline

The model domain for the CMS covered a local scale of approximately 24 km centrally located around St. Augustine Inlet, FL. Bathymetry representing the bay, entrance channel, and ocean were assembled from

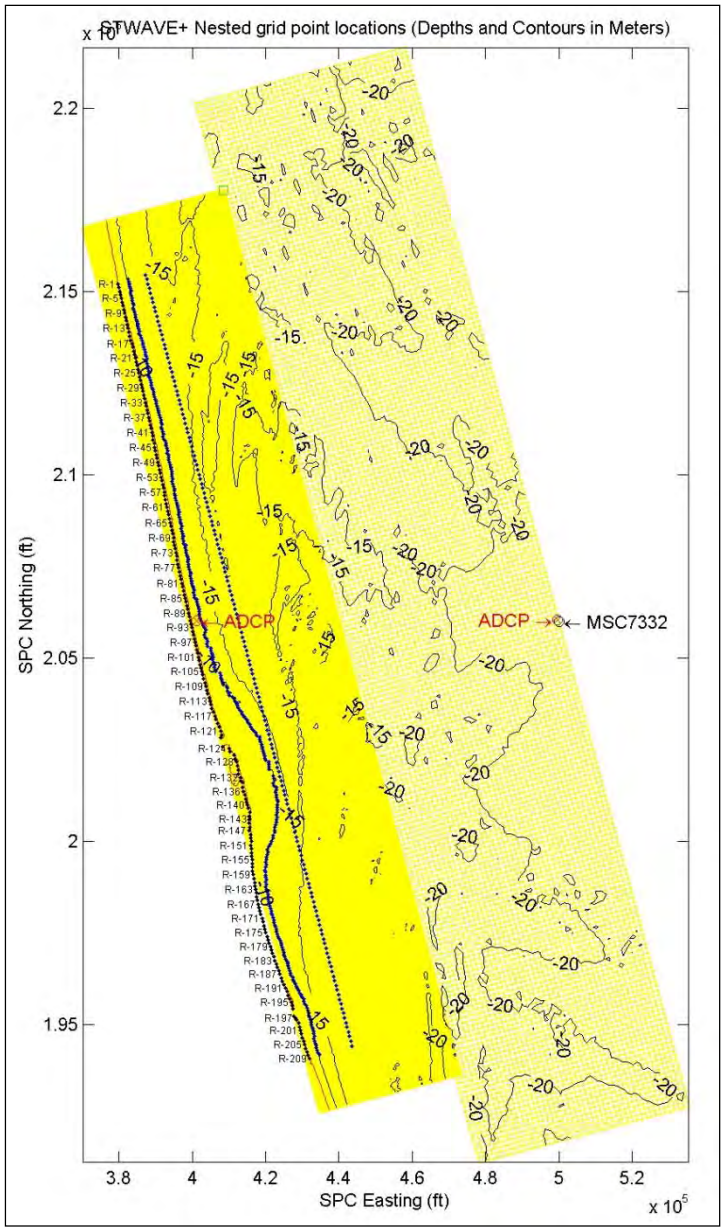

Figure 13. Study area map from the Leadon et al. (2009) report on hindcast waves for St. Johns County. Beach profiles (R-Monuments) are listed along the shoreface (black dots), and the light and dark blue dots represent the offshore and nearshore observation output points. The observation point chosen for the CMS grid is indicated in Red.

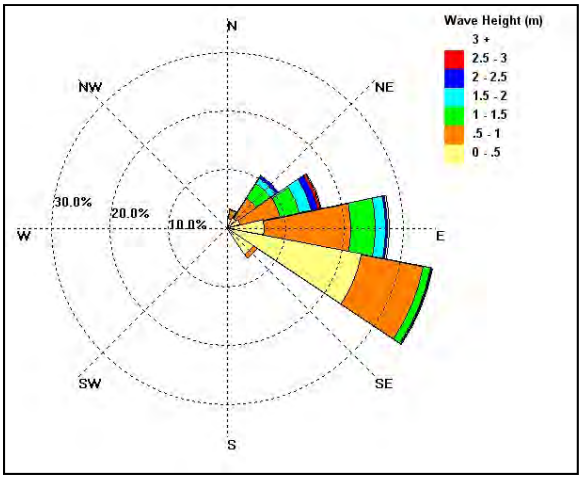

Figure 14. Rose diagram of the hindcast significant wave heights for the 2003-2005 time period.

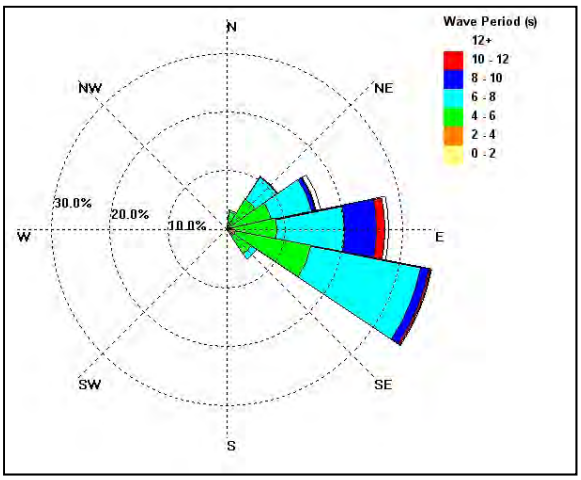

Figure 15. Rose diagram of the hindcast peak wave periods for the 2003-2005 time period.

several datasets. Bay bathymetry consisted of data collected for the AIWW (Atlantic Intracoastal Waterway), USACE entrance channel surveys, and 2004 lidar (JALBTCX 2006) for the wetlands. Nearshore and ocean bathymetric datasets were a combination of 2004 lidar (JALBTCX 2006), 2003 beach profile surveys covering the shoreline (from USACE Jacksonville District), 2003 nearshore bathymetry surveys of the ebb-tidal delta and offshore features and offshore surveys collected by the National Ocean Service (NOAA 2010b). The historical beach profile data for St. Johns County (R-1 to R-209) were collected from the Florida Department of Environmental Protection (FDEP) and analysis is provided in the first Report (Legault et al. 2012). Profiles were in FDEP format and referenced to Florida East State Plane (FIPS 0901) coordinates and the NAVD88 vertical datum. Both horizontal coordinates and vertical elevations were specified

in ft. Full data sets were available for the years 1972, 1984, 1986, 1999, 2003 and 2007; partial data sets were available for 2005 and 2006. The reader is referred to "Influence of St. Augustine Ebb-tidal delta Excavation on Near-shore Wave Climate and Sediment Pathways, St. Johns County, Florida" (USACE 2009) for bathymetric development.

The horizontal datums of all 2003 datasets were in the Florida East State Plane coordinate system. Data collected by the Jacksonville District were in the North American Datum 1927 and in feet and included beach profiles, the bathymetry for the ebb-tidal delta, and the St. Augustine Inlet federal navigation channel. The vertical datum was mean low water and in feet. The horizontal datum of the AIWW surveys from 2000 (the most recent survey), also measured by the Jacksonville District, was in geographic coordinates (NAD83), and had a vertical datum of mean low water in meters. The 2004 lidar survey was originally in the Florida East State Plane coordinate system in the NAD83 horizontal datum in feet; the vertical datum was NAVD88 in metric (JALBTCX 2006). All NOS (NOAA 2010b) offshore data were originally in geographic coordinates (NAD83) and had a vertical datum of mean low water in feet. These data were converted to the same horizontal and vertical datums used in the model through software provided by the Surface-water Modeling System, through which the CMS is operated. The final horizontal datum for all bathymetry was Florida East State Plane (NAD83) in meters, and the vertical datum was converted to mean sea level in meters, as given by the local tidal datum for St. Augustine Beach Pier, FL (NOAA 2010a).

2.4 Sediment and bottom friction characteristics

Other spatially variable features or parameters included in the CMS-Flow grid were variable median sediment grain size D50 for sediment and Manning's n for representing bottom friction. Spatially variable sediment grain sizes were incorporated in the CMS where data existed over the beach, nearshore, and ebb-tidal delta. Sediment grain-size data presented in a study by PBS&J (2009) were used as a baseline to delineate the general D50 values. Though no record exists of sediment grain sizes for the inlet throat, discussions with Jacksonville District geologists confirm that the channel thalweg is armored with large shell fragments, which is typical of Florida tidal inlets. PBS&J (2009) analyzed beach sediment from St. Johns County, FL and found that grain sizes are generally finest at depths greater than 2.7 to 4.6 m and coarsest at the shoreline.

Median sediment grain-size for the majority of the model domain was set to a constant value of 0.2 mm, representing the average sediment grain-size offshore. The inlet channel was represented with D50 values ranging from 0.2 to 10 mm (10 mm representing a shell lag for the channel thalweg). The updrift nearshore values ranged from 0.2 to 0.4 mm (from offshore to onshore) following PBS&J (2009). Finally, the ebb-tidal delta was set to the average mean grain size of 0.16 mm. CMS-Wave model parameters included a Darcy-Weisbach bottom friction value (*Cf*), which was set to the default spatially constant value of 0.005, a typical value applied in coastal inlet studies.

2.5 CMS model grid

Two CMS model grids were developed for representing St. Augustine Inlet, one for CMS-Wave and the other for CMS-Flow and sand transport. The inline version of CMS-Flow was applied in this study which contains CMS-Flow and CMS-Wave within a single code for model efficiency. The lateral extent of the CMS-Flow grid was determined through initial calibration of the hydrodynamics to resolve the appropriate bay boundaries for comparison to measured tidal prism. Additionally, the lateral extent of the model domain was defined to include several focus areas of shoreline to the north and south of the inlet. The cross-shore length of the CMS-Flow grid was set to the same location as the CMS-Wave grid, which was set to the offshore location of the contour depth of the forcing (or wave data). Therefore, the resultant two grids cover the same alongshore distance of 23.5 km and a cross-shore distance extending from the land seaward to the ocean boundary of 9 km. The finest resolution of the model grid cells were set to 15 m in the inlet throat, and 30 m in the main bay channels, ebb-tidal delta and nearshore. Maximum cells sizes in the bay reached 120 m over large open bay expanses, and to 240 m along the offshore boundary (Figure 16).

Each CMS grid was forced along the ocean boundary. CMS-Wave propagates spectral waves from the offshore ocean boundary toward land. The forcing in the CMS-Flow grid for this project was a water-surface elevation as defined by tidal constituent forcing for the full perimeter of the ocean boundary. The spatial extent of the bay area was selected to best represent the aerial-tidal prism for St. Augustine Inlet. Winds were not included because they do not generate significant currents or waves in the bay due to limited fetch. For CMS-Wave, wind stresses were already incorporated in the generation of the hindcast nearshore waves and therefore were not included in the offshore forcing of the wave model.

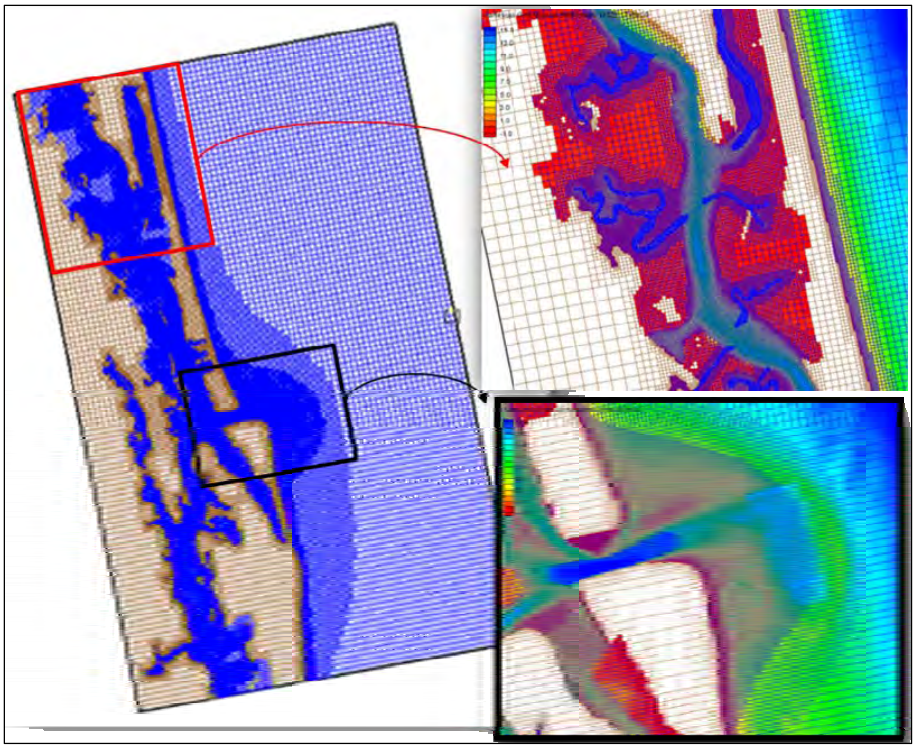

Figure 16. CMS-Flow grid for St. Augustine Inlet, FL (left), zoom-in of the northern part of the bay (top-right), and zoom-in of the entrance (bottom-right).

There is shared, or coupled, forcing that is generated in each model and subsequently passed between both models. Radiation stresses, including effects of wave shoaling and breaking, roller stresses, and water levels (with wave setup) are passed from CMS-Wave to CMS-Flow. CMS-Flow interpolates these input data from a present and future wave simulation over a certain time interval (or steering interval) and then calculates the hydrodynamics and sediment transport over that period utilizing the interpolated values. At the end of the steering interval, CMS-Flow passes water levels and current velocities back to the wave model for the next CMS-Wave simulation. Morphology is updated on a larger timescale, every 6 hours, to record updated bed topography.

Model forcing data includes hindcast waves (Dally and Leadon 2003; Leadon et al. 2009), and tidal constituent water level forcing. Calibration of the model to measured offshore water levels is described below. Tidal constituents force water levels at the offshore boundary of the grid. The vertical datums of the model grids were already set to mean sea level as defined by NOAA (see the Bathymetry and Shoreline section). The tidal constituents used were developed by NOAA for the present epoch (1983-2001; NOAA 2010a) for the St. Augustine Beach gauge (Station ID# 8720587).

3 Model Calibration

Calibration of the CMS for St. Augustine Inlet was completed in two parts: first, through comparison of measured and calculated hydrodynamics, and secondly through comparison of morphologic end-states. The hydrodynamics were calibrated through comparing measurements of water level and currents collected from 7-9 April 2010 to a simulation that was forced with the measured open ocean tide, located on the St. Augustine Beach Pier. The bathymetry used in the model grid was from the most recent bathymetry that had complete coverage, from 2008, and quality checked by both the Florida DEP and the Jacksonville District. The calculated water level variation and current velocity were forced initially by measured water levels to calibrate properly to measurements. Because there are no water level measurements in the region that span the timeframe of the 2003-2005 calibration period, tide constituent forcing was applied in the model runs. To compare the calibrated model (that used open ocean tides) to tidal constituents, the calibration period was rerun with non-astronomical forcing to validate that non-astronomical forcing was sufficient to capture the hydrodynamics of the area.

Measured morphology change from several ebb-tidal delta and navigation channel surveys were used in part in comparison with calculated morphology change. Empirically derived coefficients for sediment transport were modified to within the accepted range for calibration to sediment transport rates. Coefficient values can be increased to address the lack of transport initiated by other coastal processes not considered in this model such as swash zone processes, a known major contribution to sediment transport. Given this, the model results for sediment transport are largely dependent on the wave forcing, and therefore the calculated morphology change will be driven by the quality of wave input.

3.1 Calibration to hydrodynamics

Measured ocean water levels were used to drive CMS-Flow at the ocean boundary. Calculations of water level and current with the coupled CMS are compared here to measurements made within the modeled domain. The modeled time period from 7-9 April 2010 serves as the primary calibration period. Because there are no other available measurement periods, hydrodynamics are calibrated to two different measurement

datasets from the same period. The model run was set for a ramp period of 6 hr which is more than typically needed for implicit model runs. The hydrodynamic time step was 5 min, which was found to be sufficiently short enough to capture the tidal circulation within the bay. Table 3 summarizes the CMS-Flow setup parameters.

Table 3. CMS-Flow setup parameters for the St. Augustine Inlet field test case.

Parameter	Value
Solution scheme	Implicit
Simulation duration	2 days
Ramp period duration	6 hours
Time step	5 min
Manning's coefficient	0.025 – 0.06 $s/m^{1/3}$

Measurements from two current meters were part of the calibration to water level and currents. They were equipped with pressure gauges to measure water level and were deployed at fixed locations within 1-2 km of the inlet entrance channel and covered 50-70 m across the deepest part of the Tolomato River and the Matanzas River. Measured water levels were not correlated to a benchmark, and therefore can only be compared to model calculations with demeaned (averaged to represent a zero mean) water levels. The resultant horizontal current profiles provide temporal resolution for comparison to the calculated current velocity. Roaming vertical profiles of the ebb and flood current were also mapped across reaches of the two rivers, through the inlet entrance, and over the ebb-tidal delta and serve to spatially validate the distribution of current velocity. These profiles are compared to the modeled currents below in the Calibration to Currents section and serve as the primary calibration measurements because of the strong correlation between current velocities over the ebb-tidal delta and the resulting sediment transport as discussed in later sections.

The extent of the grid in the bay was determined by an iterative process to recreate the bay tidal prism. Because the bay system includes a secondary inlet to the south, Matanzas Inlet, there is some uncertainty involved in delineating the boundary for tidal prism between the two inlets. Calibration to both water levels and spatial current velocities was necessary to approximate this delineation of alongshore grid length, which was

ultimately selected as 23.5 km. Following this, further calibration of the bottom friction, or Manning's n, was applied to account for bridge piling locations and lag effects from the marsh and extensive lateral shape of the bay (Figure 17). This modification of Manning's n also addressed an over-prediction of flood currents in the inlet throat which significantly improved the initially predicted velocity magnitudes and phase spatially through the inlet throat (Figure 18).

The final adjustments made to the CMS grid and modeling parameters were completed during the calibration of hydrodynamics. Hardbottom, Manning's n, and D50 values are the only spatially variable parameters, and are collocated on the grid. Manning's n was modified along locations of bridges and over the inlet channel area. Other parameters included in the CMS were flooding and drying, eddy viscosity due to currents and wave breaking, and sediment transport and morphology parameters. Flooding and drying and eddy viscosity were set to default values; however, the eddy-viscosity model used was the mixing length scheme rather than other simplified formula.

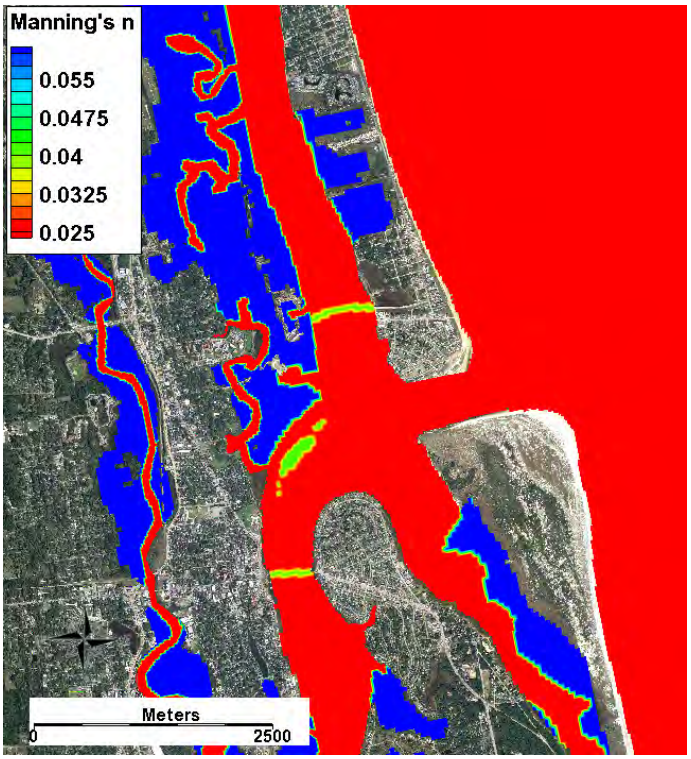

Figure 17. Variation of Manning's n in the back bay and river reaches of the CMS-Flow St. Augustine Inlet grid.

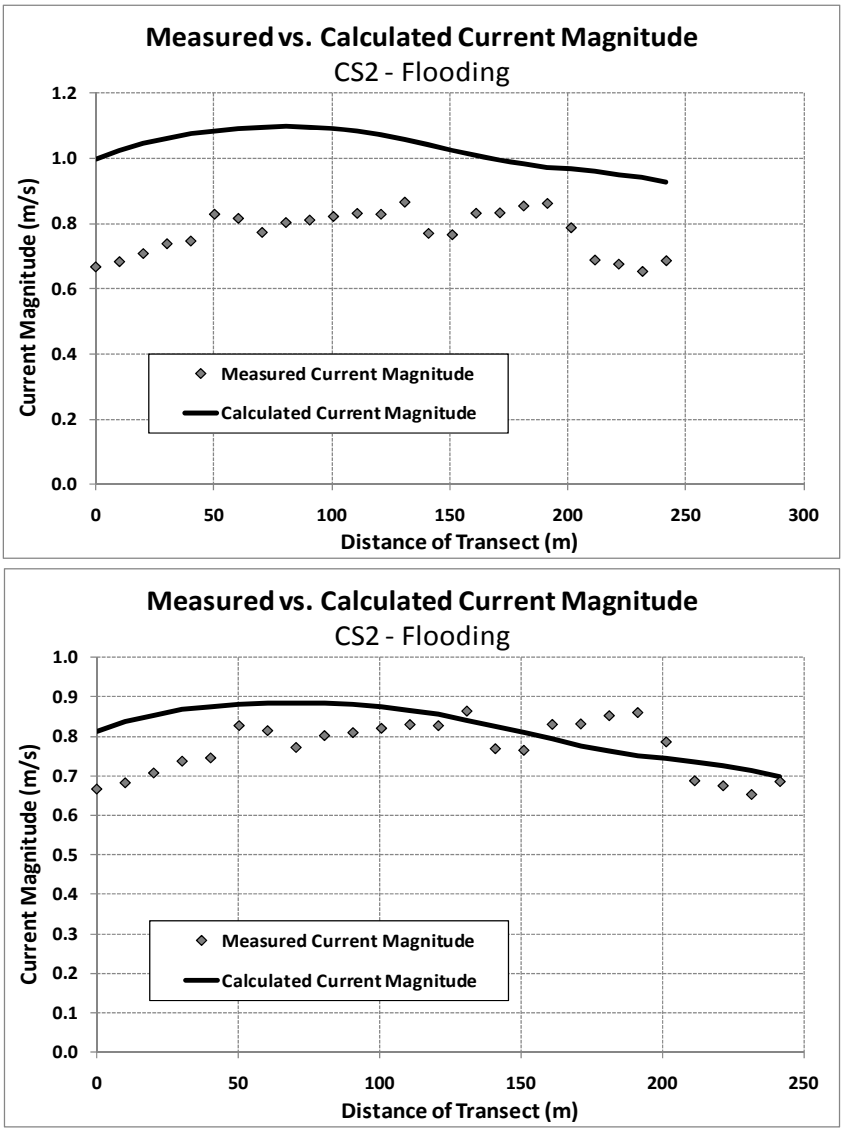

Figure 18. Comparison of measured current magnitudes before (top) and after (bottom) calibration of bottom friction. Figure 22 gives the location map.

3.1.1 Water levels

Water levels measured at the St. Augustine Municipal Marina and Vilano Beach Pier by the two H-ADCP gauges are illustrated as black and gray points, respectively, in Figure 21. Peak measurements at the St. Augustine Municipal Marina show inconsistency likely due to the proximal location to bridge-related construction and boat traffic. Other than these small fluctuations, water level measurements for the two-day measurement period had similar peaks and range in comparison to the offshore measurements which were used for the CMS forcing for initial calibration. Measurements from two current meters were also part of the calibration to water level and currents. They were equipped with pressure gauges to measure water level

and were deployed at fixed locations within 1-2 km of the inlet entrance channel and covered 50-70 m across the deepest part of the Tolomato River and the Matanzas River (Figure 4). Measured water levels were not correlated to a benchmark, and therefore can only be compared to model calculations with demeaned (averaged to represent a zero mean) water levels. The measured horizontal current profiles provided temporal resolution for comparison to the calculated current velocity.

Figures 19 and 20 show a comparison between the measured and calculated water levels at the two bay gauges. The correlation coefficient, or R2-values, between measurements and calculated are 0.82 for the St. Augustine Municipal Marina gauge, and 0.93 for the Vilano Beach Pier gauge. The measured demeaned water levels from each gauge location including the offshore gauge location are shown in Figure 21.

3.1.2 Currents

Hydrodynamics were further calibrated to current measurements collected by a boat-mounted, downward-looking acoustic Doppler current profiler (D-ADCP). The measurements compared here include depth-averaged currents across inlet throat cross-sections and several channel transects as illustrated in Figure 22. Measurements, including two ebb-shoal transects and three inlet throat cross-sections, were made at the end of an ebbing cycle. At the beginning of the flood cycle, transects were made over the northern Tolomato River and southern Matanzas River main channels. Four inlet throat cross-sections were made at or close to capturing peak flooding currents.

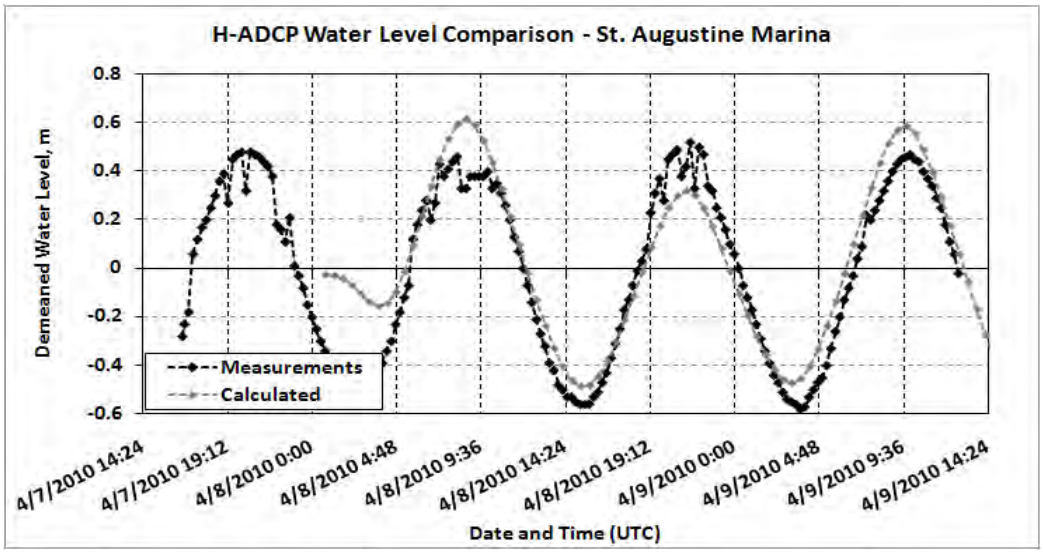

Figure 19. St. Augustine Municipal Marina measured water levels vs. calculated water levels.

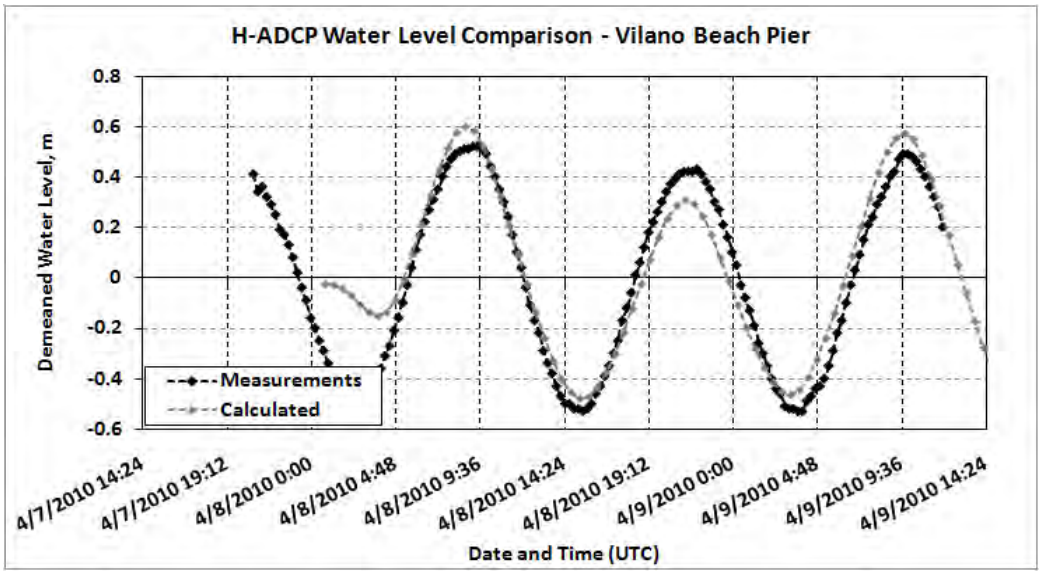

Figure 20. Vilano Beach Pier measured water levels vs. calculated water levels.

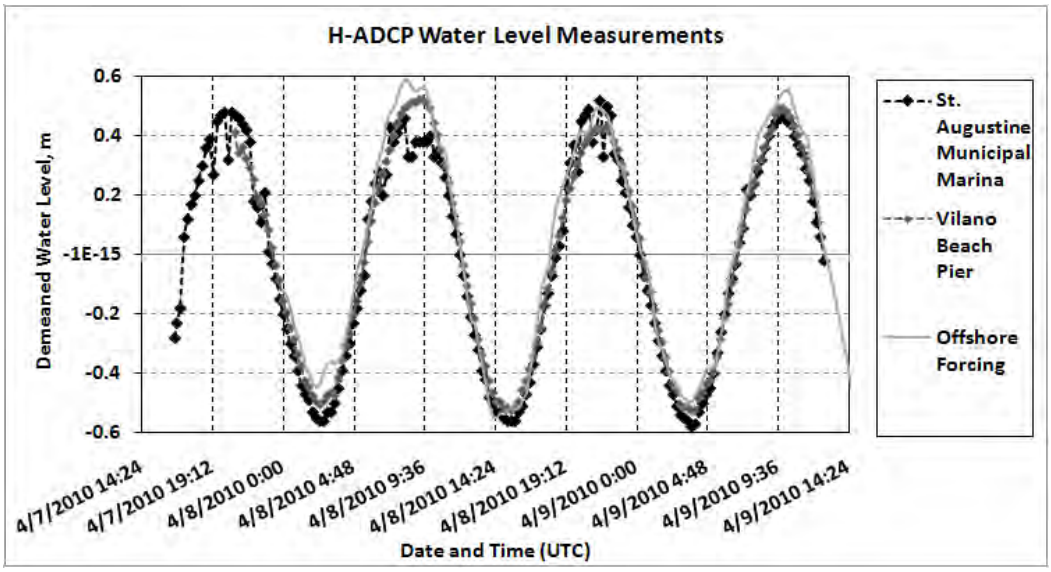

Figure 21. Measured demeaned bay water levels and measured offshore water level.

Comparisons of the measured, depth-averaged currents are given in Figures 23 to 25. Inlet throat cross-section measurements show good agreement with the calculated measurements, resulting in a Normalized Mean Average Error (NMAE) of 1- 12 percent for ebbing currents (Figures 23 to 27) and 4-8 percent for flooding currents (Figures 28 to 31). NMAE was calculated with the following formula.

$$NMAE = \frac{|x_m - x_c|}{max\, x_m - min\, x_m} \quad (1)$$

where x_m is measured values and x_c is calculated values.

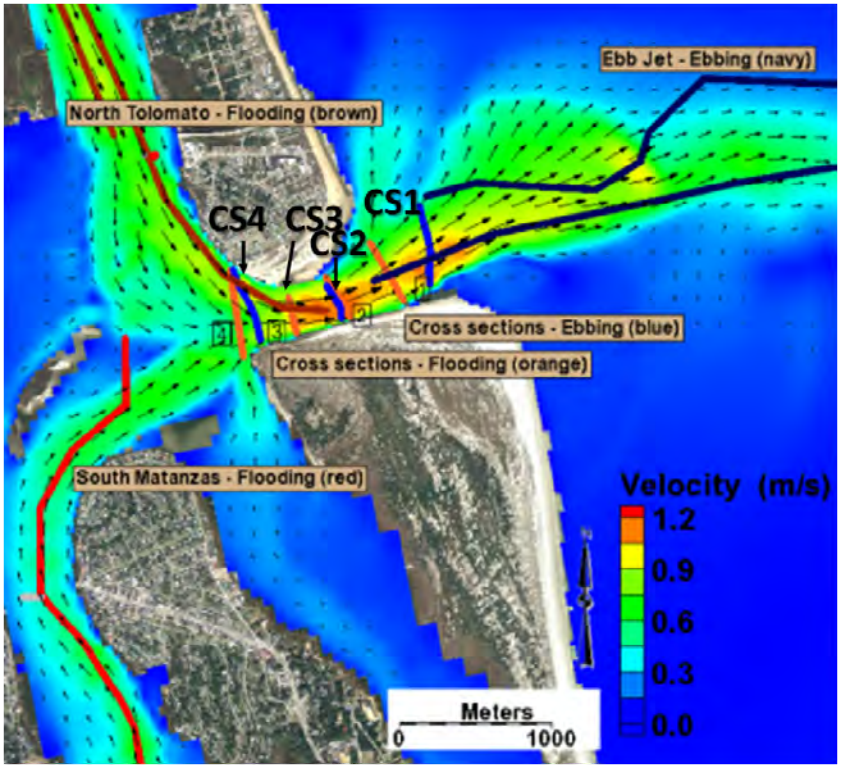

Figure 22. Location map of D-ADCP surveyed cross-sections and transects.

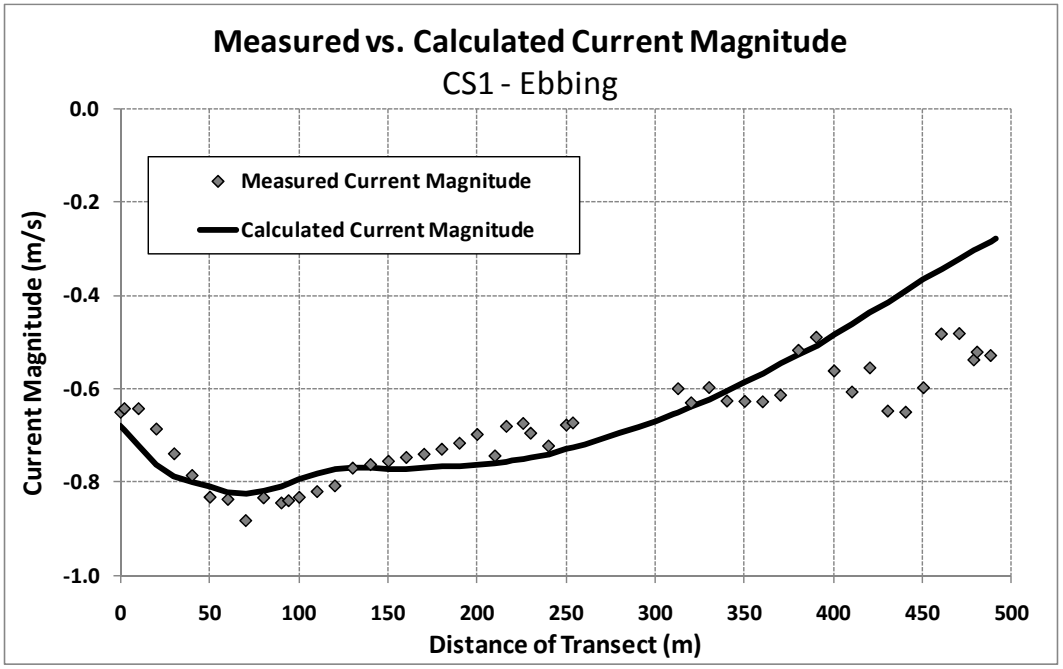

Figure 23. Measured vs. calculated current magnitude: Ebbing tide, CS1; Model time: 1440 hours; Measurement time: 1414 hours.

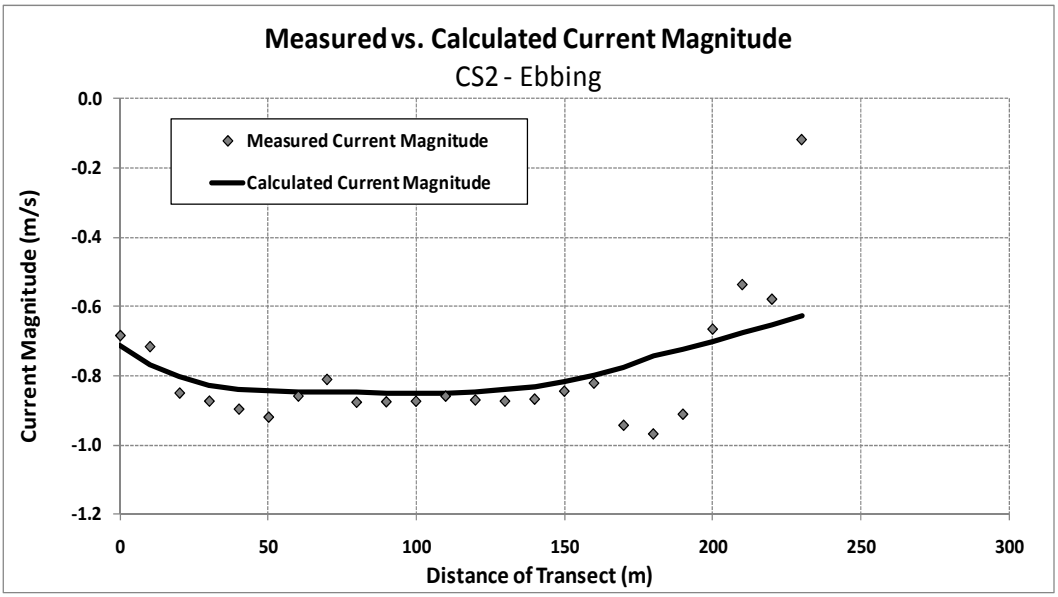

Figure 24. Measured vs. Calculated current magnitude: Ebbing tide, CS2; Model time: 1440 hours; Measurement time: 1404 hours.

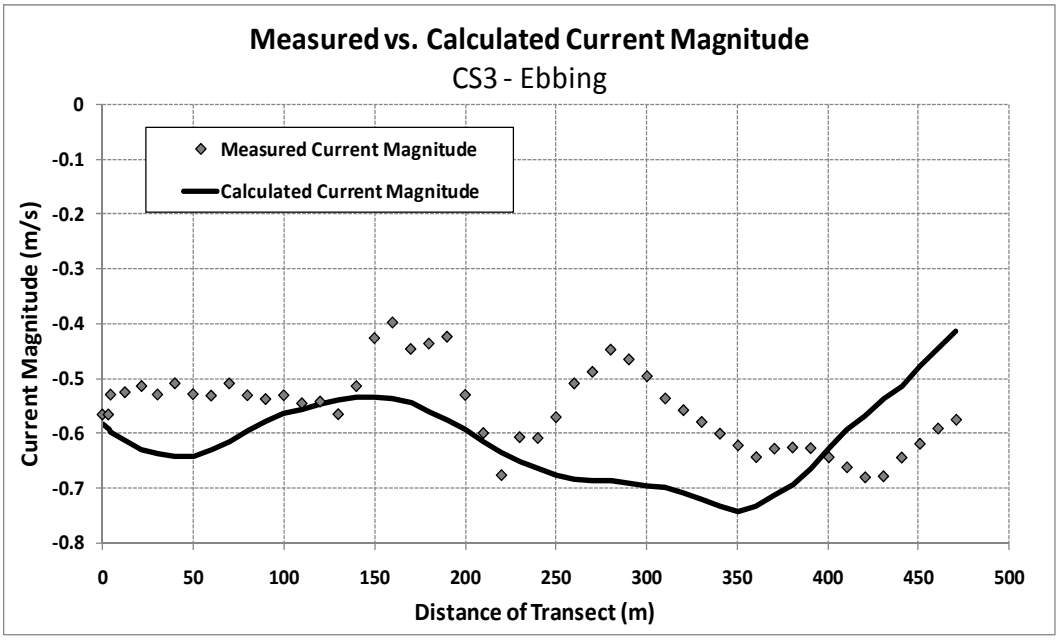

Figure 25. Measured vs. calculated current magnitude: Ebbing tide, CS3; Model time: 1440 hours; Measurement time: 1347 hours.

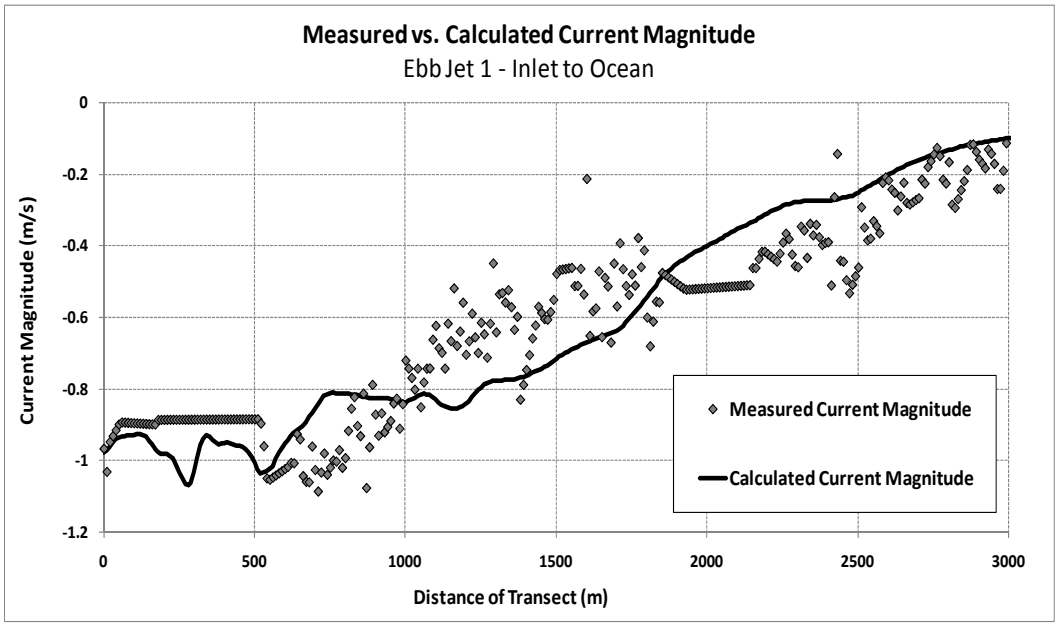

Figure 26. Measured vs. calculated current magnitude: Ebbing tide, Ebb jet 1; Model time: 1210 hours; Measurement time: 1248 hours.

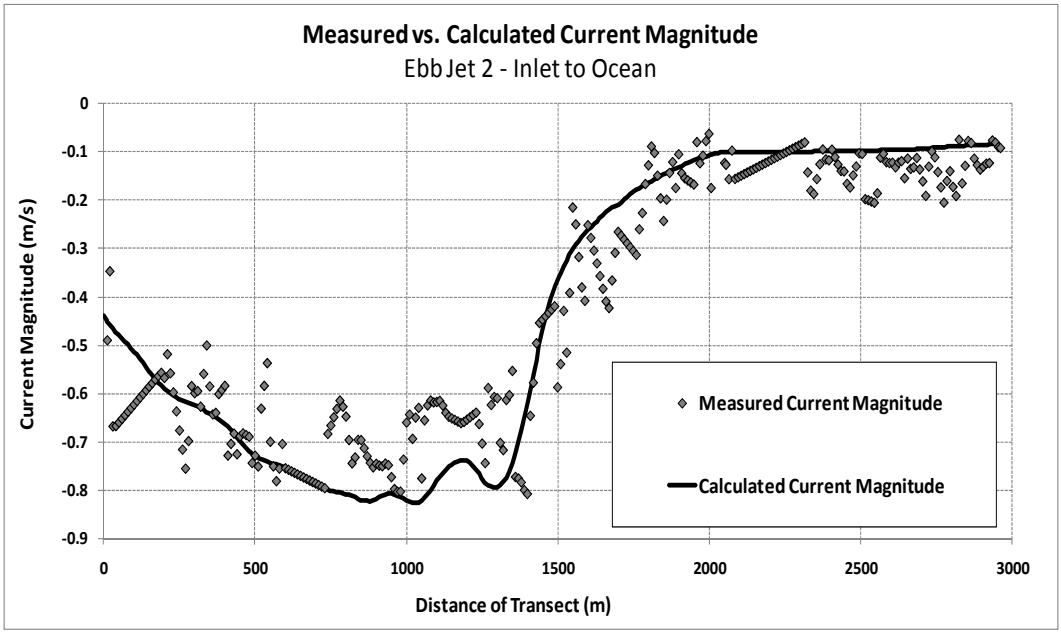

Figure 27. Measured vs. calculated current magnitude: Ebbing tide, Ebb jet 2; Model time: 1230 hours; Measurement time: 1312 hours.

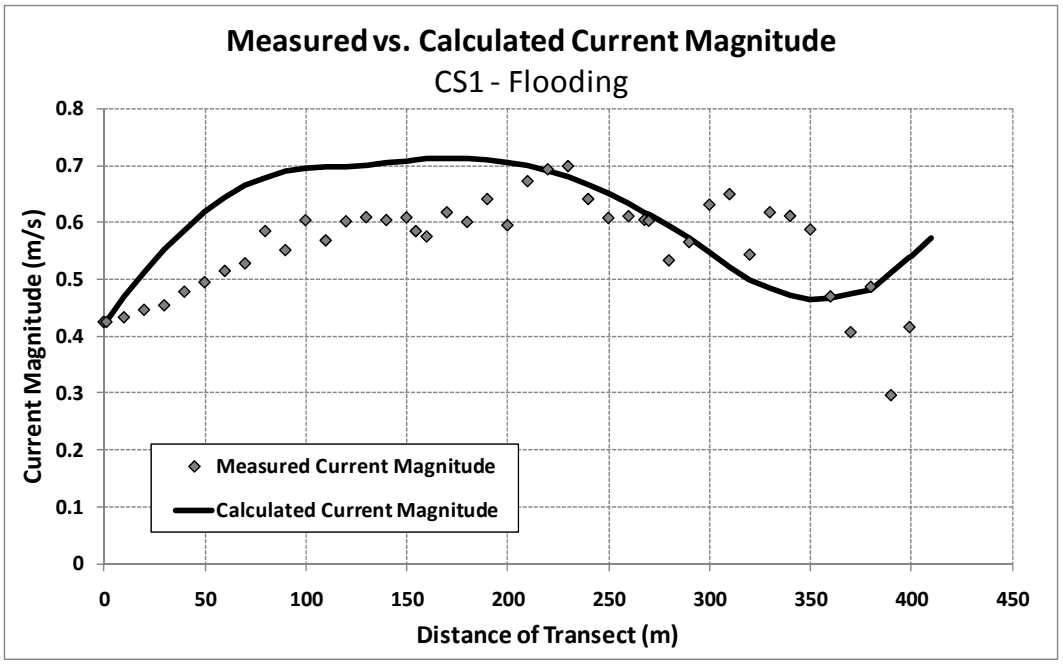

Figure 28. Measured vs. calculated current magnitude: Flooding tide, CS1; Model time: 2000 hours; Measurement time: 2018 hours.

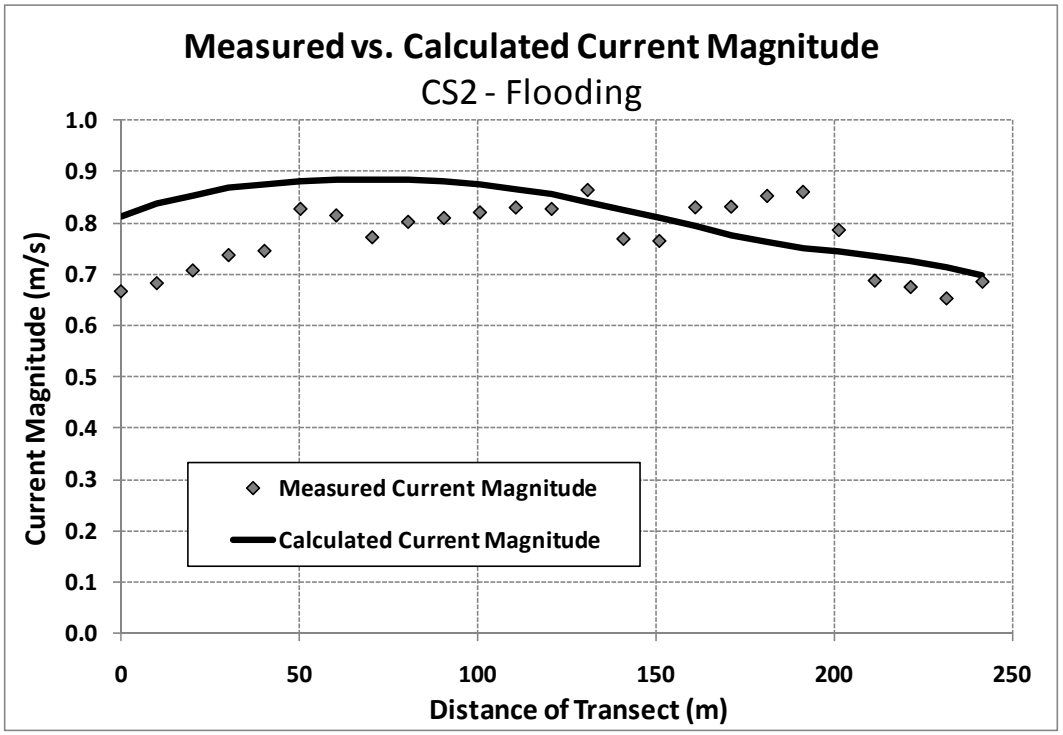

Figure 29. Measured vs. calculated current magnitude: Flooding tide, CS2; Model time: 2000 hours; Measurement time: 2026 hours.

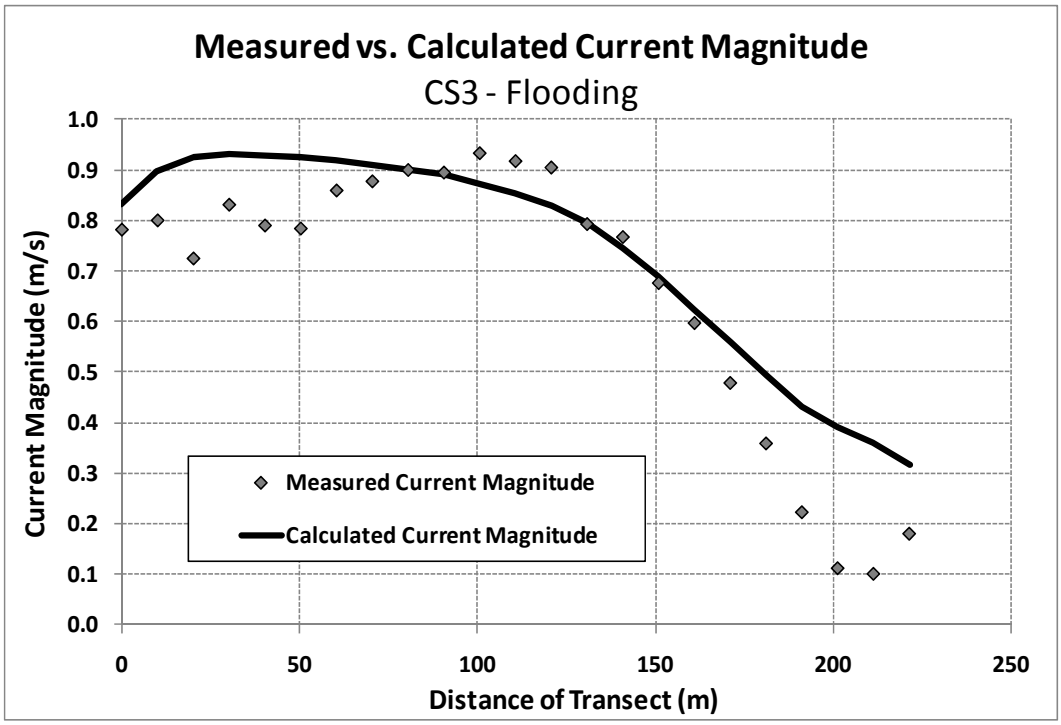

Figure 30. Measurd vs. calculated current magnitude: Flooding tide, CS3; Model time: 2000 hours; Measurement time: 2031 hours.

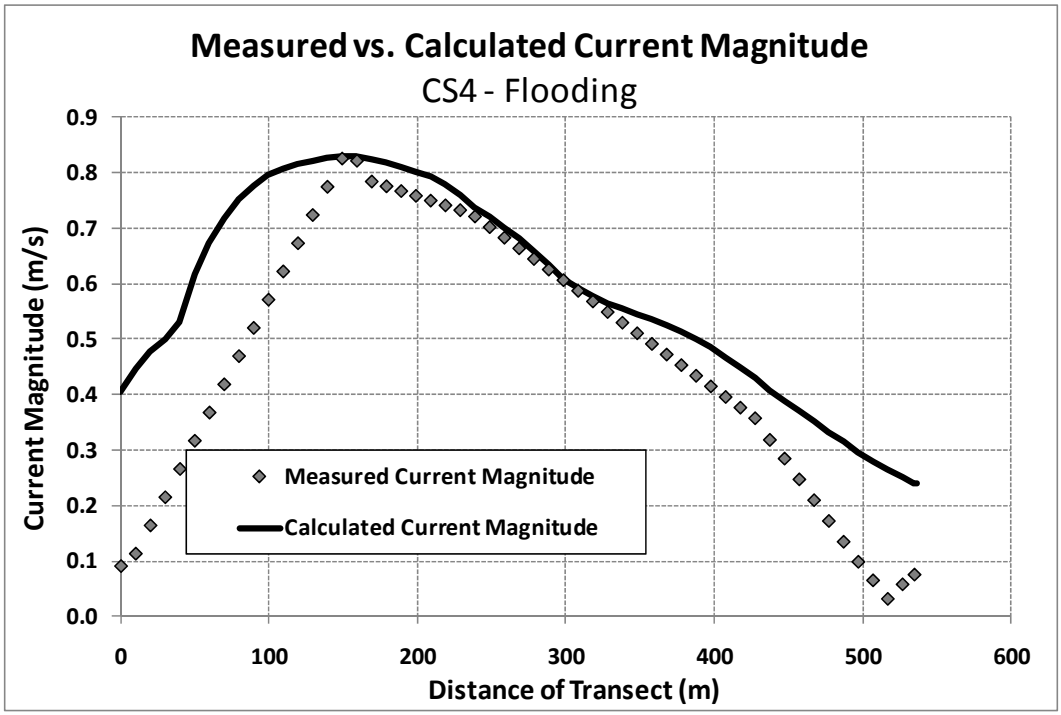

Figure 31. Measured vs. calculated current magnitude: Flooding tide, CS4; Model time: 2000 hours; Measurement time: 1954 hours.

A set of two transects over the ebb-tidal delta trace the main ebb jet through the channel and over the northern lobe of the shoal in Figures 26 and 27. The measured and calculated currents speeds have a NMAE of 8-18 percent. The velocity profiles show the strong currents near the inlet throat decreasing offshore over the distance of the ebb-tidal delta. Though the model calibration run did not include any wave-generated currents (due to a lack of wave data for the calibration period), it still predicted the ebb jet trends, which illustrate the dominance of tidal-driven flow over the ebb-tidal delta. The vertical profiles of ebb currents measured over the ebb-tidal delta with the vessel-mounted current profiler are an essential calibration dataset because of the strong correlation between current velocities over the ebb-tidal delta and the resulting tidal-driven sediment transport. In summary, the model is able to reproduce the current speed within 20 percent of measured values.

Figures 28 through 31 compare measured and calculated flood currents through the throat of the inlet. The model calculated accurate trends in both the magnitude and pattern of velocity. This is apparent in Figures 30 and 31 where the model captures the decrease in flooding velocity along the northern side of the channel where depths are shallowest adjacent to Vilano Beach.

The remaining model comparisons of transects within the bay recorded a flooding cycle that covered both the northern and southern stretches known locally as the Tolomato and Matanzas Rivers. Figures 32 and 33 are two transects stretching from the inlet throat to the north on North Tolomato (1) and south to the inlet throat on North Tolomato (2). Current velocities are largely close to measured magnitudes and within phase by less than 45 minutes. For the North Tolomato (1) transect (Figure 32), the magnitudes were over-predicted by approximately 20 percent, and slightly under-predicted near the section north of the Vilano Beach Bridge. The end of the North Tolomato 1 and beginning of the North Tolomato (2) transects are toward the far north reaches of the modeling domain. In the CMS, this boundary is considered a “no flow” walled boundary, and therefore an under-prediction of current velocity at these far reaches is acceptable. All other sections of the modeled and measured comparison are very close in magnitude and agree with the trends in velocity patterns. Figure 34 is the transect at the South Matanzas River.

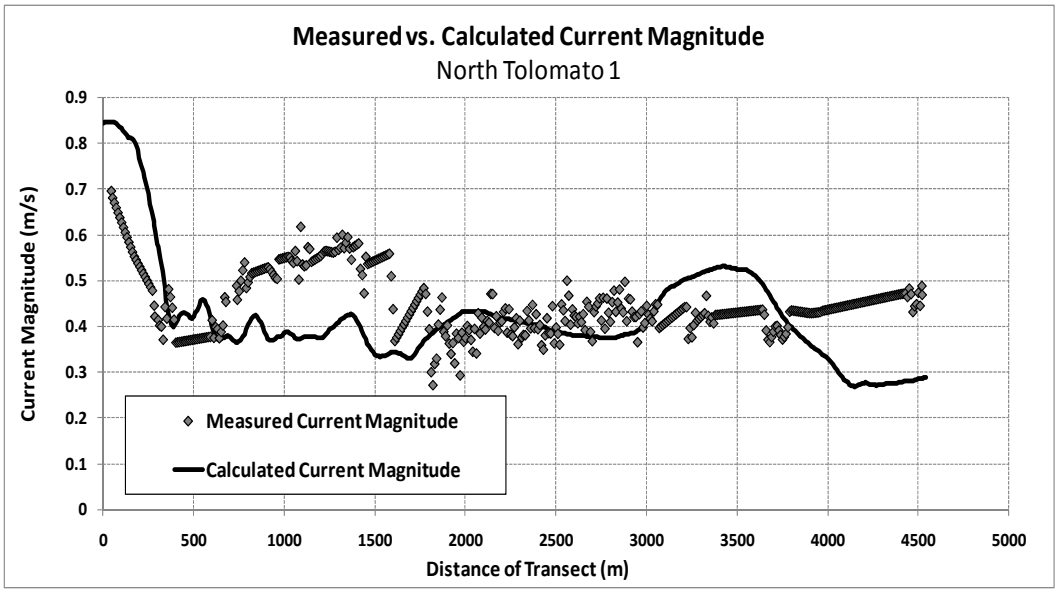

Figure 32. Measured vs. calculated current magnitude: North Tolomato River transect (1), Flooding; Model time: 1720 hours; Measurement time: 1720-1750 hours.

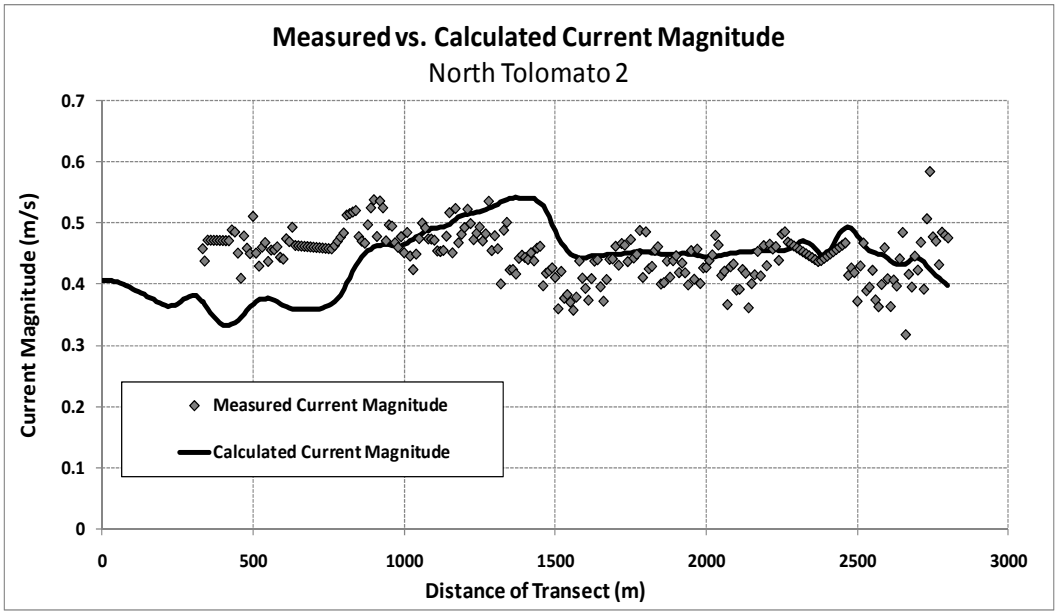

Figure 33. Measured vs. calculated current magnitude: North Tolomato River transect (2), Flooding; Model time: 1720 hours; Measurement time: 1751 hours.

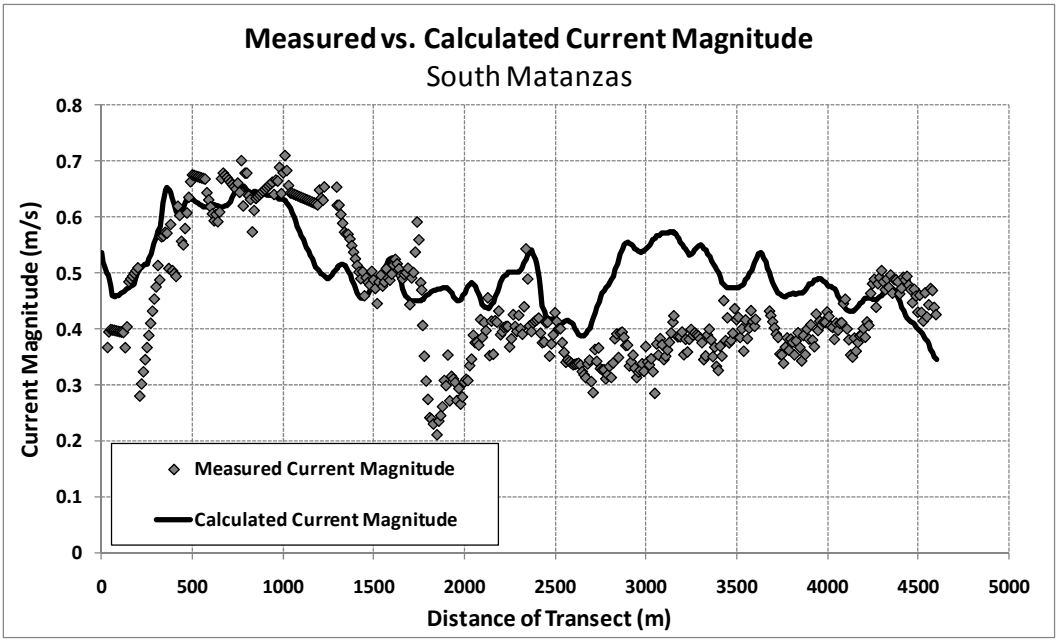

Figure 34. Measured vs. calculated current magnitude: South Matanzas River transect, Flooding; Model time: 1900 hours; Measurement time: 1854 hours.

3.2 Calibration to morphodynamics

3.2.1 Sediment transport and morphodynamics parameter selection

There are three sediment transport models available in the CMS: a sediment mass balance model, an equilibrium advection-diffusion model, and non-equilibrium advection-diffusion model. The Non-Equilibrium Transport (NET) model, which is based on a total load advection-diffusion approach (Sanchez and Wu 2010), was selected to calculate sediment transport rates in CMS-Flow. The Van Rijn transport formula (Van Rijn 2007a, b) was selected as the governing empirical formulas to calculate bedload and suspended load within CMS-Flow for combined waves (breaking and non-breaking) and current. Bed change is calculated over the same sediment transport time-step, 900 seconds (15 minutes), and was updated in the flow model. Bed change was then updated in the wave model on the steering interval of three hours.

Apart from the spatially variable parameters calibrated in the hydrodynamic calibration, sediment transport and morphology default parameters are listed in Table 4. Calibration of sediment transport is described below as an attempt to reproduce both measured transport estimates for the area and measured morphology change with long-term morphologic simulations.

Table 1. Sediment transport and morphology parameters in the CMS.

Parameter	Model Default Value	Model Value Used
Formulation	Advection-Diffusion	Advection-Diffusion
Use Non-equilibrium Transport	Yes	Yes
Sediment Transport Formula	Lund-CIRP	Van Rijn
Sediment Density	2650	2650
Bed Load Scaling Factor	1.0	1.0
Suspended Load Scaling Factor	1.0	1.0
Sediment porosity	0.4	0.4
Bed Slope Coefficient	1.0	0.1
Morphologic Acceleration Factor	1.0	1.0
Total Load Adaptation Length Method	Constant	Constant
Adaptation Length	10	10

3.2.2 Calibration to morphology

Model calibration is discussed here as the comparison of measured and calculated morphology change between the time period extending from the June 2003 post-dredging condition to the pre-dredging condition in November 2004 referred herein as 2005. Measured values of sediment transport rates over the ebb-tidal delta are between 380,000 cy (USACE 1998) to 440,000 cy (Walton and Adams 1976) toward the south. Calibration of morphology change to capture these apparent trends in transport direction requires modifications to the sediment transport formula, the bed slope coefficient, and the bed load and suspended load scaling factors.

The Van Rijn unified sediment transport formula was chosen for the St. Augustine application because of its good representation of morphology change over the ebb-tidal delta. Transport rates between Van Rijn and Lund-CIRP formulas proved to be very close in magnitude. Watanabe, the third sediment-transport formula option, was not considered appropriate for this application because it is a transport formula developed for bed load transport only. The bed slope coefficient, important for the equilibrium advection-diffusion sediment transport models, is not necessary for non-equilibrium model. Because the sediment transport model selected includes terms that smooth the bed slope, the bed slope coefficient was reduced to 0.1 for closer representation to the morphology of channel slopes at St. Augustine. The default CMS suspended load and bed load sediment transport scaling factors were not modified.

A non-uniform sediment transport scheme was used in the CMS to represent the various grain sizes being transported and the significant impact of sediment hiding and exposure. Five different sediment grain sizes were defined based on the D50 grain sizes in the grid. Including hiding and exposure of multiple grain size distributions reduced scour within the channel thalweg, accurately representing the shell hash observed in this region. In addition, sediments that are transported over the nearshore and ebb-tidal delta are within the mobile grain size range for the prevailing hydrodynamic forcing, and are more realistically represented with varying grain size distributions.

The Non-Equilibrium Transport (NET) method also controls the capacity of sediment transport through scaling factors such as adaptation lengths or times, generally dependent upon length-scales of morphologic features such as bed-forms or timescales of sediment movement. As a total load formulation is used with the NET, the Adaptation Length must be modified to calibrate to morphology. The Adaptation Length is a length scaling factor that is typically based on localized bed-forms. The smaller the Adaptation Length, the closer the model is to Equilibrium Transport which results in greater rates of transport that is more localized. Adaptation Lengths tested included 1, 2, 3, 4, 5, 10, and 100 meters. An Adaptation Length of 10 meters was selected for the entire domain of the final calculations because of the realistic patterns and trends observed in the calculations as compared to the measurements. Final parameter values were chosen to produce calibration of results to specific regions of interest, such as channel infilling in the dredged pit.

3.2.3 Test of model skill

Model skill was tested through a comparison of the calculated morphology change and measured morphology change for the 1.4-year simulation extending from 2003 to 2005. Figure 35 is a comparison of the measured bathymetry for the pre-dredging condition of 2005 with the calculated bathymetry. Morphology change, illustrated in Figure 36, is red for deposition and blue for erosion, is close in comparison with the volume of channel infilling and also captures the overall trends of erosion and deposition. Modeled results were filtered for morphology change within a range of +1 m, which is considered well within the error of morphologic modeling. Therefore, the delineated polygons in Figure 36 are areas with a significant trend of erosion or deposition associated with major morphologic features.

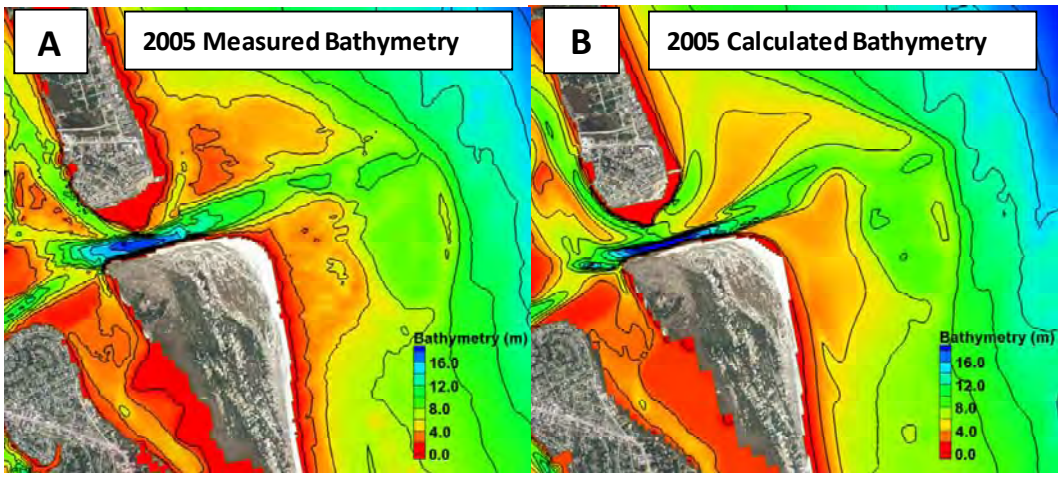

Figure 35. Comparison of measured 2005 pre-dredging bathymetry with calculated 2005 pre-dredging bathymetry.

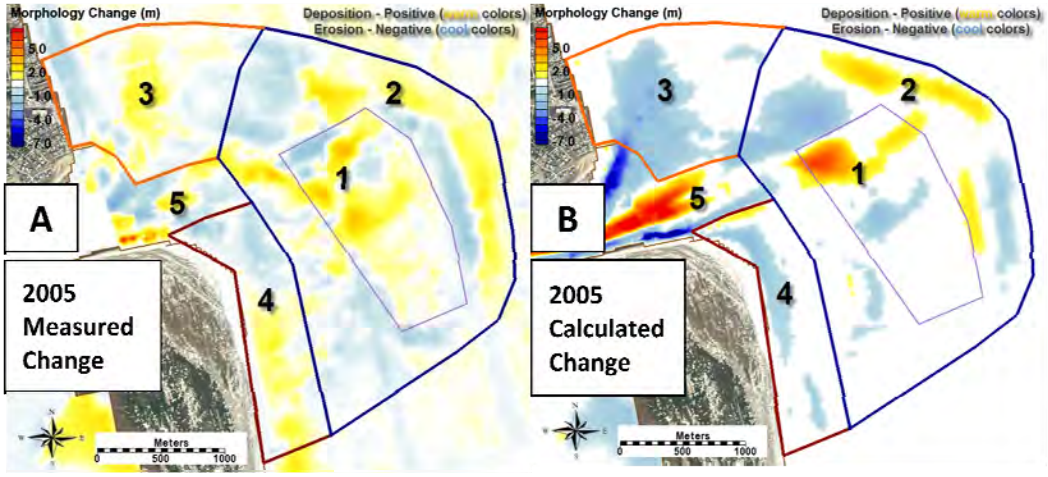

Figure 36. Comparison of A) measured 2005 bathymetry with B) calculated 2005 bathymetry.

In the present formulation of CMS, cross-shore processes and swash processes are only qualitatively represented in that alongshore generated currents will move sediments in this region but to a lesser magnitude. The northern and southern parts of the shoal closest to the nearshore beaches show a reduction in offshore platform elevation, which follows the measured trend (Figure 36a). Figure 36b shows some erosion in the offshore portion of the updrift ebb-tidal delta, however there is a poor correlation closer to the shoreline. These eroded sediments in the vicinity of Vilano Beach are not modeled properly due to lack of onshore sediment transport processes. Because the objective of the calibration of sediment transport and morphology change was to capture the channel infilling and overall ebb-tidal delta morphologic patterns, the nearshore areas were not considered as important in the final analysis and therefore were not analyzed (polygons 3, 4, and 5). The main polygon (areas 1 and 2) representing the

ebb tidal shoal was used to compute correlation coefficients for determining model skill in reproducing morphology change. The comparisons of volume change for the polygons are given in Table 5. Polygon 2 represents the ebb delta-mining imprint, and the calculated accretion indicates that the model predicted shoaling along the northern portion of the mining footprint. Total volume change for the measured and calculated ebb-tidal delta is compared in Table 6.

Table 5. Volume change of ebb-tidal delta to 9 m contour for 1.4 years.

Dredged Pit/Channel (1)	Remainder of Ebb-tidal delta (2)
2005 Measured = 369,000 cy	2005 Measured = 240,000 cy
2005 Calculated = 383,000 cy	2005 Calculated = 127,500 cy
3.6 % Difference	-50 % Difference

Table 6. Measured and calculated ebb-tidal delta volume over the full delta imprint for 1.4 years.

2005 Calculated Volume
2005 Measured = 32,655,700 cy
2005 Calculated = 32,576,000 cy
-1 % Difference

Though analysis of these volume changes can provide insight into the morphologic behavior, a qualitative analysis of the results bears substantial information about the inlet processes. Overall, there are five areas with significant morphologic change occurring in the modeled results, three of which are the result of a lack of representative processes as described above.

As the non-uniform sediment transport sorts sediments over the domain, the main channel thalweg increases in average grain sizes, and finer sediments are redistributed. There is little erosion in the deep part of the inlet channel, which scours 1- 2 meters, as the hydraulic radius goes to equilibrium with the tidal currents and bottom grain size. Sediments fill in the channel along the northern spit, also called Porpoise Point, which is an active tidal process of re-curved spits in the ebb and flood direction. The representation of sedimentation in this area supports the ability of CMS to reproduce tidally driven sedimentation and erosion patterns associated with inlet throat processes.

Changes to the updrift shoal platform are a result of initial redistribution of sediments in addition to the model error induced by a lack of appropriate processes in the nearshore. A similar effect is seen along the nearshore portion of the downdrift platform adjacent to St. Augustine Beach. All other offshore ebb-tidal delta attributes, including the main ebb channel and offshore shoals, were well represented in the model. The processes that control erosion and deposition over much of the ebb-tidal delta were the focus of the calibration. The CMS successfully reproduced sedimentation patterns and quantities within the area of focus.

4 Role of Historical Mining Activities on Morphology: Model Results

CMS was used to examine the role of previous ebb-tidal delta mining activities on the morphological trajectory of the ebb-tidal delta. We sought to answer the scientific question: "Has the evolution of the ebb-tidal delta been diverted from its natural (no engineering activity) trajectory?" To answer this question with respect to model results, sediment pathways and overall volumetric change are compared to a non-engineering trajectory.

To determine ebb-tidal delta trajectory for the pre-dredging period, the existing condition post-dredging survey of the first dredging in 2003 is compared to "no mining" condition. These two alternatives, the 2003 existing and 2003 filled (no mining), were modeled over the calibration time-period with the same waves. Since no pre-dredge bathymetry is available, the 2003 no-mining alternative initial bathymetry was created from the 2003 existing bathymetry by digitally filling the dredged pit with the volume of sediment removed (4.5 mcy). Table 7 describes the bathymetric datasets underlying the two main simulations and the wave dataset used.

Table 7. Time periods for initial and end conditions of each model run.

Initial Condition Bathymetry/Topography (2003)			End Condition Bathymetry/Topography (2005)		
2003 Existing	2003 Filled	Wave Forcing (FCFP Waves)	2003 Existing	2003 Filled	Wave Forcing (FCFP Waves)
2003 Ebb-tidal delta Bathymetry	Modified 2003 Ebb-tidal delta Bathymetry	17 June 2003 to 17 November 2004	2005 Ebb-tidal delta Bathymetry	2005 Ebb-tidal delta Bathymetry	17 June 2003 to 17 November 2004
2003 beach profiles R1 – R209	2003 Beach Profiles R1 – R209	17 June 2003 to 17 November 2004	2005 Beach Profiles R110 – R152	2005 Beach Profiles R110 – R152	17 June 2003 to 17 November 2004

4.1 Ebb-tidal delta planform area

Resultant planform area change is analyzed here to clarify the changes to 1) the overall planform change of the active shoal, and 2) the sediment pathways over the active shoal. The "active shoal" is defined here as water

depths less than nine meters. The authorized dredging depth is 30 feet (9 m) below mean sea level, which is deeper than the depth of closure (7.6 m) or active zone of sediment transport on the ebb-tidal delta for normal (non-extreme) conditions. A second planform area is determined for the 6-m contour, which better depicts large-scale movement of the active parts of the shoal under normal wave and tidal conditions. Figure 37 includes a polygon delineating the shoal area over which calculations were based on for both the planform area of the ebb-tidal delta above 9 m and 6 m. Because the simulation is for 1.4 years, the 6 m and 9 m (20 and 30 ft) contours illustrate the general trend of the long-term trajectory. Long-term adjustment of the existing condition back to the unexcavated condition's planform area may take as long as 5 to 15 years. The dashed grey and black lines in Figure 37a are the locations of the planform area for the 6 m and 9 m contours, respectively, and illustrate the projected long-term adjustment of the ebb-tidal delta. The calculated 6 m contour for the existing bathymetry clearly shows the extension of the shallow, updrift portion of the shoal toward the location of the final position of the filled bathymetry.

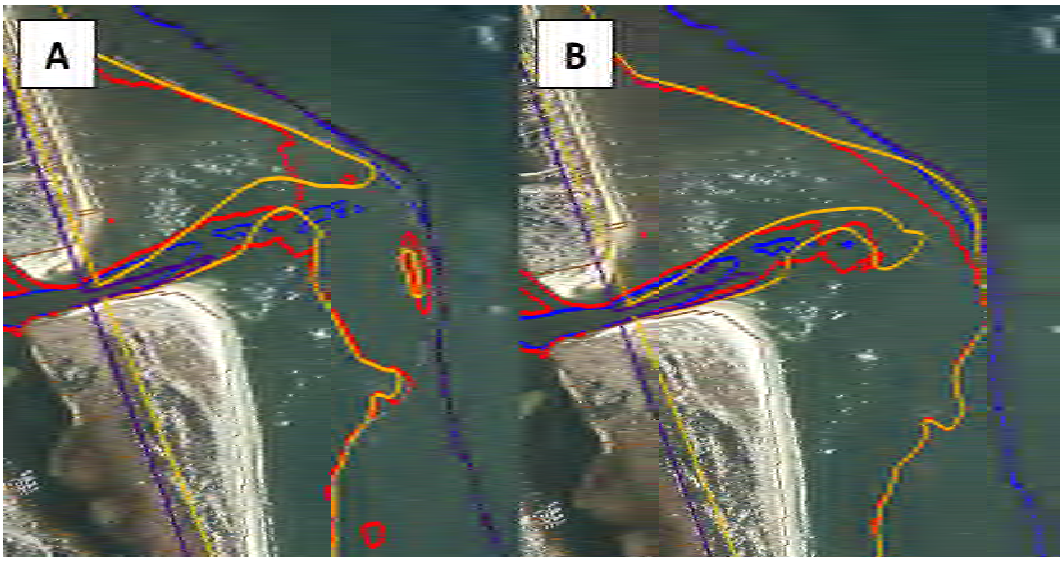

Figure 37. Planform of the 6 m and 9 m contours (warm and cool colors, respectively) and estimate of the natural 6-m and 9-m contours (light gray and dark gray, respectively) for the a) initial 2003 existing bathymetry (red, blue) and final calculated 2005 bathymetry (orange, purple), and b) 2003 "Filled" bathymetry and calculated 2005 bathymetry.

A comparison of the existing and filled condition areas are given in Table 8. The percent difference between the 2003 existing condition and the final 2005 calculated condition is six percent for the 6 m contour and 1.9 percent for the 9 m contour. The percent difference between the 2003 filled condition and the final 2005 calculated filled condition is three percent for the

Table 8. Aerial change from the 6 m and 9 m contour for each model run.

Planform Surface Area of Ebb-tidal delta to 6 m Contour				Planform Surface Area of Ebb-tidal delta to 9 m Contour			
2003 Existing Planform Area	2005 Calculated Planform Area	Change	Difference %	2003 Existing Planform Area	2005 Calculated Planform Area	Change	Difference %
2003 Existing = 6,795,700 yd^2	2005 Calculated Existing = 7,220,200 yd^2	424,450 yd^2	6%	2003 Existing = 13,795,700 yd^2	2005 Calculated Existing = 14,067,500 yd^2	271,800 yd^2	1.9%
2003 Filled = 8,071,300 yd^2	2005 Calculated Filled = 8,313,500 yd^2	242,200 yd^2	3%	2003 Filled = 13,809,225 yd^2	2005 Calculated Filled = 14,053,800 yd^2	244,575 yd^2	1.7%

6 m contour and 1.7 percent for the 9 m contour. The difference in the evolution of the planform area of the 6 m contour between the existing and filled condition is three percent, and the difference in the evolution of the planform area of the 9 m contour between the existing and filled condition is 0.2 percent. Because this difference is within tolerable levels depicting no change, we conclude that the previous mining activities do not affect the planform area of the ebb-tidal delta to the 6 and 9 m contours, and that this change would not have implications for the wave climate and far-field effects upon the shoreline.

4.2 Ebb-tidal delta volume

In addition to calculating ebb-tidal delta planform changes, volumetric changes of the ebb-tidal delta (Figure 38) are calculated here to determine the effect of the initial ebb-tidal delta mining on the trajectory of ebb-tidal delta morphology. The same area as used in the volume change analysis for determining model skill (Figure 36) is also applied to calculate the ebb-tidal delta volumes. Table 9 gives the percent difference as the volume of the initial ebb-tidal delta as compared to the calculated ebb-tidal delta for the existing and filled conditions. The volume of the ebb-tidal delta grew above the 9 m contour by two percent for the existing condition and grew by three percent for the filled condition. This describes the capacity of the inlet system to modify the sediment fluxes entering the system either laterally from the adjacent beaches, or internally from the channel and flood shoal sediments. The difference is within tolerable levels, depicting little change from the effects of the dredged pit on morphologic evolution in the modeled 1.4 years.

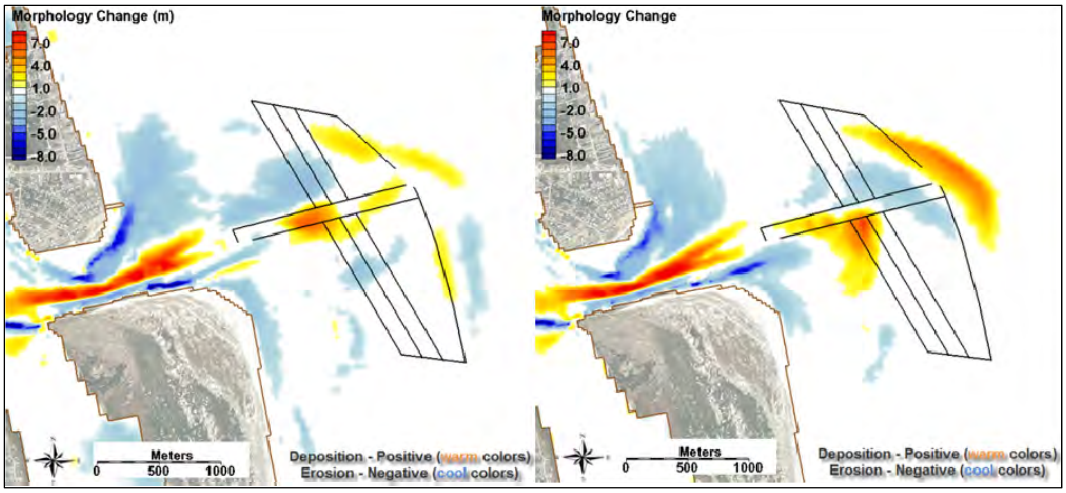

Figure 38. Final ebb-tidal delta morphology change with the dredge design template overlaying the a) 2003 existing bathymetry and b) 2003 "filled" bathymetry.

Table 9. Volumes and differences of the 2003-2005 existing and filled conditions.

Volume of Ebb-tidal delta to 9 m Contour		Accreted	Difference %
2003 Existing = 32,066,000 cy	2005 Calculated Existing = 32,576,000 cy	510,000 cy	2%
2003 Filled = 36,566,000 cy	2005 Calculated Filled = 37,564,000 cy	998,000 cy	3%
2003 Existing = 32,066,000 cy	2005 Calculated Existing = 32,576,000 cy	510,000 cy	2%

We conclude that the previous mining activities did not affect the volume change of the ebb-tidal delta to the 9 m contour and that this did not collapse or deflate the overall ebb-tidal delta volume. This difference in volume should also not have any implications for the wave climate and far-field effects upon the shoreline.

4.3 Ebb-tidal delta trajectory

Increased volume change over the active part of the ebb-tidal delta, typically channel infilling, tends to occur under energetic periods, particularly during the high-energy winter months. However, channel infilling and overall shoal volume increase at a near constant rate, as shown in Figure 39. This constant rate suggests that sedimentation over the inlet channel is largely driven by the more regular tidally driven transport rather than the influence of storm event-driven transport. Thus, large-scale sediment transport at the inlet is tidally dominated. It is important to note that Hurricanes Frances and Jean moved through the area during Month 14, and the ebb-tidal delta volume during Months

15 and 16 (Figure 39) show the morphologic response as a drop in volume. The greater response in the existing scenario is partially due to exposure to storm waves or the lack of protection over the outer shoal because of the open, mined area. In addition, there is a greater flux over the features that volume change was measured over, namely the channel and outer portion of the ebb-tidal delta. The filled scenario shows less change/flux over the measured area because the ebb-tidal delta dissipates enough of the hurricane wave energy, and therefore responds less to the forcing.

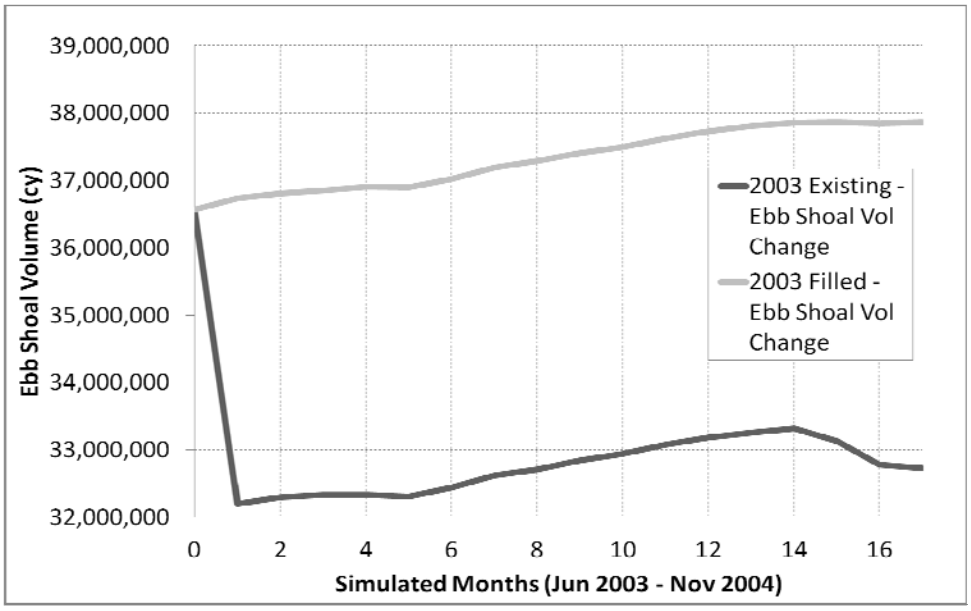

Figure 39. Calculated ebb-tidal delta volume change over the 1.4-year simulation for the 2003 Existing condition and 2003 Filled condition. Note that the 2003 Existing condition includes the dredging of 4.2 million cy.

4.4 Sediment transport pathways and sediment fluxes

Sediment pathways are examined here to determine the effects of the 2003 mining on the performance of the ebb-tidal delta to bypass sediments. Figures 40 through 47 illustrate sediment transport pathways under ebbing and flooding currents for north and south orientated waves. Figures 40-41 and Figures 44-45 are of initial conditions at the beginning of the 1.4-year simulation, and Figures 42-43 and Figures 46-47 are of final conditions near the end of the 1.4-year simulation. Both ebbing and flooding conditions are illustrated to show the different pathways sediment transport occupies under the ambient tidal conditions, and the color intensity in each image illustrates the quantity of sediment suspended (kg/m^3) or transported in the water column. The black vectors in each figure illustrate the direction of transport. Color is not directly related to pathway location, only to areas of increased sediment concentration in the water column.

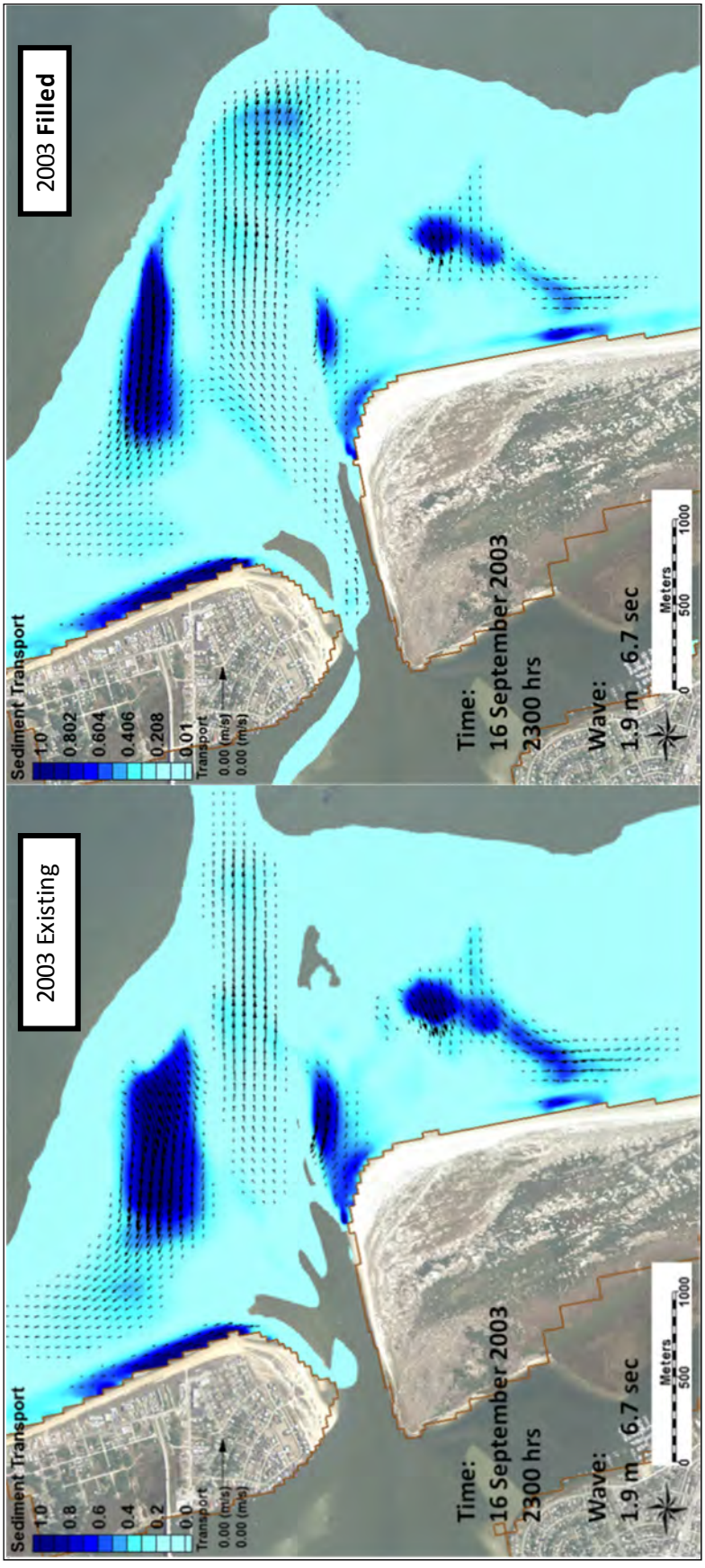

Figure 40. Initial sediment transport (in kg/m3) pathways for the 2003-2005 existing condition and 2003-2005 filled condition during mid-2003 under northerly waves and an ebbing current.

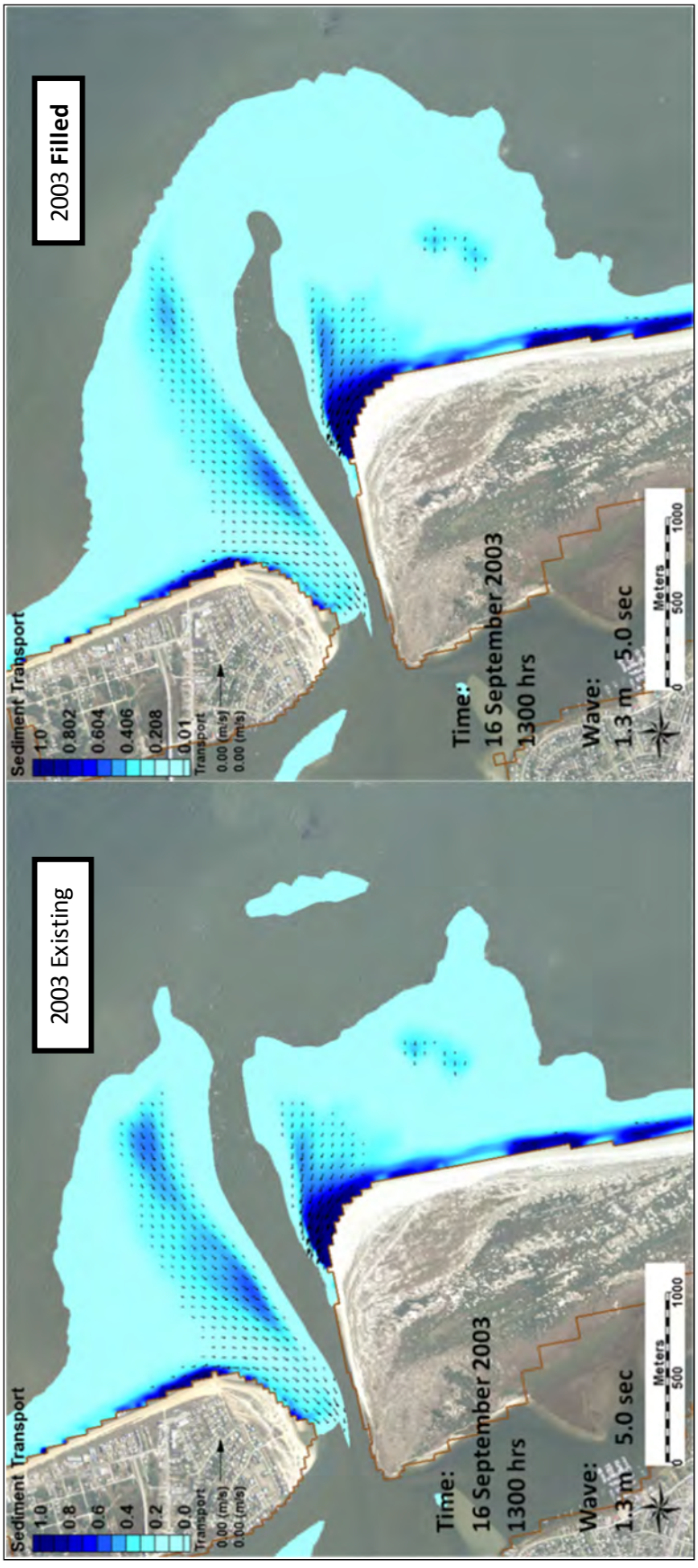

Figure 41. Initial sediment transport (in kg/m³) pathways for the 2003-2005 existing condition and 2003-2005 filled condition during mid-2003 under northerly waves and a flooding current.

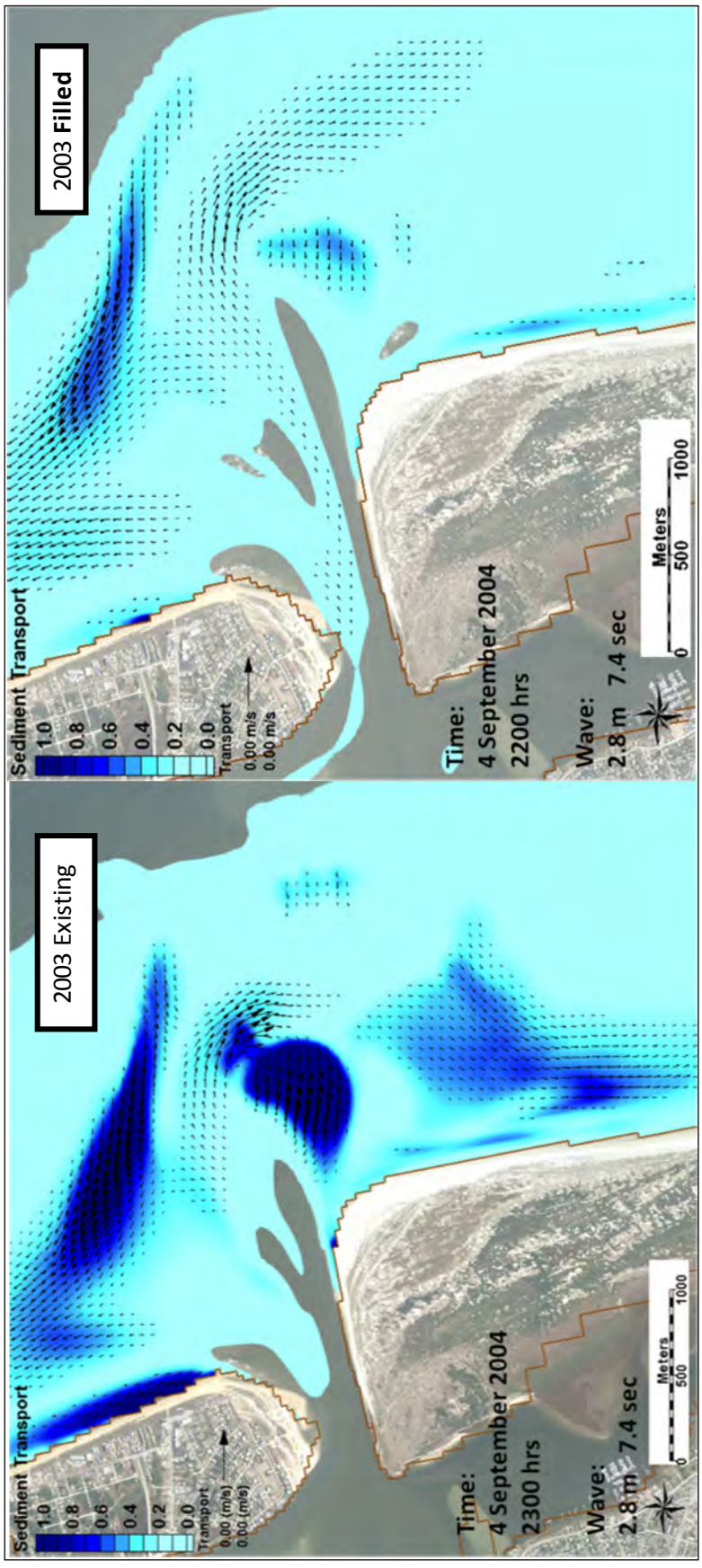

Figure 42. Final sediment transport (in kg/m³) pathways for 2003-2005 existing condition and 2003-2005 filled condition during late-2004 under northerly waves and an ebbing current.

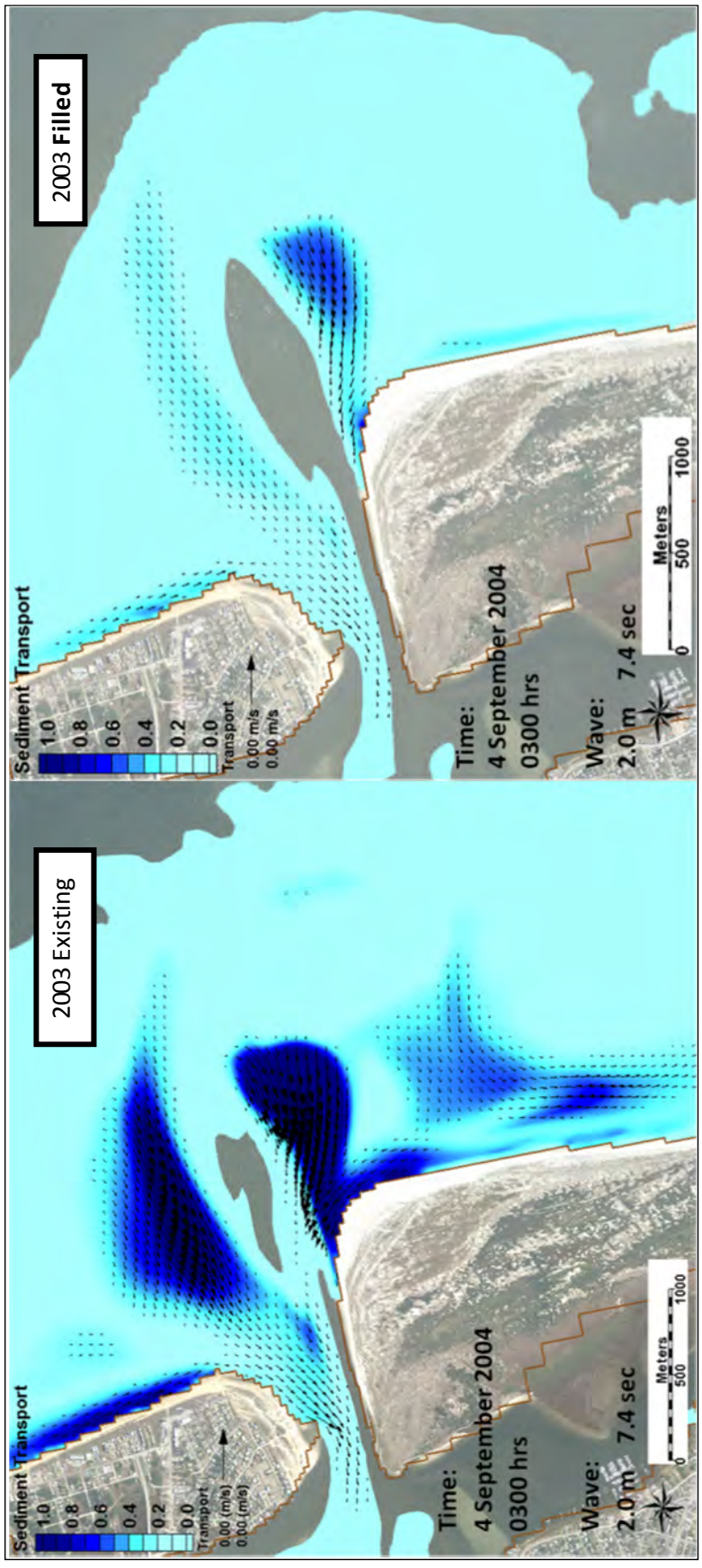

Figure 43. Final sediment transport (in kg/m³) pathways for 2003-2005 existing condition and 2003-2005 filled condition during late-2004 under northerly waves and a flooding current.

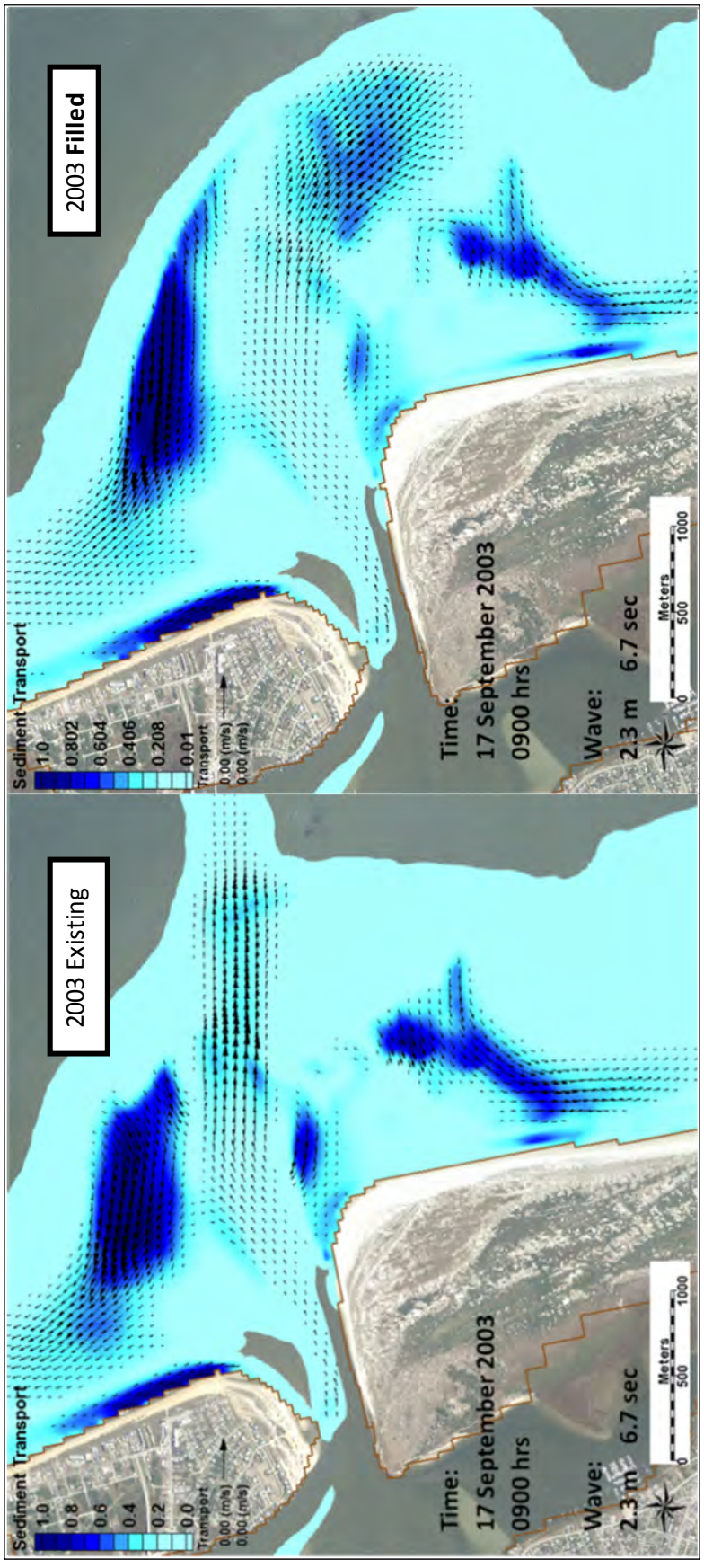

Figure 44. Initial sediment transport (in kg/m³) pathways for 2003-2005 existing condition and 2003-2005 filled condition under during mid-2003 southerly waves and an ebbing current.

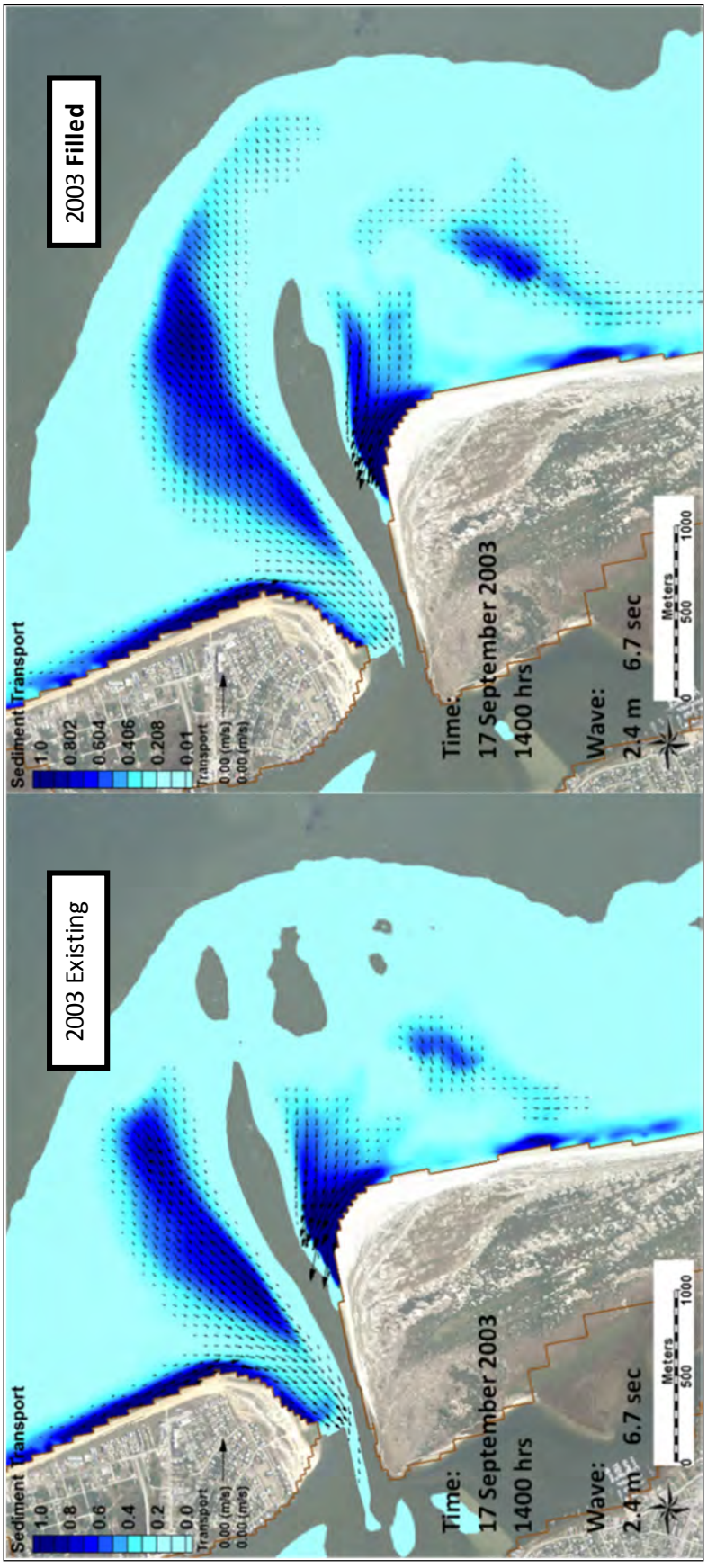

Figure 45. Initial sediment transport (in kg/m³) pathways for 2003-2005 existing condition and 2003-2005 filled condition under during mid-2003 southerly waves and a flooding current.

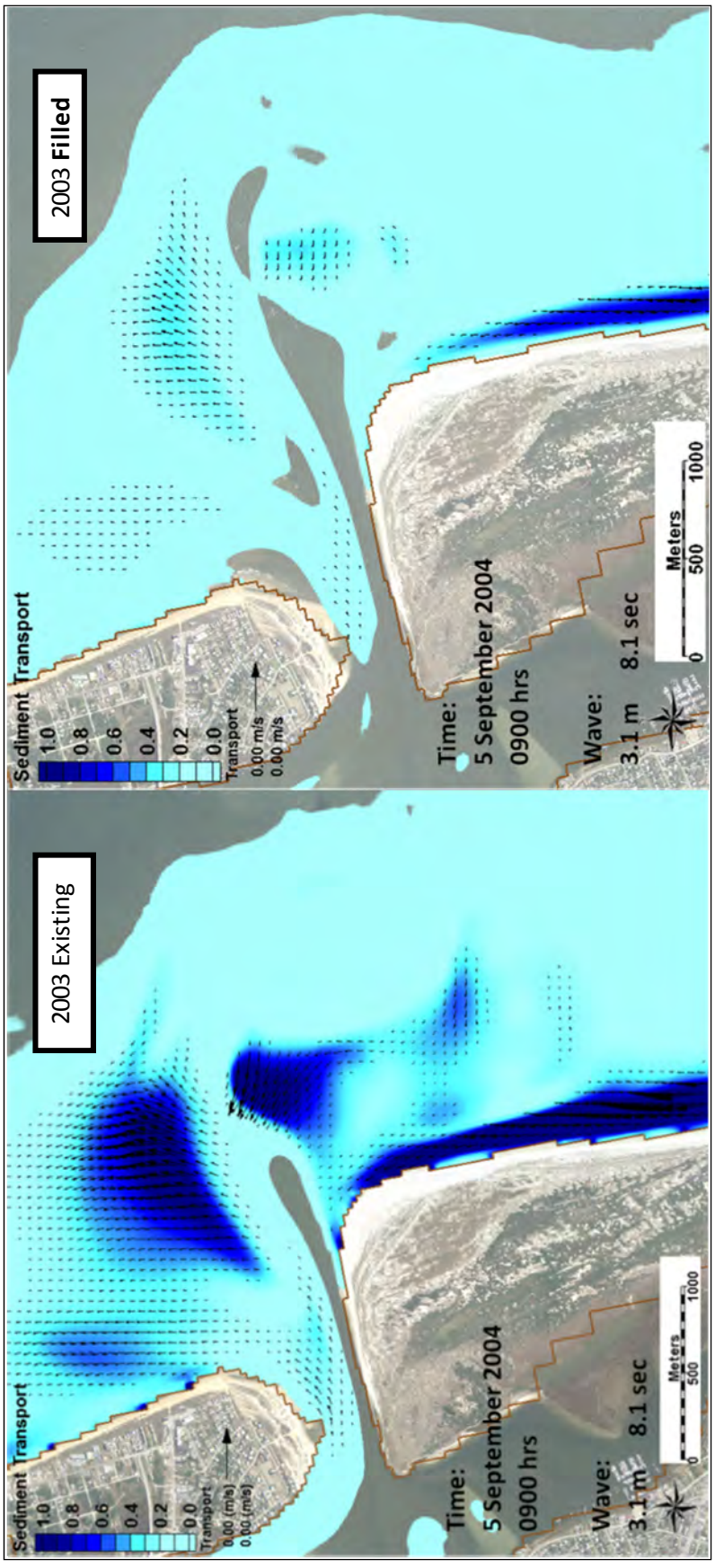

Figure 46. Final sediment transport (in kg/m^3) pathways for 2003-2005 existing condition and 2003-2005 filled condition during late-2004 under very energetic southerly waves and an ebbing current.

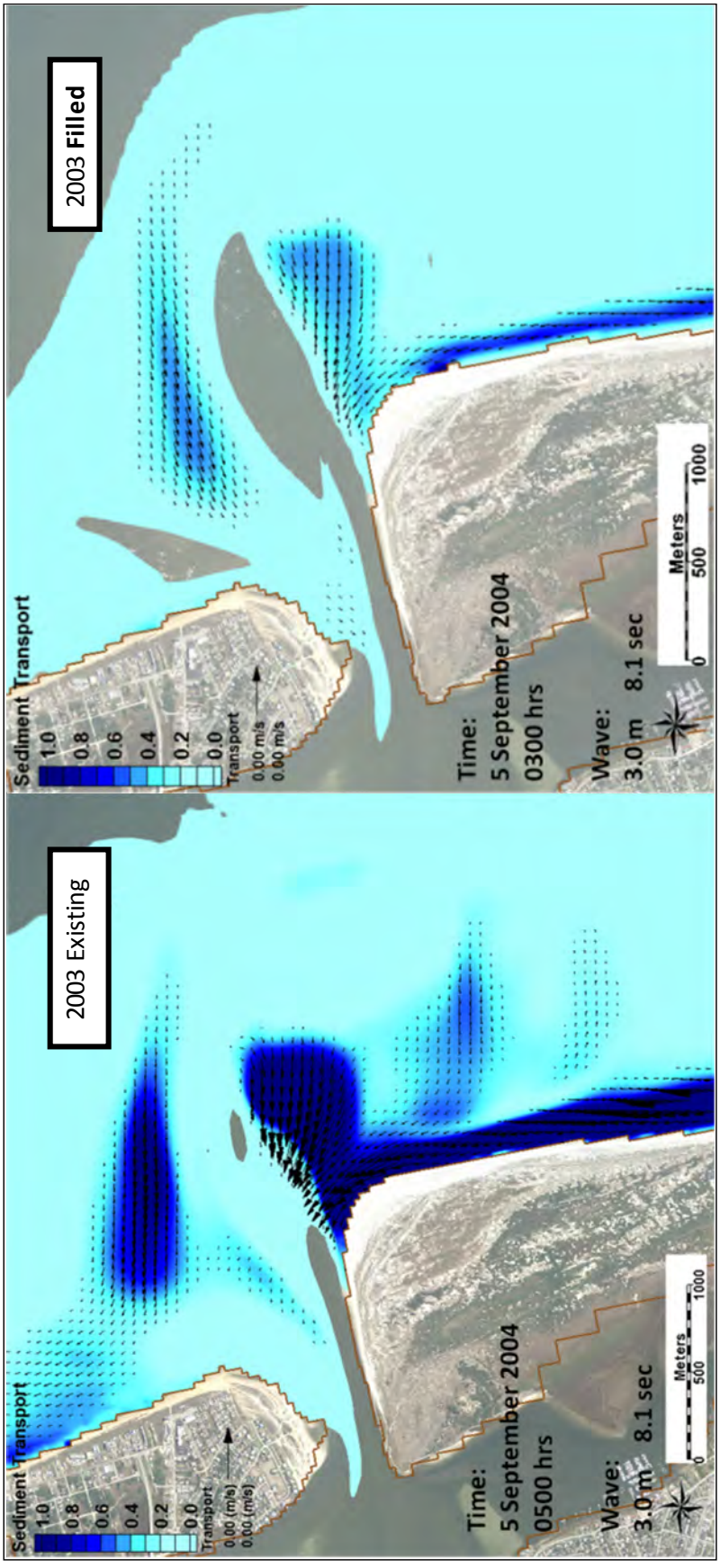

Figure 47. Final sediment transport (in kg/m3) pathways for 2003-2005 existing condition and 2003-2005 filled condition during late-2004 under very energetic southerly waves and a flooding current.

Transport over the northern lobe, or updrift platform, of the ebb-tidal delta is active under ebbing and flooding conditions, and north and south directed waves. Wave direction does not have as great an effect on transport direction as do tidal currents. This is especially true under higher energy waves that tend to refract over the ebb-tidal delta to very acute angles or shore normal (typically -30 to 30 degrees from shore normal). However, there is a distinct difference in transport direction under ebb versus flood currents. The CMS reproduces wave-wave and wave-current interactions, and Figures 40 through 47 illustrate clearly a shift in transport direction from updrift and offshore during ebbing conditions, to landward and inlet-directed transport during flooding conditions. As the ebb jet exits through the main ebb channel, an eddy forms near the offshore, updrift part of the shoal, inducing a force on the wave-generated currents that would normally be directed landward (Figures 40 and 41). This redirected transport tends to orient east-west, facilitating sediment to be transported north of the ebb-tidal delta and in the vicinity of Vilano Beach. Under each condition given in the figures below, transport over the updrift platform is very similar in aerial extent and magnitude. While the 2003 existing condition shows no initiation of transport over the inactive dredged pit, there is sedimentation; however, for the filled condition there is some transport predicted (Figures 37 and 44).

Most of the ebb-directed flow in the ebb jet transports sediment toward the location of the dredged pit, or in the case of the filled condition, toward the offshore outer lobe of the ebb-tidal delta. Transport vectors show sediment moving in the direction of the ebb jet, which exits the shoal or is carried further offshore. Direction of transport over this area was examined throughout the simulation and does not show a lateral pathway (in this case, a more north-south direction) for transport to move around the entire ebb-tidal delta under wave-induced currents.

Under ebbing currents, the southern ebb-tidal delta lobe, or downdrift platform, has very similar patterns and intensity for both the 2003 existing and filled conditions. There is some difference in transport over the southern ebb-tidal delta lobe, or downdrift platform, under ebbing versus flooding currents (Figures 40 and 41). Both the 2003 existing and filled conditions illustrate a stronger inlet-directed transport under flooding currents over the channel-adjacent portion of the shoal. Inlet directed currents carry the sediments over the shallow northern part of the

downdrift platform, and spillover in to the main channel to be redistributed by tidal currents.

Similarly, under both northerly and southerly waves, the updrift platform tends to focus transport in the inlet direction under flooding conditions, with current and transport vectors oriented northeast to southwest (Figures 41, 43, 45 and 47). Sediments moving alongshore of Vilano Beach (updrift) are dominated by flooding currents, due to their proximity to the flood marginal channel, and are always oriented from north to south. The main ebb channel typically does not carry significant flow or prism under flooding conditions, and so less sediment transport occurs here.

The final pathways illustrated in Figures 42, 43, 46 and 47 show some long-term differences between the 2003 existing and filled conditions. Toward the end of the 1.4-year simulation, the channel marginal-portions of the updrift and downdrift shoals become shallower and more active in the 2003 existing condition. As a result, more sedimentation tends to occur closer to the nearshore and more inlet-adjacent for both ebbing and flooding conditions.

The general pathways of current-induced sediment transport are illustrated in Figures 48 and 49 for both 2003 existing and filled conditions. There is no identifiable difference between flooding current patterns. However, there is a slight offset in offshore-directed ebbing current patterns for the filled condition to preferentially orient toward the southeast. Figures 50 and 51 illustrate the dominant pathways of wave-induced sediment transport over the shoal. Transport over the north and south shoals tend to be oriented into the channel on flooding current and offshore during ebbing currents. The ultimate direction of these sediments either places them onto the nearshore or injects them into the inlet channel to be redistributed on tidally dominated currents. The transport pathways are dominated by tidal currents, and function identically in both the 2003-2005 existing condition and the 2003-2005 filled condition. Overall, sediment transport pathways were not found to be interrupted by the present dredging footprint.

Sediment fluxes into and out of the ebb-tidal delta were integrated over the 1.4 yr model run through arc lines orthogonal to major sediment pathways. The arcs include 1) the main inlet channel, 2) the downdrift or main ebb channel, 3) the updrift flood marginal channel, 4) offshore of the

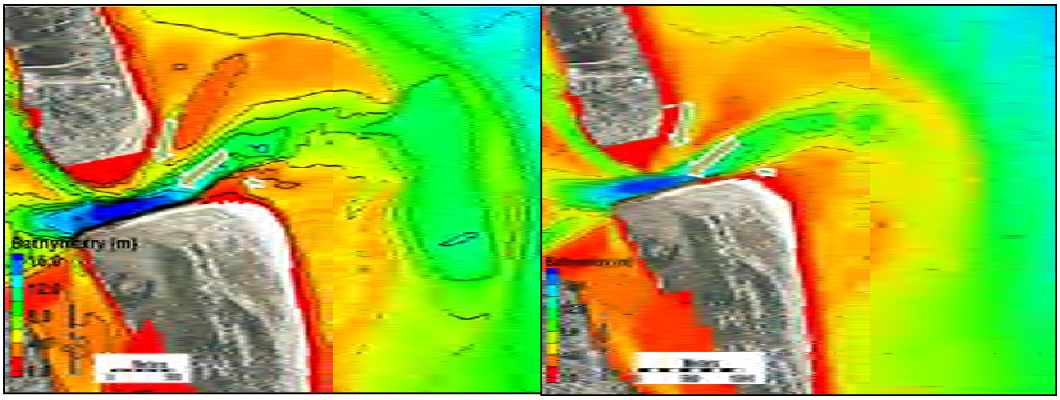

Figure 48. General sediment transport pathways under flood currents for 2003-2005 existing condition and 2003-2005 filled condition; size of arrows indicates relative magnitude.

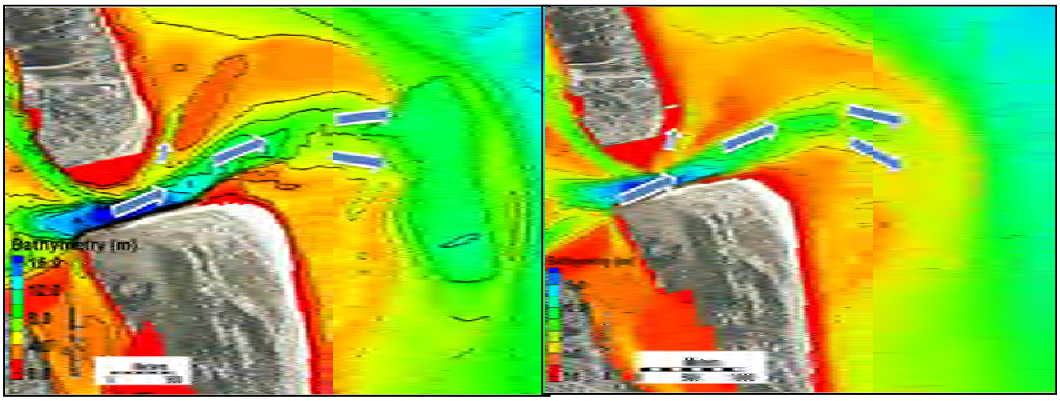

Figure 49. General sediment Transport under ebb currents for 2003-2005 existing condition and 2003-2005 filled condition; size of arrows indicates relative magnitude.

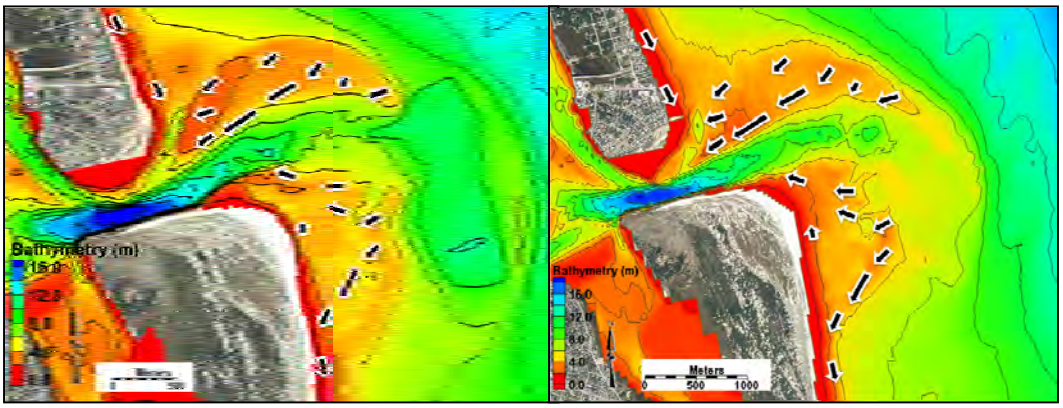

Figure 50. General sediment transport pathways under northerly waves for 2003-2005 existing condition and 2003-2005 filled condition; size of arrows indicates relative magnitude.

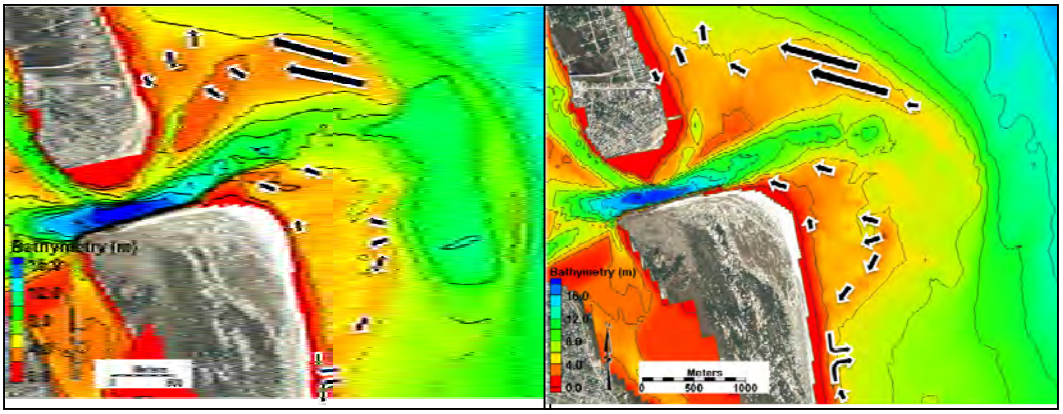

Figure 51. General sediment transport pathways under southerly waves for 2003-2005 existing condition and 2003-2005 filled condition; size of arrows indicates relative magnitude.

ebb-tidal delta, 5) downdrift of the ebb-tidal delta, 6) updrift of the ebb-tidal delta, and 7) across the ebb-tidal delta proper or channel infilling in to the dredged pit (Figure 52).

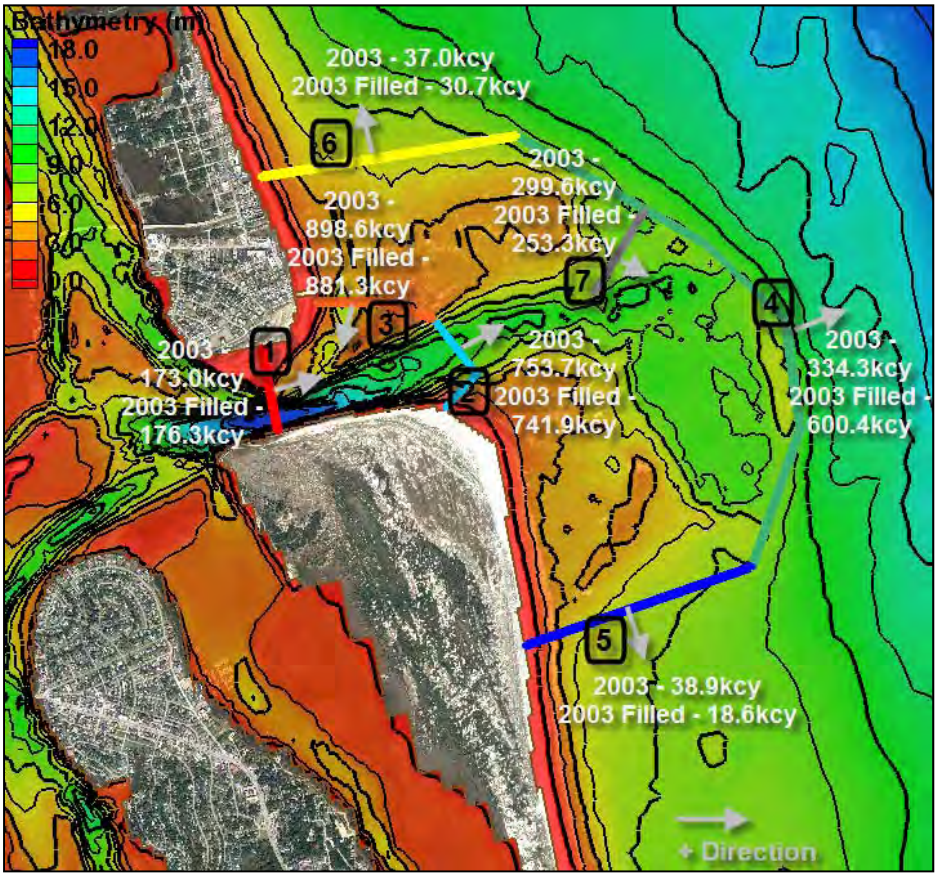

Figure 52. Orientation of arc lines over which sediment fluxes are calculated (over 2003 bathymetry). Directions of arrows indicate net direction of transport. The inset image is of the final bathymetry (November 2004) with arcs.

The magnitude of net sediment fluxes is given in Tables 10 and 11. The greatest sediment transport occurs over the dominant pathways of transport through the main tidally driven channels. Both modeled scenarios were similar in magnitude of gross and net transport; however, there was significantly more sedimentation offshore in the filled scenario (see Figure 52, arc line 4). In addition, a slightly higher transport of 50 kcy/yr was calculated across the ebb-tidal delta into the dredged pit for the 2003 existing condition as compared to the 2003 filled condition. This was determined to be a function of accommodation space, where the dredged pit acts as a greater sediment trap than the filled condition.

Table 10. Calculated sediment fluxes for arcs 1-3.

ARC LINE #	Arc 1 - Inlet Throat (Ebb-Oriented)	Arc 2 - South Channel (Ebb-Oriented)	Arc 3 – North Channel (Flood-Oriented)
FLUX (kcy/yr) Existing	173.0	753.7	898.6
FLUX (kcy/yr) Filled	176.3	741.9	881.4

Table 11. Calculated sediment fluxes for arcs 4-6.

ARC LINE #	Arc 4 – Offshore (East)	Arc 5 – Downdrift (South) R-127	Arc 6 – Updrift (North) R-120
FLUX (kcy/yr) Existing	334.3	38.9	30.7
FLUX (kcy/yr) Filled	600.4	18.6	37.0

5 Role of Planned Mining Activities on Future Morphology

CMS was used to assess whether additional excavations of the ebb-tidal delta would significantly change the entire ebb-tidal delta bathymetry, not just the borrow area excavation alone, by reducing its depth either through deflation or collapse, and/or by reducing its planform such that it would result in a significant adverse impact to the coastal littoral system and adjacent beaches.

We sought to answer the scientific question, "How many cubic yards of sediment can be mined from the ebb-tidal delta in the future which does not cause large-scale morphological change to the ebb-tidal delta/ inlet complex?" Ebb-tidal delta collapse or deflation means migration of a portion or the entire ebb-tidal delta onshore, alongshore, and/or offshore because of loss of the ebb-tidal current (abandonment) over the shoal (Hansen and Knowles 1988; Pope 1991). Byrnes et al. (2003) document collapse of the southern (updrift) and northern (down drift) flanks of the ebb-tidal delta at Grays Harbor, Washington, and seaward translation of the central portion of the ebb-tidal delta in response to construction of long jetties at the turn of the 20th Century. Kana and McKee (2003) discuss the twice-relocated Captain Sams Inlet in South Carolina, for which collapse of the ebb-tidal delta at the closed inlet was anticipated to nourish the beach (Kana and Mason 1988).

To determine the role of additional excavations of the ebb-tidal delta on future morphology, the most recent survey bathymetry from 2008 (existing) is compared to several dredging scenarios. Table 12 describes the bathymetric datasets underlying the two main simulations and the wave dataset used. These four alternatives were modeled over the same time period with the same waves as those used in the model skill and above section on the 2003 analysis. The 2003 wave dataset was used for consistency in wave input for comparison of volume change and sediment transport pathways to other results. Figure 53 illustrates the bathymetry of the different dredging scenarios. The dredging scenarios for 1.5 mcy removed and three mcy removed were created from the 2008 existing bathymetry by digitally removing the volume of sand from authorized dredging location. These two

Table 12. Time periods for initial and end conditions (2008) of each model run.

2008 Existing	2008 – 1.5 mcy Removed	2008 – 3 mcy Removed	2008 – 4 mcy Removed	Wave Forcing (FCFP Waves)
2008 Ebb-tidal Delta Bathymetry	Modified 2008 Ebb-tidal Delta Bathymetry	Modified 2008 Ebb-tidal Delta Bathymetry	Modified 2008 Ebb-tidal Delta Bathymetry	17 June 2003 to 17 November 2004
2007 beach profiles R1 – R209	2007 beach profiles R1 – R209	2007 beach profiles R1 – R209	2007 beach profiles R1 – R209	17 June 2003 to 17 November 2004

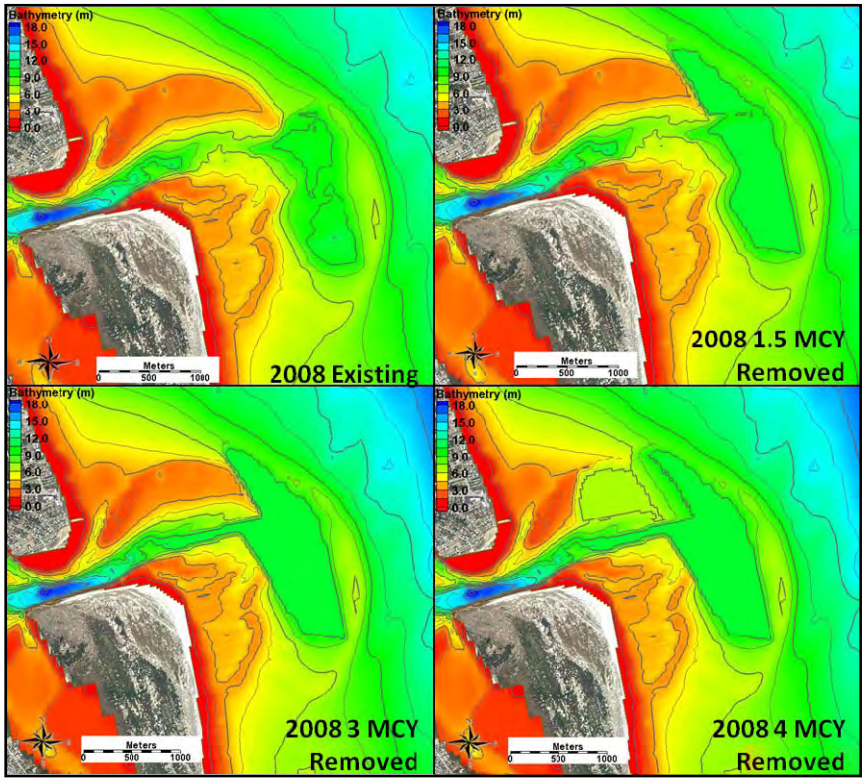

Figure 53. Model grid bathymetry for the 2008 existing condition and the three dredging scenarios.

alternatives also were strictly designed to only impact the furthest offshore reaches of the authorized dredging location. The scenario with 1.5 mcy required removal of sediments from the downdrift platform and offshore. The 3 mcy removed scenario required the 1.5 mcy design with more sediments removed from the offshore updrift platform, and all available sediments within the authorized channel to 9 m below MLW. The 4 mcy of sediment removed scenario was designed to further modify the updrift platform of the ebb-tidal delta, which was necessary to remove an additional 1 mcy of sediment.

To estimate the ebb-tidal delta response for future mining events, approximately scheduled to occur in 2011, it would be expected that, using previous estimates of ebb-tidal delta borrow site infilling, approximately 600,000 cy/yr (Taylor Engineering Inc. 2010), would infill into the borrow site between 2008 and 2011. It is estimated that the borrow site will have accreted approximately 1.5 mcy of sediment between 2008 and 2011.

Results for sediment transport pathways and planform adjustment are shown in detail for the 2008 existing condition and the 2008 1.5 mcy removed condition in the following sections. We selected to further analyze the 2008 1.5 mcy removed condition as it was closest to the proposed permit for a 2011 dredging event. The permitted dredge volume is subject to potentially change to 3 mcy following this study. However, due to the expected accretion rates (infilling) between 2008 and 2011, this scenario may also represent the dredging footprint of a greater quantity in 2011.

5.1 Sediment transport pathways

Sediment transport pathways are compared here for the 2008 existing condition and the 2008 1.5 mcy removed condition. Figures 54 through 61 illustrate sediment transport pathways under ebbing and flooding currents for north and south-orientated waves. Figures 54-55 and Figures 58-59 are of initial conditions, and Figures 56-57 and Figures 60-61 are of final conditions. The color intensity in each image illustrates the sediment suspended concentration (kg/m^3) in the water column and transportation direction is indicated by the black vectors.

Overall, each condition (ebbing and flooding, northerly and southerly approaching waves) appears to produce the nearly identical pathways and transported sediments for both the initial and the final conditions. In comparison to the 2003 scenarios, there is also no difference in the general pathways of transport because all of the major morphological features are still intact, in equivalent shape, and therefore modeled similarly. Some difference is notable in the orientation of the ebb jet directed sediments, which are skewed more toward the south-southeast for the 2008 existing condition. All dredging scenarios tend to allow for a more easterly oriented ebb jet where part of the shoal has been removed. Ebbing conditions are modeled to show sediment transport directed away from the inlet offshore and toward the adjacent beaches, and flooding conditions produce inlet-directed transport.

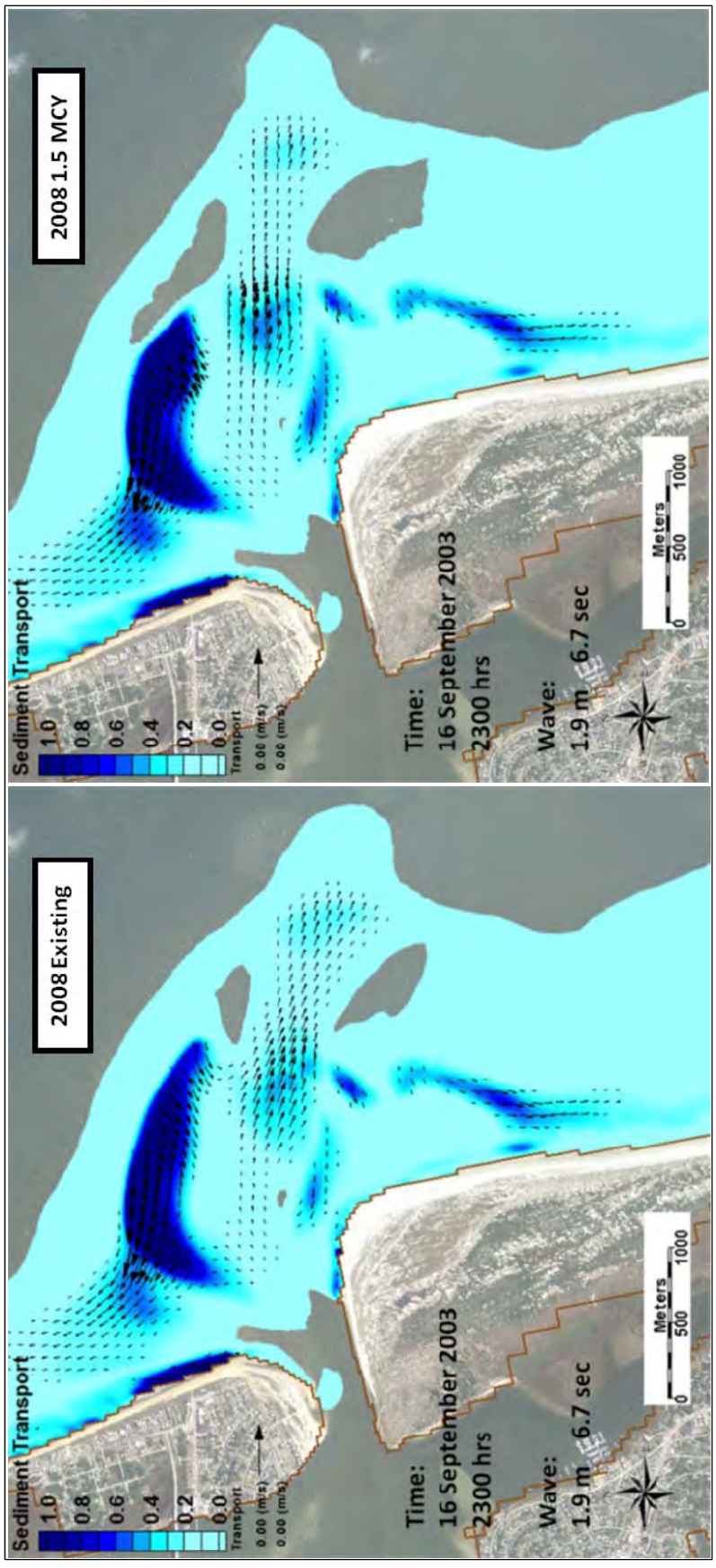

Figure 54. Initial sediment transport (in kg/m³) pathways for the 2008 existing condition and 2008 1.5 mcy removed condition during mid-2003 under northerly waves and an ebbing current.

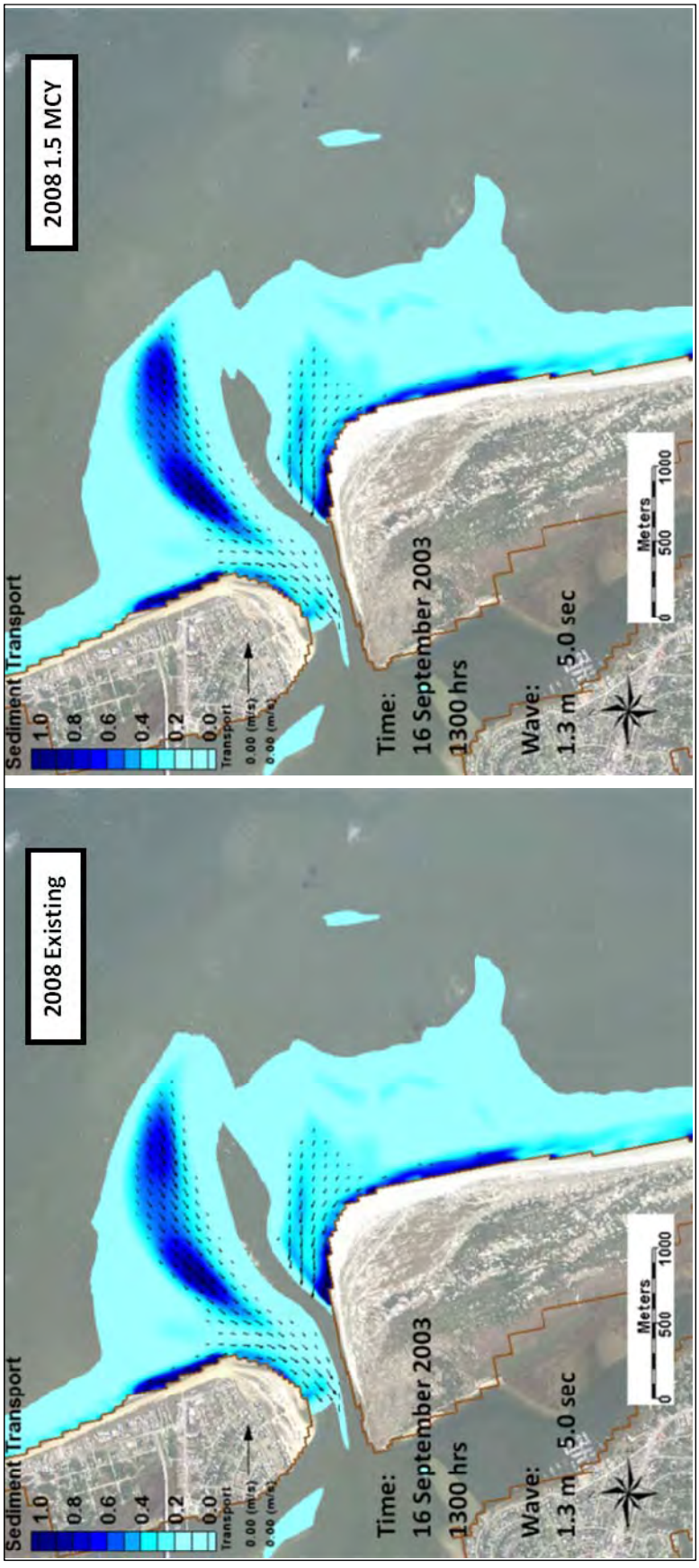

Figure 55. Initial sediment transport (in kg/m³) pathways for the 2008 existing condition and 2008 1.5 mcy removed condition during mid-2003 under northerly waves and a flooding current.

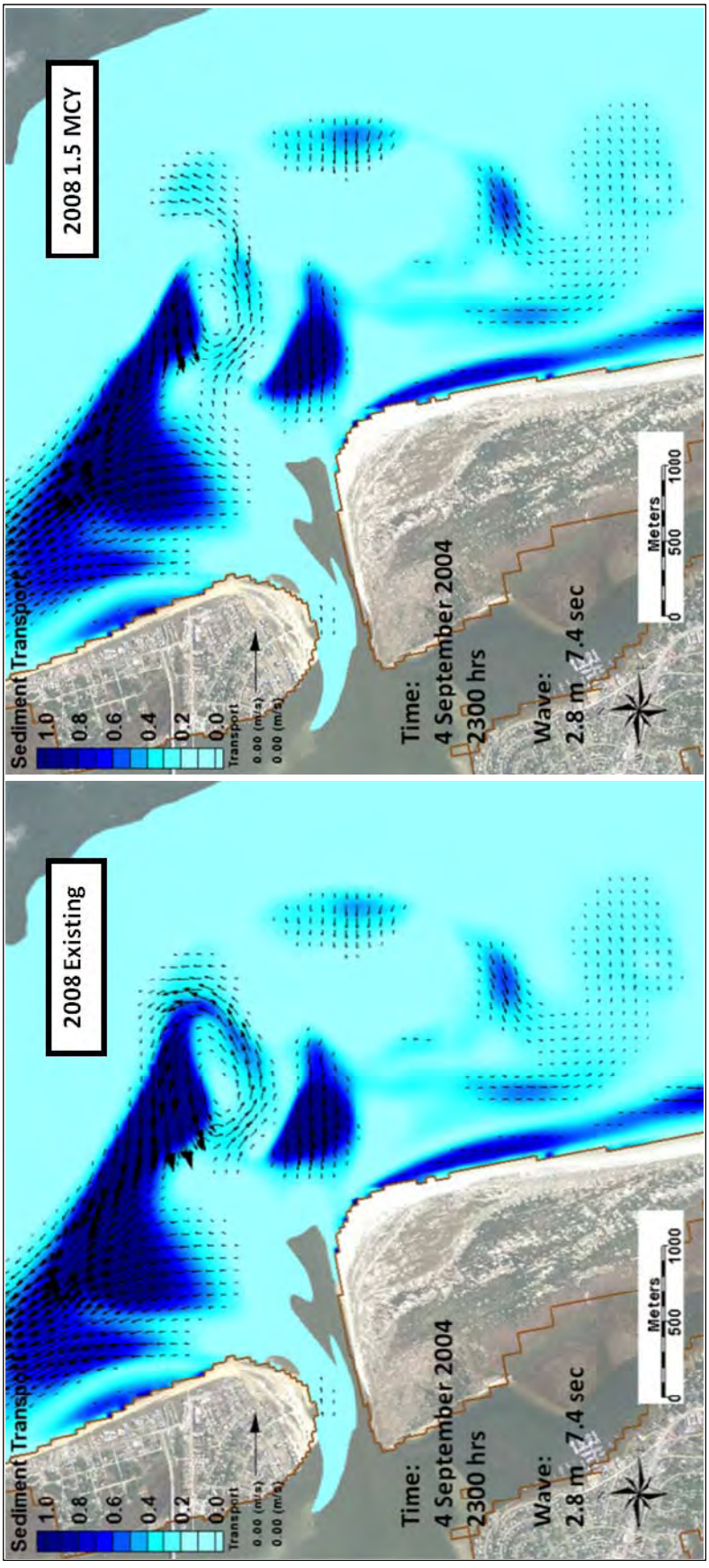

Figure 56. Final sediment transport (in kg/m^3) for the 2008 existing condition and 2008 1.5 mcy removed condition during late-2004 under northerly waves and an ebbing current.

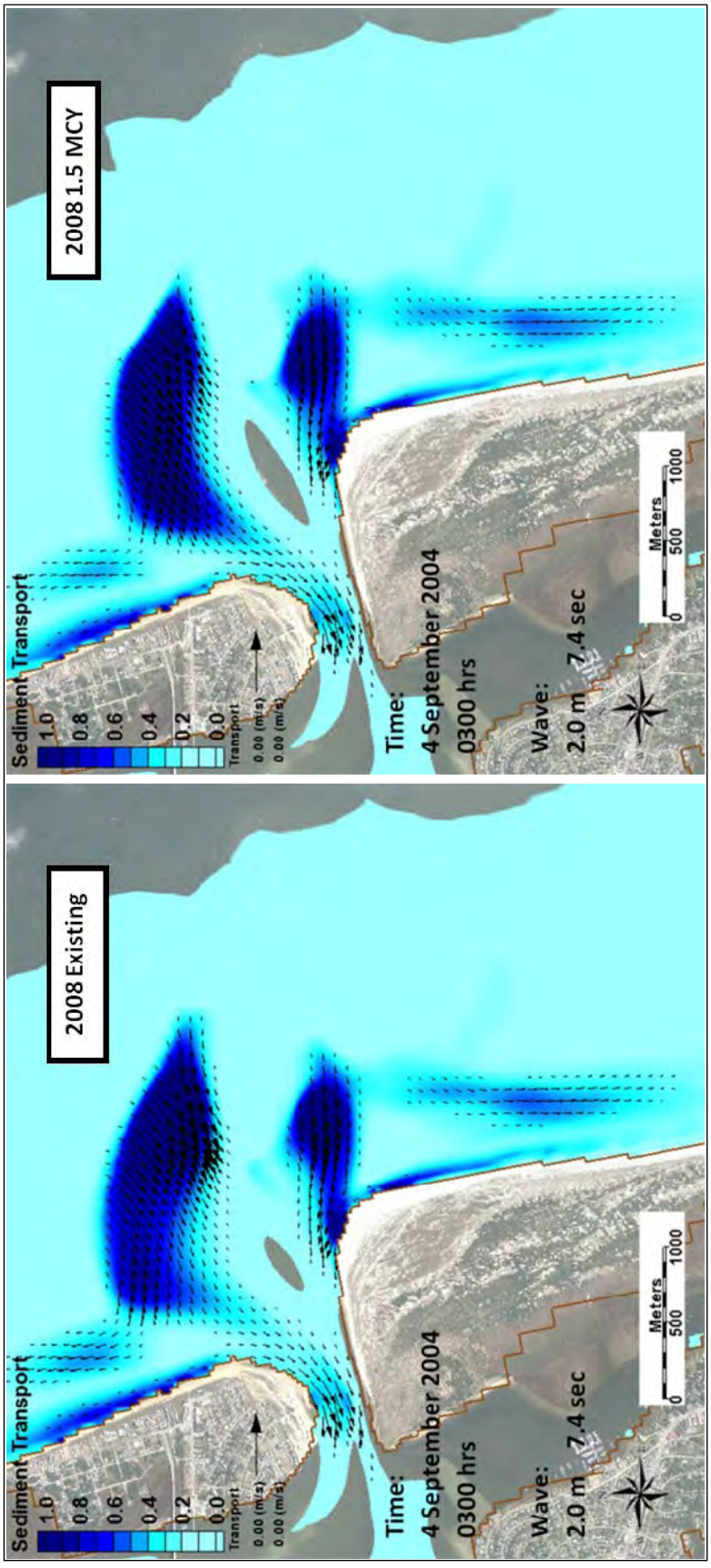

Figure 57. Final sediment transport (in kg/m3) pathways for the 2008 existing condition and 2008 1.5 mcy removed condition during late-2004 under northerly waves and a flooding current.

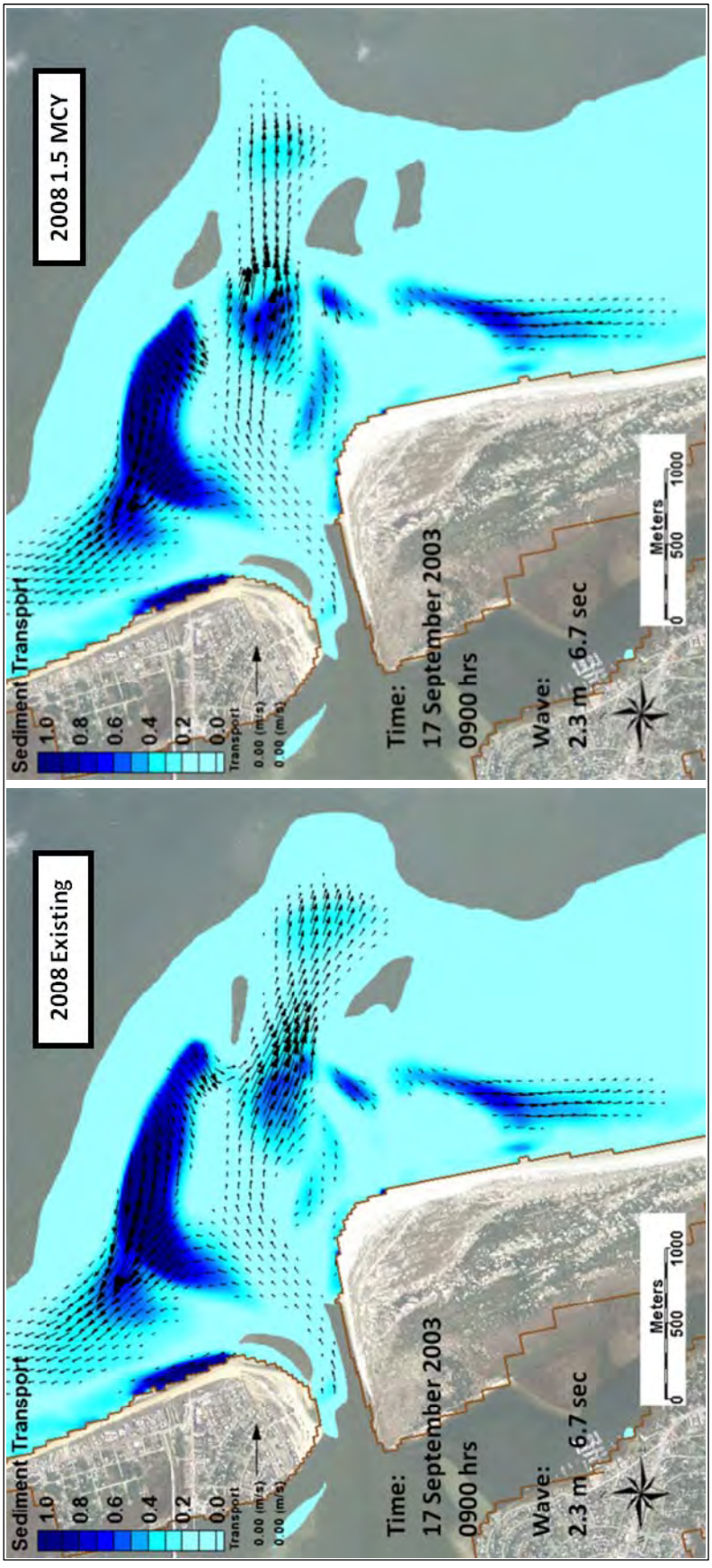

Figure 58. Initial sediment transport (in kg/m^3) pathways for the 2008 existing condition and 2008 1.5 mcy removed condition during mid-2003 under southerly waves and an ebbing current.

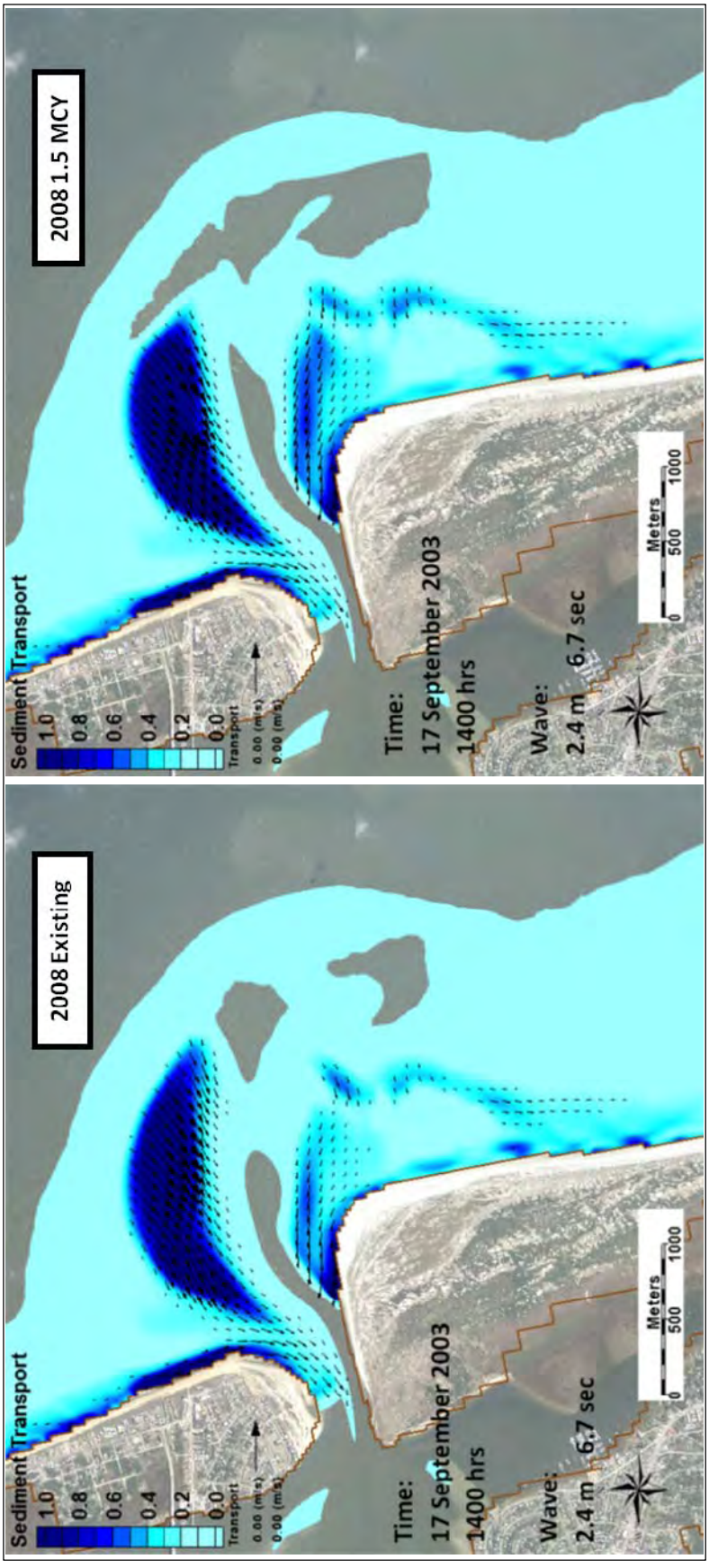

Figure 59. Initial sediment transport (in kg/m³) pathways for the 2008 existing condition and 2008 1.5 mcy removed condition during mid-2003 under southerly waves and a flooding current.

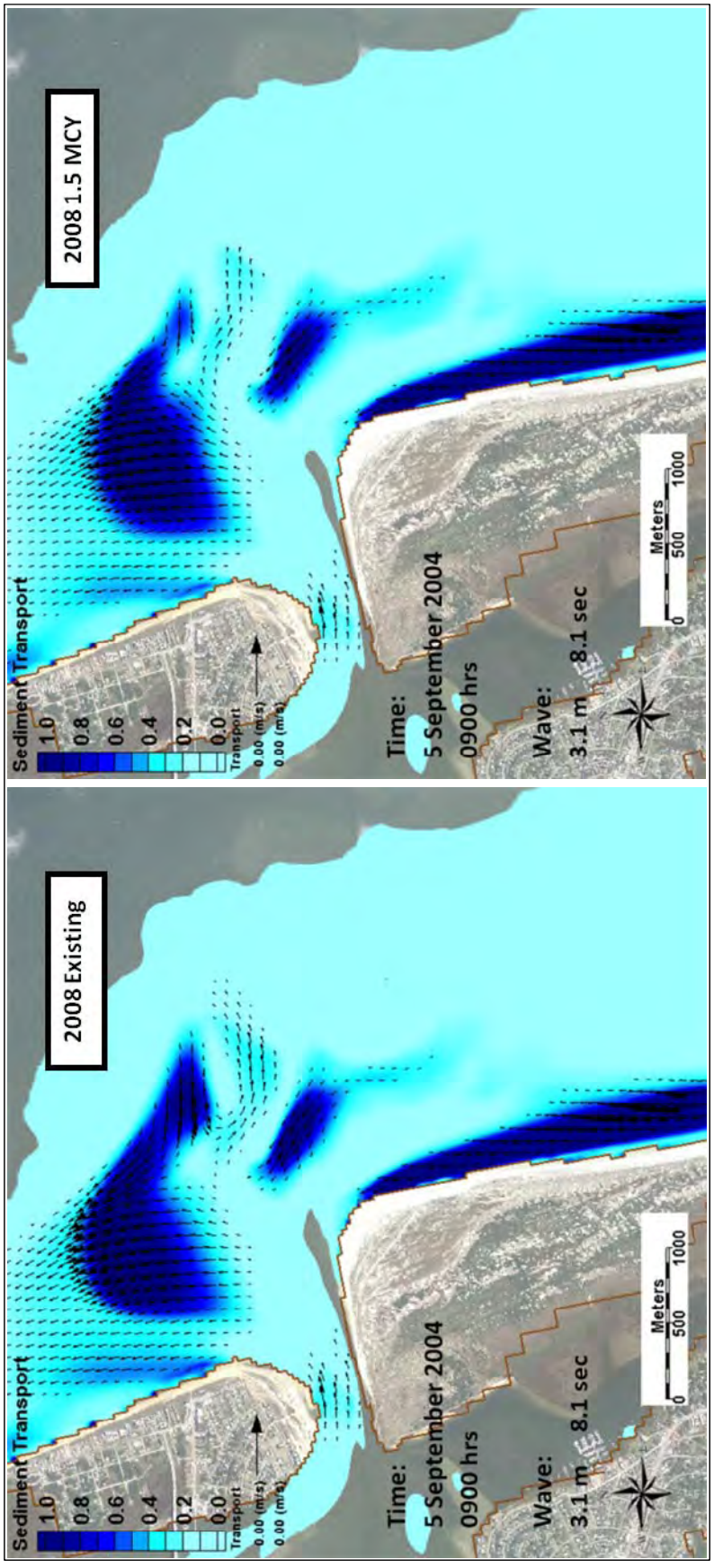

Figure 60. Final sediment transport (in kg/m³) pathways for the 2008 existing condition and 2008 1.5 mcy removed condition during late-2004 under southerly waves and an ebbing current.

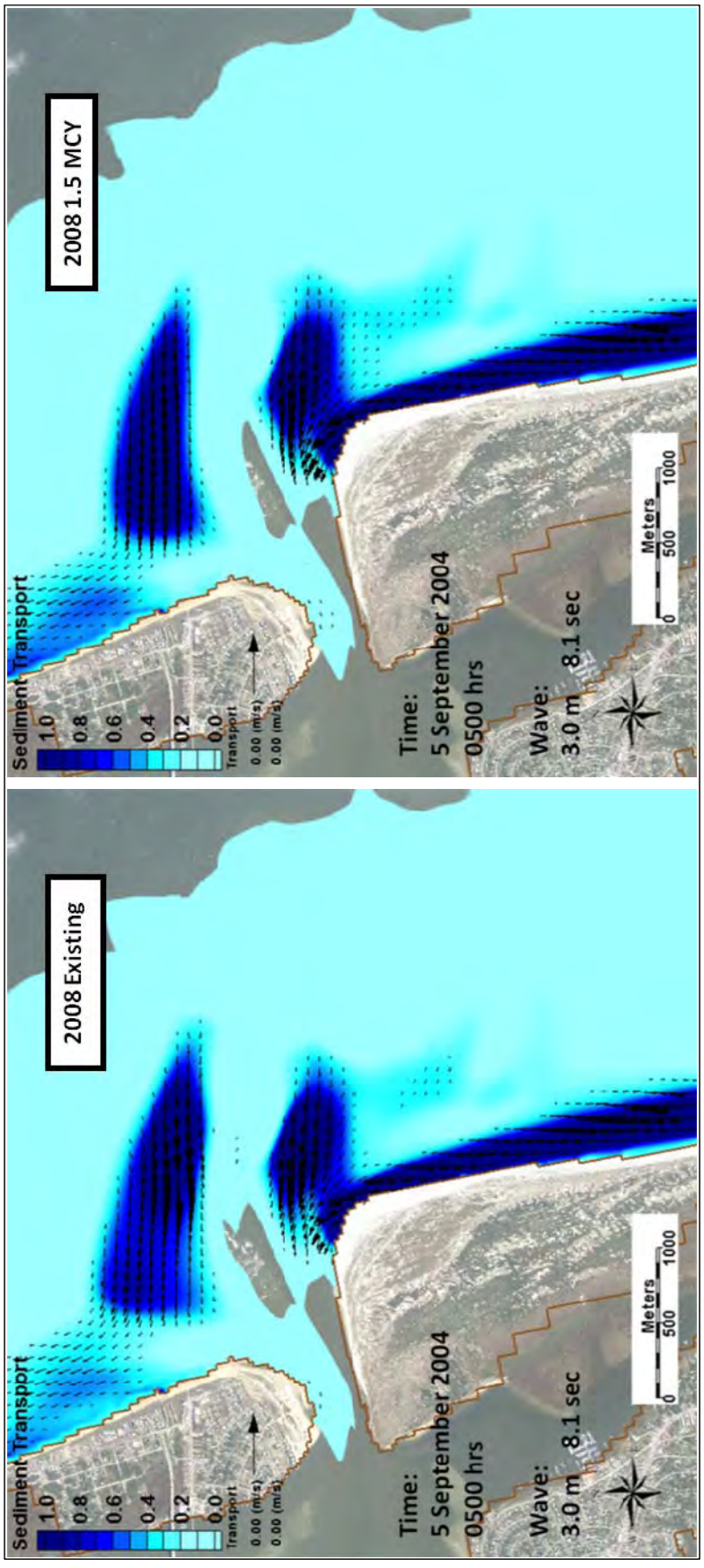

Figure 61. Final sediment transport (in kg/m3) pathways for the 2008 existing condition and 2008 1.5 mcy removed condition during late-2004 under southerly waves and a flooding current.

5.2 Ebb-tidal delta planform area

The comparison of different dredged quantities modeled, illustrated in this section as the total morphologic volume change, provides a scale for dredging scenarios. As stated before, the quantitative analysis of morphology change can provide insight in to the behavior of the inlet, however, a qualitative analysis of the results provide equal or more substantial information about the inlet processes and modeled changes under each scenario. Planform area change and volumetric change are analyzed quantitatively and finally ebb-tidal delta morphologic change is examined to determine ebb-tidal delta stability for all dredging scenarios.

Figure 62 illustrates polygons delineating the planform area of the ebb-tidal delta above the 6 m (20 ft) and 9 m (30 ft) contours. The planform change for a 1.4-year simulation illustrates the medium-term trajectory of the ebb-tidal delta planform. The dashed grey and black lines are the projected locations of the planform area of the ebb-tidal delta for the 6 m (20 ft) and 9 m (30 ft) contours, respectively. Similarly, the 2003 scenarios, the final 9 m (30 ft) contour shows little change. However, the 6 m contour shows the extension of the shallow, updrift portion of the shoal extending toward the dredged pit location. This is consistent with the historical trend of the updrift shoal growing toward the south-southeast, in the net direction of sediment transport. Table 13 gives the calculations of planform area change. The planform area to the 6 m (20 ft) contour for the 2008 existing condition grew by four percent and the planform area to the 6 m contour for the 1.5 mcy dredging condition grew by two percent. Similarly, planform area to the 9 m (30 ft) contour for the 2008 existing condition grew by 1.6 percent and the planform area to the 9 m contour for the 1.5 mcy dredging condition grew by 2.5 percent.

Morphology change for each scenario is given as a plot of bathymetry at the end of the 1.4-year simulation and a final morphology-change (erosion/deposition) plot in Figures 63 through 66. Ebb-tidal delta volume change was calculated based on the polygons illustrated in the morphology change plots from Figure 36 and is given in Table 14. The rate of volumetric recovery for the entire ebb-tidal delta was similar for each alternative, which is to be expected when using identical forcing. Figure 67 shows the volumetric recovery rates of the 1.5 mcy removed condition with the 2008 Existing condition are identical. The volume change for the 2008 Existing and the 1.5 and 3 mcy sediment removed scenarios are calculated to increase over the calculated 1.4 years at approximately the same rate.

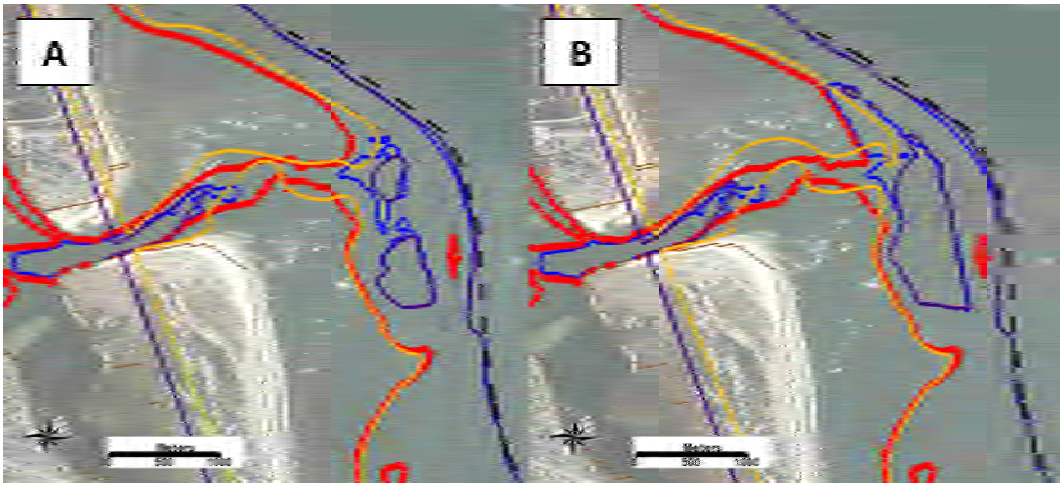

Figure 62. Planform of the 6 m and 9 m contours (warm and cool colors, respectively) and estimate of the natural 6-m and 9-m contours (light gray and dark gray, respectively) for the a) initial 2008 existing bathymetry (red, blue) and calculated final bathymetry (orange, purple), and b) 2008 1.5 mcy Removed bathymetry and calculated final bathymetry.

Table 13. Aerial changes for each model run.

Planform Surface Area of Ebb-tidal delta to 6 m Contour				Planform Surface Area of Ebb-tidal delta to 9 m Contour			
Existing Planform Area	Calculated Planform Area	Change	Difference %	Existing Planform Area	Calculated Planform Area	Change	Difference %
2008 Existing = 7,214,800 yd^2	2008 Existing Calculated = 7,471,447 yd^2	256,647 yd^2	4%	2008 Existing = 14,024,900 yd^2	2008 Existing Calculated = 14,267,200 yd^2	242,300 yd^2	1.6%
2008 1.5 mcy Removed = 7,111,700 yd^2	2008 1.5 mcy Removed Calculated = 7,243,700 yd^2	132,000 yd^2	2%	2008 1.5 mcy Removed = 13,579,500 yd^2	2008 1.5 mcy Removed Calculated = 13,939,300 yd^2	359,800 yd^2	2.5%

Sedimentation patterns are slightly different; however, overall the volume fluxes remain the same. The 2008 4 mcy removed scenario has a greater difference in aerial change of ebb-tidal delta morphology, and the calculated morphology change results in a greater variance in both aerial and volumetric change. The morphologic change is so great the shoals in the ebb-tidal delta reorient themselves and build a Northeast-oriented ebb channel. This modeled scenario illustrates morphologic change of the ebb-tidal delta that is beyond the tipping point of stable inlet processes.

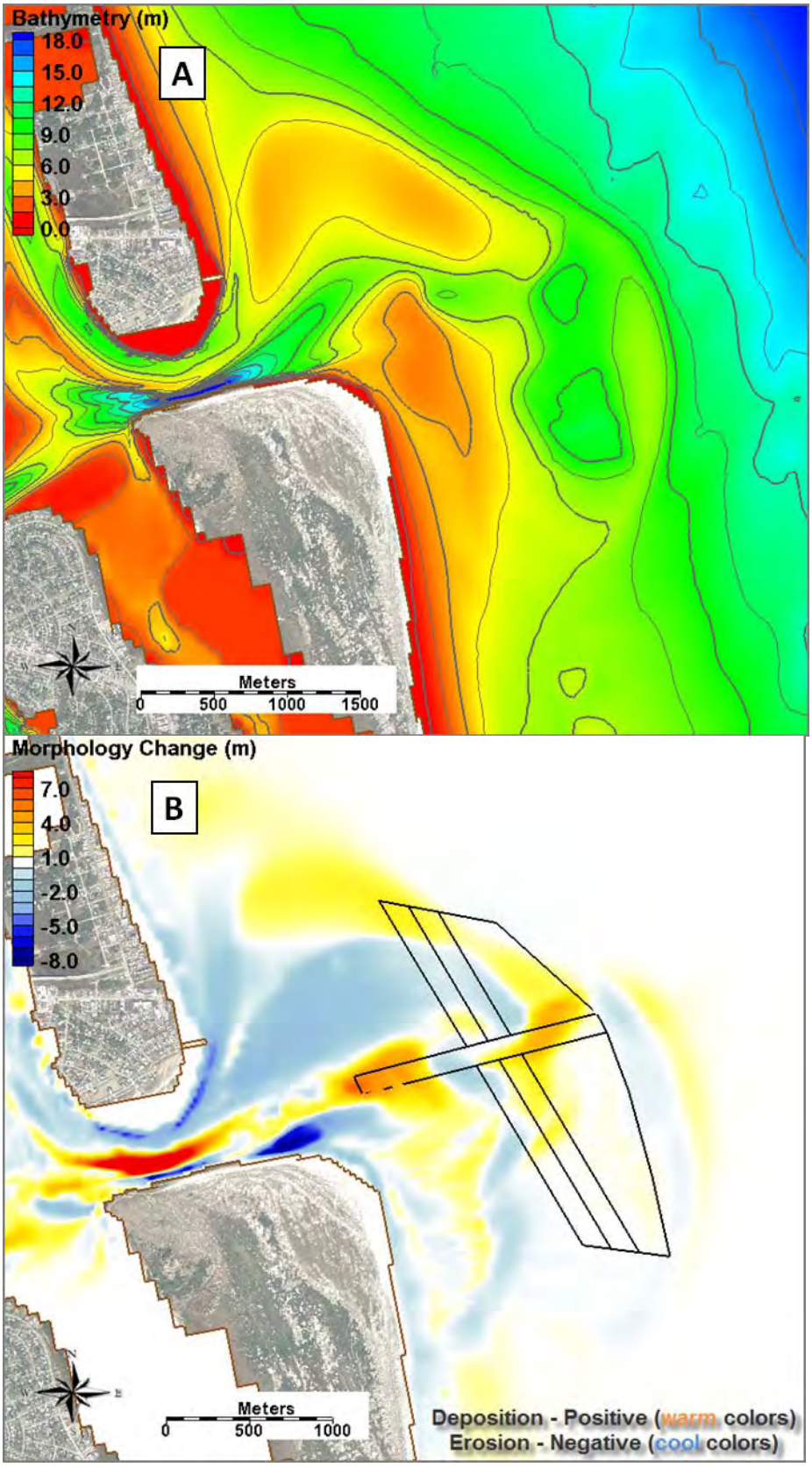

Figure 63. Final ebb-tidal delta change of the existing condition after a 1.4-year simulation.

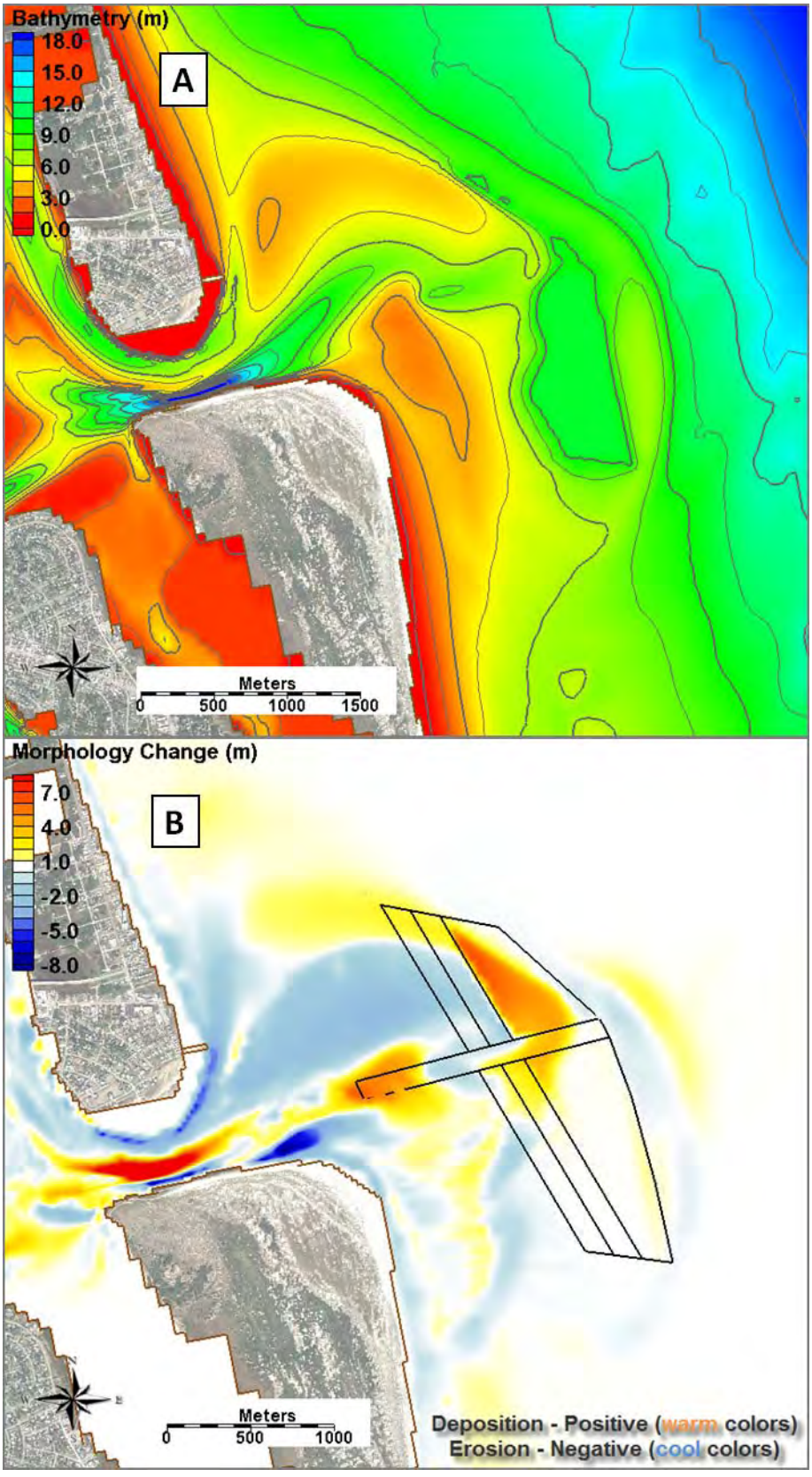

Figure 64. Final ebb-tidal delta change of the 1.5 mcy removed condition after a 1.4-year simulation.

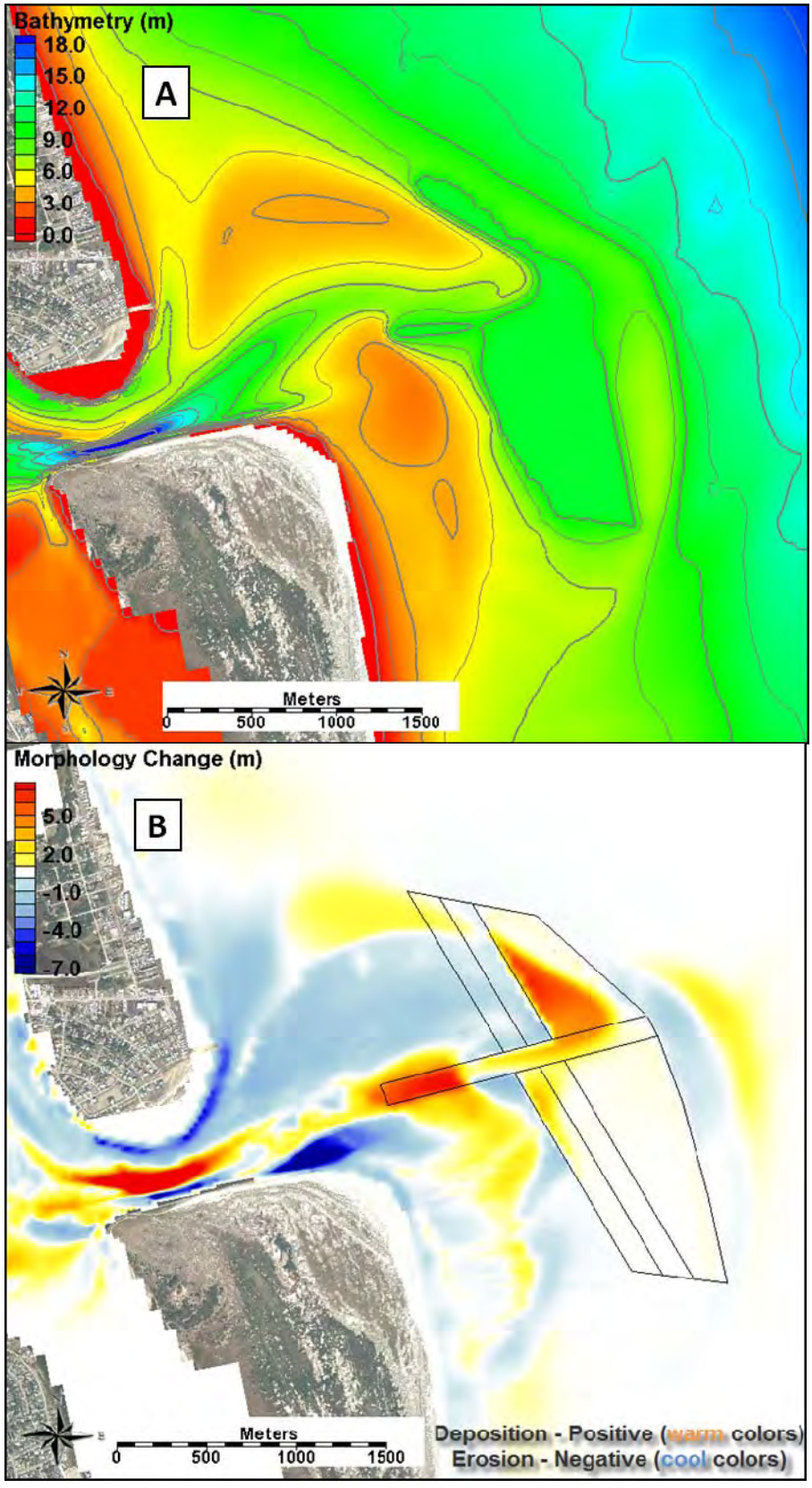

Figure 65. Final ebb-tidal delta change of the 3 mcy removed condition after a 1.4-year simulation.

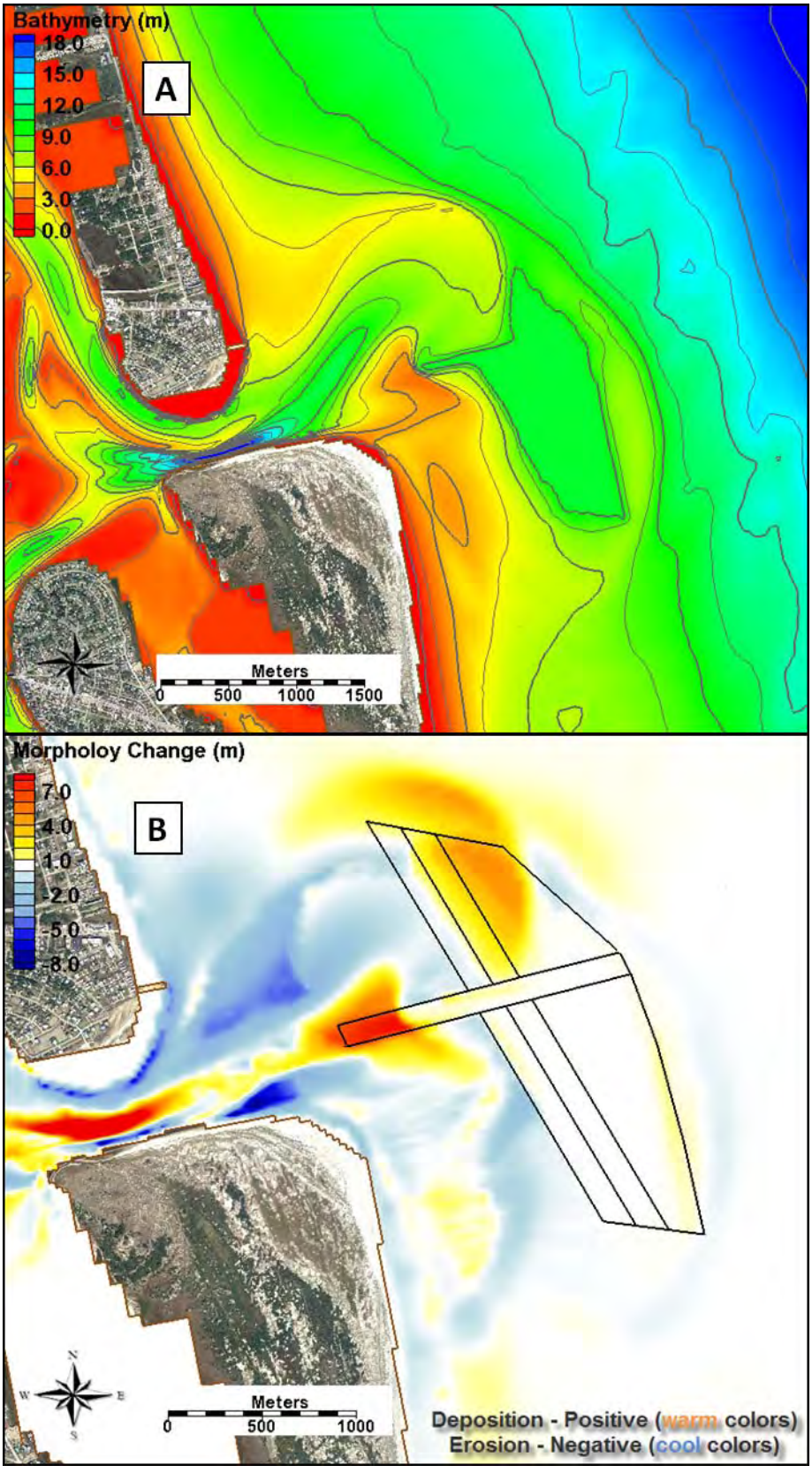

Figure 66. Final ebb-tidal delta change of the 4 mcy removed condition after a 1.4-year simulation.

Table 14. Volumes of ebb-tidal delta to 9 m contour and differences of the 2008 existing and 1.5 mcy removed conditions.

Initial	Final	Accreted	Difference %
2008 Existing = 30,566,500 cy	2008 Calculated Existing = 30,965,800 cy	399,300 cy	1.3%
2008 1.5 mcy Removed = 29,066,500 cy	2008 1.5 mcy Removed = 29,431,300 cy	364,800 cy	1.2%

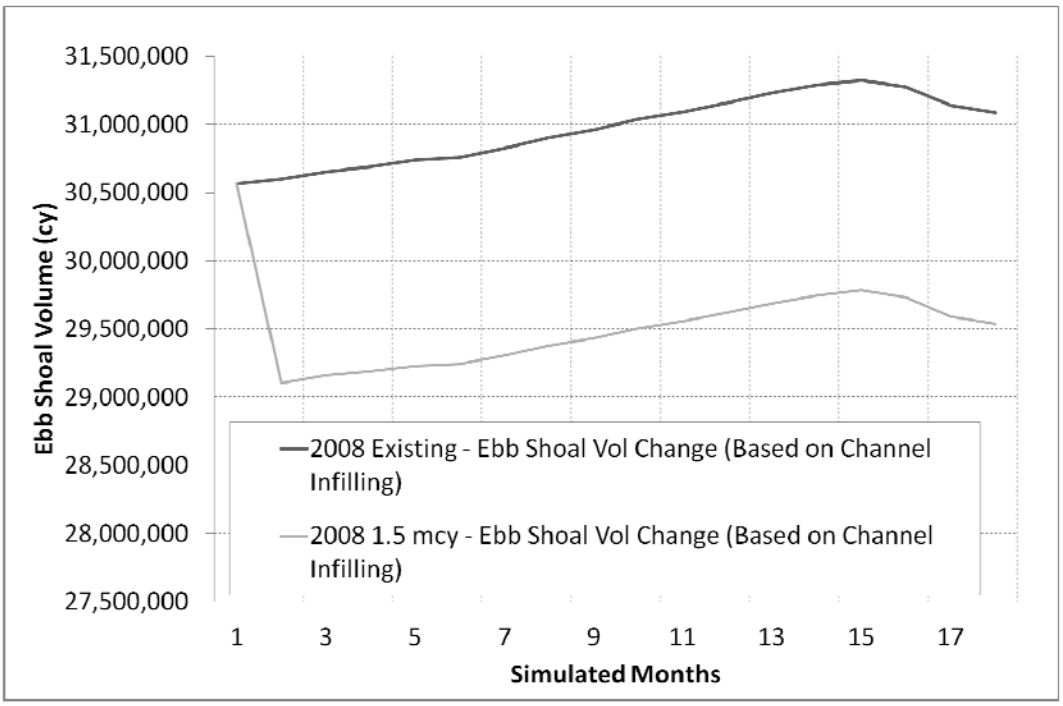

Figure 67. Ebb-tidal delta volume change of the 2008 existing condition and 2008 1.5 mcy removed condition.

6 Discussion and Conclusions

6.1 Role of historical mining activities on morphology

The primary goal of this project was to determine the role of mining activities on the morphological trajectory of the ebb-tidal delta at St. Augustine Inlet, FL. The CMS modeled results were first used to determine if the evolution of the ebb-tidal delta had been diverted from its natural (non-engineered) trajectory for previous mining activities. To perform this activity the model was setup for two comparative scenarios: 1) modeling the existing 2003 bathymetry in which the borrow site was excavated over the ebb-tidal delta, and 2) modeling the existing scenario with the borrow site digitally filled through replacing the volume that had been removed, thus creating a smooth, continuous surface across the ebb-tidal delta. Using the CMS, 1.4 years of morphology change were simulated for each scenario.

The planform extent of the ebb-tidal delta was examined to determine whether significant changes had occurred which would potentially cause a realignment of the shoreline. CMS calculations were compared for planform differences between the first (existing) and second (filled) scenarios. Here, significant change is defined as variations in the shape and extent of the planform at the active depth of transport of 6m, and, in addition, at the estimated depth of the ebb-tidal delta proper at approximately 9 m. The former more clearly describes the active zones of transport above the depth of closure whereas the latter more clearly defines the ebb-tidal delta proper. Both contours were examined to determine change to the planform of the ebb-tidal delta.

The 9 m contour was considered because tracking this contour would demonstrate whether there was significant geometrical change (for example, a morphological feature being sub-divided, or growing/shrinking extensively). The 6 m contour was also considered, because as the active zone of transport, examination of change in this contour would more clearly describe if significant changes had been made to a) the geometrical shape of the active zone of transport (had it widened or become more narrow?) and b) had the location of active transport changed (did it move onshore or offshore?)

The calculated 6 m contour for the existing bathymetry clearly shows the extension of the shallow, updrift portion of the shoal toward the location of the final position of the filled bathymetry. In Figure 37a, the orange line depicts the calculated 6 m contour for the existing condition, and it begins to follow the exact contour line for the orange line in Figure 37b, which represents the filled condition, at most north-eastern section of the north lobe. The 6 m contour is evolving toward the same planform equilibrium state in both model scenarios; however the existing condition does not recover the continuous active sediment transport at the 6 m contour in 1.4 years, because there is no active sediment transport over the borrow site, and it would be unreasonable to expect recovery of that site within 1.4 years.

In line with accepted principles of coastal geomorphology, the lack of change of the planform of the ebb-tidal delta proper would indicate that there would be no commensurate change in the far-field wave climate. Significant changes in the planform extent of the ebb-tidal delta, thus modifying the far-field wave climate, would lead to a realignment of the shoreline. At the 9 m contour, which represents the ebb-tidal delta proper, there was a 0.2 percent difference in planform area change between the existing and filled conditions at the conclusion of the model runs, indicating that significant change in the planform extent was not observed. There would be no expected change in the distribution of wave energy and incident wave angle along the adjacent beaches beyond the local change, at the 6 m contour that was described in previous STWAVE analyses (USACE 2009). Ultimately, the trajectory of the ebb-tidal delta proper was not diverted between the existing and filled cases and we conclude that previous engineering activities did not cause significant change to the planform extent and thus did not influence shoreline position.

Generally, accepted principles of coastal geomorphology also hold that the position of the shoreline along the adjacent beaches is in alignment with the wave climate as a function of the volume of the ebb-tidal delta. Comparisons of the ebb-tidal delta volume between existing and filled conditions indicated a one percent difference in volume. Because this is within tolerable levels depicting no change, we conclude that the previous mining activities did not affect the volume change of the ebb-tidal delta to the 9 m contour and that this did not collapse or deflate the overall ebb-tidal delta volume. This difference in volume should also not have any implications for the wave climate and far-field effects upon the shoreline.

Both modeled scenarios were similar in magnitude of gross and net transport; however, there was more sedimentation offshore in the filled scenario (arc line 4; Figure 52) and a slightly higher transport rate across the ebb-tidal delta into the dredged pit for the existing scenario (arc line 7; Figure 52). Transport was not expected to continue over the dredge pit and therefore sediment that would be transported offshore in the filled scenario instead would be deposited into the dredge pit in the existing scenario. For all other regions of the ebb-tidal delta, sediment fluxes were not significantly different.

Sediment transport pathways between the existing and filled conditions were examined to identify any appreciable change in the location, dominant direction, or aerial extent of active transport. There is no identifiable difference between flooding and ebbing current patterns save for the slight offset in the ebb jet pattern for the filled condition, which is oriented preferentially to the southeast. Transport over the north and south shoals tend to be oriented either into the channel on flooding currents or offshore during ebbing currents. The ultimate direction of these sediments either places them onto the nearshore or injects them into the inlet channel to be redistributed on tidally-dominated currents. This type of inlet is dominated by tidal processes rather than wave energy, and functions identically in both the 2003-2005 existing condition and the 2003-2005 filled condition. Overall, sediment transport pathways were not found to be interrupted by the present dredging footprint.

6.2 Role of planned mining activities on future morphology

We sought to answer the scientific question: “How many cubic yards of sediment can be mined from the ebb-tidal delta in the future which does not cause large scale morphological change to the ebb-tidal delta and inlet complex?” Large-scale morphological change includes significant change to the elevation and planform extent of the ebb-tidal delta as well as volumetric change. Ebb-tidal delta collapse or deflation means migration of a portion or the entire ebb-tidal delta onshore, alongshore, and offshore because of loss of the ebb-tidal current (abandonment) over the shoal (Hansen and Knowles 1988; Pope 1991).

The following analysis was used to assess whether additional excavations of the ebb-tidal delta would significantly change the entire ebb-tidal delta bathymetry, not just the borrow area excavation alone, by reducing its depth either through deflation or collapse, and/or by reducing its planform area such that it would result in a significant adverse impact to the coastal littoral

system and adjacent beaches. A geomorphologic model that couples wave, current and sediment transport processes was necessary to determine if additional excavation of the ebb-tidal delta that further reduces its size would change the distribution of wave energy and incident wave angle along the adjacent beaches.

To determine the role of additional excavations of the ebb-tidal delta on future morphology, the most recent survey bathymetry from 2008 (existing) is compared to several dredging scenarios. Three alternatives were developed by digitally removing 1.5 mcy, 3 mcy, and 4 mcy of sediment from authorized dredging locations over the 2008 existing bathymetry.

Sediment transport pathways were compared for the existing condition and the condition for which 1.5 mcy of sediment was removed from the authorized borrow site. Because we found no impact due to previous dredging events, we digitally mined in the same region and extended slightly into the north lobe to obtain the required 1.5 mcy. Of note, these volumes were based upon the 2008 bathymetry, and the borrow area would be greatly reduced in aerial extent if the 2010 survey presently underway demonstrates that there is a greater amount of available sediment in the previous borrow site. Overall, under different environmental forcing (ebbing and flooding, northerly and southerly approaching waves) there appears to be nearly identical sediment transport pathways for the existing condition and the condition for which 1.5 mcy of sediment was removed.

Ebb-tidal delta morphologic change is examined to determine ebb-tidal delta stability for all dredging scenarios (existing, 1.5 mcy removed, 3 mcy removed and 4 mcy removed). At the conclusion of the model runs, at the 9 m contour, which represents the ebb-tidal delta proper, there was a 0.9 percent difference in planform area change and a 0.1 percent difference in ebb-tidal delta volume change between the existing and 1.5 mcy mining alternative. The 6 m contour of both alternatives shows the extension of the shallow, updrift portion of the shoal into the dredged pit location with a two percent difference between the two alternatives. This is consistent with the historical trend of the updrift shoal growing toward the south-southeast, in the net direction of sediment transport. The lack of significant morphological change is reflected in the lack of significant change in wave refraction and wave energy at the ebb-tidal delta (e.g. shown in Figures 68 and 69 as wave height squared). Owing to this, there would be no expectation of an adjustment of the shoreline as a function of a significant change in wave refraction patterns.

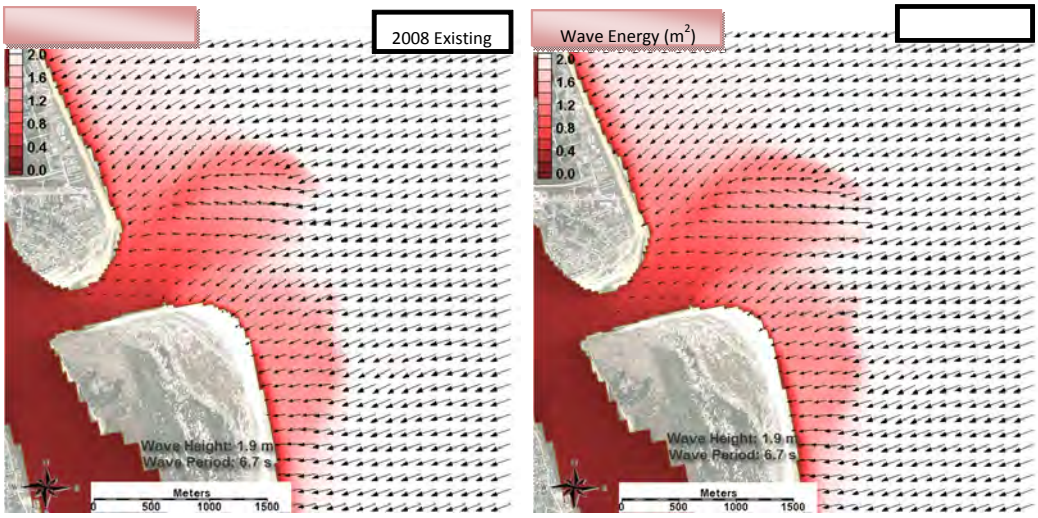

Figure 68. Vector plots of wave height squared illustrated in color intensity for the 2008 existing condition and 2008 1.5 mcy removed condition during mid-2003 under energetic northerly waves.

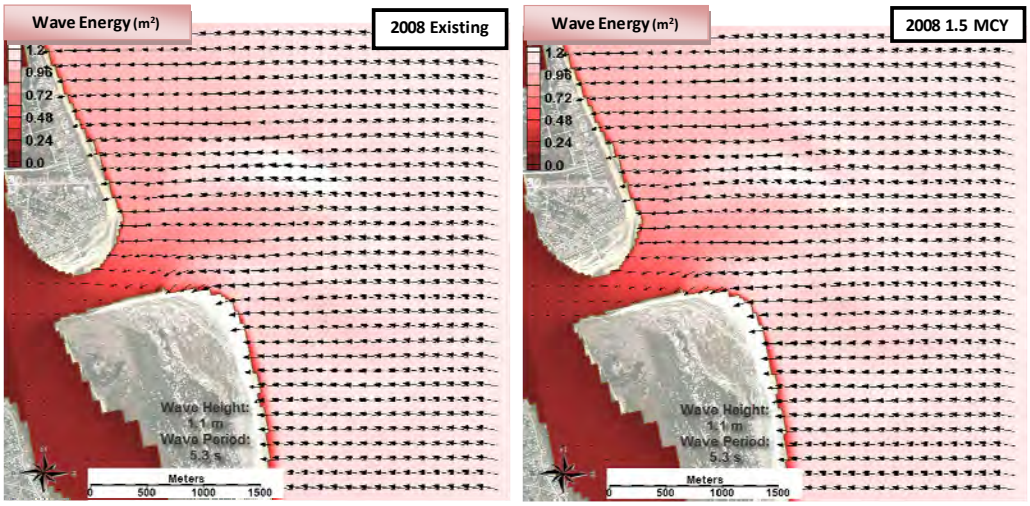

Figure 69. Vector plots of wave height with wave energy illustrated in color intensity for the 2008 existing condition and 2008 1.5 mcy removed condition during mid-2003 under energetic southerly waves.

An analysis of the ebb-tidal delta bathymetric changes contained in the 2006 monitoring report (Taylor Engineering Inc. 2007) indicated some deflation of the ebb-tidal delta elevations outside the limits of the borrow area following the initial 2003 beach restoration. There is a present concern that removal of too large a quantity of sediment from the borrow site would cause further deflation and possible collapse of the ebb-tidal delta. Significant changes in the depth and planform extent of the ebb-tidal delta would lead to a realignment of the shoreline to such a degree that beach erosion would threaten upland infrastructure. Large-scale changes of the ebb-tidal

delta bathymetry, as demonstrated in the 4 mcy removed scenario, would interfere with gross southerly sediment transport to the downdrift beaches. It may also change wave refraction patterns that could induce more erosion of adjacent beaches than predicted by consideration of the borrow area excavation alone. The variance in dredging imprint and volumes removed for the four scenarios provided guidance on the potential result of the removal of too much sediment, and aided in the conservative dredging quantity request the Jacksonville District submitted for the 2011 and future permits.

6.3 Conclusions

The morphodynamics and sediment bypassing patterns that occur at St. Augustine Inlet are indicative of a mixed-energy straight morphology with stable inlet processes and modest planform change (no migration) since it's relocation in 1942. Historical morphology has indicated that the updrift, northern portion of the inlet shoal is wave-dominated; whereas the northern flood marginal channel and southern shoal complex are greatly influenced by tidal currents. The resultant sediment pathways are a combination of wave-driven transport over the active shoals, and subsequent tidally-driven transport redistributing the sediment to all ebb- and flood-tidal delta shoals.

Geomorphological model results indicated that previous mining of the ebb-tidal delta did not significantly change the planform (or footprint) of the ebb-tidal delta proper. In line with accepted principles of coastal geomorphology, the lack of change of the planform of the ebb-tidal delta proper would indicate that there would be no commensurate change in the far-field wave climate. Significant changes in the planform extent of the ebb-tidal delta, thus modifying the far-field wave climate, would lead to a realignment of the shoreline. At the 9 m contour, which represents the ebb-tidal delta proper, there was a 0.2 percent difference in planform area change between the existing and filled conditions, indicating that significant change in the planform extent was not observed. Ultimately, the trajectory of the ebb-tidal delta proper was not diverted between the existing and filled cases, indicating that previous engineering activities did not cause significant change to the planform extent and thus did not influence shoreline position. Sediment transport pathways were not found to be interrupted by the present dredging footprint when comparing sediment transport spatial patterns and magnitudes. Comparisons of the ebb-tidal delta volume between existing and filled conditions indicated a one percent difference,

also indicating that the previous mining activities did not greatly affect the volumetric growth of the ebb-tidal delta and that this did not collapse or deflate the overall ebb-tidal delta volume.

Ebb-tidal delta morphologic change was examined to determine ebb-tidal delta stability for four future dredging scenarios (existing, 1.5 mcy removed, 3 mcy removed and 4 mcy removed). At the 9 m contour, which represents the ebb-tidal delta proper, there was a 0.9 percent difference in planform area change and a 0.1 percent difference in ebb-tidal delta volume change between the existing and 1.5 mcy mining alternative. At the 6 m contour, which represents the active ebb-tidal delta, there was a two percent difference in planform area change between the existing and 1.5 mcy mining alternative, indicating that significant change in the planform extent was not observed. For a 1.5 mcy mining alternative, there would be no expectation of an adjustment of the shoreline as a function of a significant change in wave refraction patterns. In addition, this alternative would not impact sediment transport pathways over the inlet/ebb-tidal delta complex.

All modeled future alternatives except for the 4 mcy removed alternative did not show significant variance in volumetric change over the time period simulated. Modeling of planned alternatives including the removal of an additional 1.5, 3, and 4 mcy of sediment also illustrated a tipping point in morphodynamic response in varying volume removed and mining design. For the expansive dredging design in the 4 mcy alternative, the resulting planform represents a significant change in morphology that indicates large-scale migration of a portion of the ebb-tidal delta. Future borrow site plans should be designed with an eye toward avoiding migration of morphological features, for example, realignment of the inlet channel, or a reposition of the north, south and terminal lobes, or relocation of attachment bars.

References

Beck, T.M., and N.C. Kraus. 2010. Shark River Inlet, New Jersey, Entrance Shoaling: Report 2, Analysis with Coastal Modeling System. ERDC/CHL-TR-10-4, US Army Engineer Research and Development Center, Coastal and Hydraulics Laboratory, Vicksburg, MS.

Buttolph, A. M., C.W. Reed, N.C. Kraus, N. Ono, M. Larson, B. Camenen, H. Hanson, T. Wamsley, and A.K. Zundel. 2006. Two-Dimensional Depth-Averaged Circulation Model CMS-M2D: Version 3.0, Report 2, Sediment Transport and Morphology Change. Technical Report ERDC/CHL-TR-06-7, US Army Engineer Research and Development Center, Coastal and Hydraulics Laboratory, Vicksburg, MS.

Byrnes, M.R., J.L. Baker, and N.C. Kraus. 2003. Coastal sediment budget for Grays Harbor, Washington. Proc. Coastal Sediments '03, CD-ROM, World Sci. Press and East Meets West Productions, Corpus Christi, TX ISBN-981-238-422-7, 10 p.

Camenen, B., and M. Larson. 2007. A Unified Sediment Transport Formulation for Coastal Inlet Application. Contract Report ERDC/CHL-CR-07-1, US Army Engineer Research and Development Center, Coastal and Hydraulics Laboratory, Vicksburg, MS.

Dally, W.R. and M.E. Leadon. 2003. Comparison of Deep-Water ADCP and NDBC Buoy Measurements to Hindcast Parameters. Report submitted to the U.S. Army Corps of Engineers, Jacksonville District.

Davis, Jr., R.A., and M.O. Hayes. 1984. What is a wave dominated coast? *Marine Geology* 60, 313-329.

Fitzgerald, D.M. 1988. Shoreline Erosional-Depositional Processes Associated with Tidal Inlets. Hydrodynamics and Sediment Dynamics of Tidal Inlets, D.G. Aubrey and L. Weishar, eds., New York. p. 412-439.

Hansen, M., and S.C. Knowles. 1988. Ebb-tidal delta response to jetty construction at three South Carolina inlets. in Hydrodynamics and Sediment Dynamics of Tidal Inlets, D.G. Aubrey and L. Weishar, eds., Lecture Notes on Coastal and Estuarine Studies 29, Springer, 364-381Hayes, M.O. 1979. Barrier island morphology as a function of tidal and wave regime. In: Barrier Islands. Leatherman, S.P., ed., Academic Press, 1-28.

Hayes, M.O. 1979. Barrier island morphology as a function of tidal and wave regime. In: *Barrier Islands form the Gulf of St. Lawrence to the Gulf of Mexico*, S.P. Leatherman (Ed.). Academic Press, NY, pp. 1-27.

JALBTCX. 2006. 2004 US Army Corps of Engineers (USACE) Topo/Bathy Lidar: Alabama, Florida, Mississippi and North Carolina. *Joint Airborne LiDAR Bathymetry Technical Center of Expertise (JALBTCX).* NOAA's Ocean Service, Coastal Services Center (CSC): <http://www.csc.noaa.gov/ldart>; Charleston, SC.

Kana, TW, and P.M. McKee. 2003. Relocation of Captain Sams Inlet – 20 years later. Proc. Coastal Sediments 03, CD-ROM, World Sci. Press and East Meets West Productions, ISBN-981-238-422-7, 14 p.

Kana, T. W., and J.E. Mason. 1988. Evolution of an ebb-tidal delta after an inlet relocation. in Hydrodynamics and Sediment Dynamics of Tidal Inlets, D.G. Aubrey and L. Weishar, eds., Lecture Notes on Coastal and Estuarine Studies 29, Springer, 382-411.

Kana, T.W., E. J. Hayter, and P. A. Work. 1999. Mesoscale Sediment Transport at Southeastern U.S. Tidal Inlets: Conceptual Model Applicable to Mixed Energy Settings. *Journal of Coastal Research*; Vol. 15, No. 2 (Spring, 1999), pp. 303-313.

Leadon, M.E., W.R. Dally, D.A. Osiecki. 2009. The Florida Coastal Forcing Project. Report submitted to the Florida Department of Environmental Protection.

Lin, L., Z. Demirbilek, H. Mase, J. Zheng, and F. Yamada. 2008. CMS-Wave: A Nearshore Spectral Wave Processes Model for Coastal Inlets and Navigation Projects. ERDC/CHL-TR-08-13, US Army Engineer Research and Development Center, Coastal and Hydraulics Laboratory, Vicksburg, MS.

Legault, K., J.D. Rosati, J. Engle, and T.M. Beck. 2012. St. Johns County, St. Augustine Inlet, FL Report 1: Historical Analysis and Sediment Budget. ERDC/CHL-TR-12-X, US Army Engineer Research and Development Center, Coastal and Hydraulics Laboratory, Vicksburg, MS.

NOAA. 2010a. Tides and currents. National Oceanographic and Atmospheric Administration. http://tidesandcurrents.noaa.gov/ , accessed 17 April 2010.

NOAA. 2010b. NOAA Bathymetry. National Oceanographic and Atmospheric Administration. https://www.ngdc.noaa.gov/mgg/bathymetry/relief.html , accessed 3 March 2010.

PBS&J. 2009. St. Johns County Shore Stabilization Feasibility Study for South Ponte Vedra and Vilano Beach Regions. Tampa, Florida.

Pope, J. 1991. Ebb delta and shoreline response to inlet stabilization, examples from the southeast Atlantic Coast. *Proc. Coastal Zone '91*, ASCE, 643-654.

Sanchez, A., and W. Wu.(2010. A non-equilibrium sediment transport model for coastal inlets and navigation channels. *Journal of Coastal Research*, submitted.

Taylor Engineering, Inc. 1996. Inlet Baseline Conditions Physical and Environmental Characteristics. St. Augustine Inlet Management Plan – Part 2, St. Johns County, Florida.

Taylor Engineering, Inc. 2007. 2006 Monitoring Report. St. Johns County Shore Protection Project, St. Johns County, Florida.

Taylor Engineering, Inc. 2010. 2009 Monitoring Report. St. Johns County Shore Protection Project, St. Johns County, Florida.

USACE 1998. St. Johns County, Florida Shore Protection Project, General Reevaluation Report with Final Environmental Assessment. Jacksonville District Internal Report.

USACE 2009. Influence of St. Augustine Ebb-tidal delta Excavation on Near-shore Wave Climate and Sediment Pathways, St. Johns County, Florida. Jacksonville District Internal Report.

USACE 2010. Wave Information Studies Project Documentation: WIS Hindcast Database. Developed by the US Corps of Engineer Research and Development Center. http://frf.usace.army.mil/wis2010.

van Rijn, L.C. 2007a. Unified View of Sediment Transport by Currents and Waves. I: Initiation of Motion, Bed Roughness, and Bed-load Transport. *Journal of Hydraulic Engineering*, 133(6), 649-667.

van Rijn, L.C. 2007b. Unified View of Sediment Transport by Currents and Waves. II: Suspended Transport. *Journal of Hydraulic Engineering*, 133(6), 668-689.

Walton, T. L., and W. D. Adams. 1976. Capacity of inlet outer bars to store sand. *Proceedings 15th Coastal Engineering Conference*, ASCE, 1,919-1,937.

Wu, W., M. Zhang, and A. Sanchez. 2010. An implicit 2-D shallow water flow model on unstructured quadtree rectangular mesh. *Journal of Coastal Research*, submitted.

REPORT DOCUMENTATION PAGE

Form Approved
OMB No. 0704-0188

1. REPORT DATE *(DD-MM-YYYY)*	2. REPORT TYPE	3. DATES COVERED *(From - To)*
August 2012	Report 2 of a series	

4. TITLE AND SUBTITLE

St. Augustine Inlet, Florida: Applying the Coastal Modeling System, Report 2

5a. CONTRACT NUMBER

5b. GRANT NUMBER

5c. PROGRAM ELEMENT NUMBER

6. AUTHOR(S)

Tanya M. Beck and Kelly Legault

5d. PROJECT NUMBER

5e. TASK NUMBER

5f. WORK UNIT NUMBER

7. PERFORMING ORGANIZATION NAME(S) AND ADDRESS(ES)

Coastal and Hydraulics Laboratory
U.S. Army Engineer Research and Development Center
3909 Halls Ferry Road
Vicksburg, MS 39180-6199

8. PERFORMING ORGANIZATION REPORT NUMBER

ERDC/CHL TR-12-14

9. SPONSORING / MONITORING AGENCY NAME(S) AND ADDRESS(ES)

U.S. Army Engineer District, Jacksonville
701 San Marco Blvd.,
Jacksonville, FL 32207

10. SPONSOR/MONITOR'S ACRONYM(S)

11. SPONSOR/MONITOR'S REPORT NUMBER(S)

12. DISTRIBUTION / AVAILABILITY STATEMENT

Approved for public release; distribution is unlimited.

13. SUPPLEMENTARY NOTES

14. ABSTRACT

This report, the second in a series, documents a numerical modeling study performed with the Coastal Modeling System (CMS), supported by field data collection, to quantify the impact of historical and future planned mining of the ebb-tidal delta at St. Augustine Inlet, FL. Recently, in the years 2001-2003 and 2005, two nourishment intervals utilized beach-quality sediment from the ebb-tidal delta at St. Augustine Inlet, resulting in 4.7 and 2.5 million cubic yards of sediment removed from the inlet system, respectively, for the two time periods. The CMS was used to determine the impact of these historical mining operations, as well as potential future minings on the natural littoral system in the vicinity of the inlet as well as the morphodynamics of the inlet. Quantitative comparisons of planform evolution, volumetric change, and transport pathway spatial distribution and magnitude were made for the historical and future scenarios. Results showed little to no changes in the ebb-tidal delta trajectory in these three quantitative comparisons. The footprint of the ebb-tidal delta mining did not change the bypassing patterns in a way such as to cause significant morphologic change to the inlet system. Modeling of planned alternatives including the removal of an additional 1.5, 3, and 4 million cubic yards (mcy) of sediment also illustrated a tipping point in morphodynamic response in varying volume removed and mining design.

15. SUBJECT TERMS

Channel infilling
Coastal modeling system
Coastal processes
Ebb-shoal mining
Ebb-tidal delta
Inlet morphodynamics
Sediment transport
Tidal inlets

16. SECURITY CLASSIFICATION OF:			17. LIMITATION OF ABSTRACT	18. NUMBER OF PAGES	19a. NAME OF RESPONSIBLE PERSON: Tanya Beck
a. REPORT	b. ABSTRACT	c. THIS PAGE			19b. TELEPHONE NUMBER *(include area code)*
Unclassified	Unclassified	Unclassified	Unclassified	96	(601) 634-2603